MASTER THESIS

Thermochemical Energy Storage –
Basic design of a lab-scale test plant for
oil-suspended boric acid cycles

carried out for the purpose of obtaining the academic degree of

Diplomingenieur (Dipl.-Ing.)

submitted at

TU Wien

Faculty of Mechanical and Industrial Engineering

by

Mathias Berlinger BSc

Mat. Nr. 01327627

under the direction of

ao.Univ.Prof. Dipl.-Ing. Dr. Franz Winter

Institute of Chemical, Environmental and Bioscience Engineering

Getreidemarkt 9/E166, A-1060 Vienna

Vienna, May 2022

Affidavit

I declare in lieu of oath, that I wrote this thesis and performed the associated research myself, using only literature cited in this volume. If text passages from sources are used literally, they are marked as such.

I confirm that this work is original and has not been submitted elsewhere for any examination, nor is it currently under consideration for a thesis elsewhere.

I acknowledge that the submitted work will be checked electronically-technically using suitable and state-of-the-art means (plagiarism detection software). On the one hand, this ensures that the submitted work was prepared according to the high-quality standards within the applicable rules to ensure good scientific practice "Code of Conduct" at the TU Wien. On the other hand, a comparison with other student theses avoids violations of my personal copyright.

I confirm, that going to press of this thesis needs the confirmation of the examination committee.

I emphasize that the thesis contains confidential information and internal company data. Therefore, publication or disclosure of contents to third parties is not permitted without the prior consent of the Institute of Chemical, Environmental and Bioscience Engineering.

_____   _____

City and Date   *Mathias Berlinger*

To my father

To whom I promised this work seven years ago.

May you find rest on your invisible path.

To my mother

To whom I owe this joyful existence.

May you find silence to listen to the whispers from within.

To my allies and enemies

To light and darkness guiding and evolving us forever eversince.

Do not lose faith

For we will look back on our lives one day

The regrets of yesterday

The worries about tomorrow

The suffering of today

And smile

Smile lightheartedly

Together with all sentient beings we have helped to overcome their suffering.

What has been will be again, what has been done will be done again;

There is nothing new under the sun.

Ecclesiastes 1:9

Table of contents

Abstract

Throughout the majority of industrial plants, large quantities of waste heat are released into the atmosphere. Tapping these heat sources could potentially yield a year's district heating energy demand next to appropriate plants. To store this energy from season to season, thermochemical energy storage is of growing interest, with boric acid being a candidate for low-temperature energy capture.

The aim of this thesis is to design the apparative and operational requirements for a laboratory-scale plant that enables continuous full-cycle experiments with the thermochemical energy storage (TCES) system orthoboric acid - metaboric acid - boron oxide. So far, experiments have been conducted in small batch reactors under different temperature and pressure profiles to better understand the reaction kinetics; Once these results represent a found empirical knowledge of the novel approach to TCES - the operation in a suspension of thermal oil - the plant will serve as a platform for experiments of heat transfer, conversion, phase separation, convection through different conveying units, cyclic stability, dehydration/rehydration efficiency and byproduct generation. This thesis is limited to theoretical modelling of the basic process steps in the simplified reaction system orthoboric acid - metaboric acid, calculating heat and mass flows as well as visualizing them with Sankey-diagrams, and designing the experimental plant's basic P&ID. A few operation modes are compared to maintain flexibility in a yet undiscovered field of research, and considerations about possibly occurring phenomena are discussed.

Kurzfassung

In den meisten Industriebetrieben werden große Mengen an Abwärme an die Atmosphäre abgegeben. Die Erschließung dieser Wärmequellen bei geeigneten Industrien könnte den Energiebedarf für die gesamte Fernwärme einer Heizperiode liefern. Um diese Energie über die Jahreszeiten zu speichern, ist die thermochemische Energiespeicherung von wachsendem Interesse, wobei Borsäure ein Kandidat für die Energiegewinnung bei Niedertemperatur ist.

Ziel dieser Arbeit ist es, die apparativen und betrieblichen Grundlagen für eine Anlage im Labormaßstab zu schaffen, die kontinuierliche Vollzyklusexperimente mit dem thermochemischen Energiespeichersystem (TCES) Borsäure - Metaborsäure - Boroxid ermöglicht. Bisher wurden Experimente in kleinen Batch-Reaktoren unter verschiedenen Temperatur- und Druckprofilen durchgeführt, um die Reaktionskinetik besser zu verstehen. Sobald diese Ergebnisse ein fundiertes empirisches Wissen über den neuartigen Ansatz der TCES - den Betrieb in einer Suspension von Thermoöl - darstellen, wird die Anlage als Plattform für Experimente zu Wärmeübertragung, Umwandlung, Phasentrennung, Konvektion durch verschiedene Fördereinheiten, zyklischer Stabilität, Dehydratisierungs-/Rehydratisierungseffizienz und Nebenproduktbildung dienen. Diese Arbeit beschränkt sich auf die theoretische Modellierung der grundlegenden Prozessschritte im vereinfachten Reaktionssystem Borsäure - Metaborsäure, die Berechnung von Wärme- und Massenströmen sowie deren Visualisierung mit Sankey-Diagrammen und den Entwurf des grundlegenden P&ID der Versuchsanlage. Eine Auswahl von Betriebsarten wird verglichen, um die Flexibilität in einem noch frischem Forschungsgebiet zu gewährleisten, und mögliche auftretende Phänomene werden diskutiert.

List of figures

List of tables

Notation

I. Symbols

H_3BO_3	Orthoboric acid, boric acid	mol
HBO_2	Metaboric acid	mol
B_2O_3	Boron oxide	mol
H_2O	Water/steam	mol
M	Molar mass	g/mol
$\dot{n}$	Molar flow	mol/h
m	Mass	kg
$\dot{m}$	Mass flow	kg/h
ρ	Density	kg/m³
V	Volume	m³
$\dot{V}$	Volume flow	m³/h
ε	Void volume	-
T	Temperature	K or °C
$\overline{T}$	Mean temperature	K or °C
T_m	Melting point	K or °C
c_p	Specific heat capacity	kJ/kgK
h	Specific enthalpy	kJ/kg
$\Delta_f H°$	Standard enthalpy of formation	kJ/mol
$\Delta_r H°$	Standard reaction enthalpy (r…chg, dcg)	kJ/mol
$\Delta_r h°$	Specific standard reaction enthalpy (r…chg, dcg)	kJ/kg
Δh_V	Condensation/evaporation enthalpy	kJ/kg
P	Power	kW
$\dot{Ex}$	Exergy flow	kW
X	Reaction conversion rate	-
t	Time	min
τ	Residence time	min
L	Length	m
n	Cycle count	-

II. Abbreviations

BA	Orthoboric acid (boric acid)
MB	Metaboric acid
oil	process oil: Fragoltherm Q-32-N (Fragol AG)
H_2O	process water (not necessarily pure water)

chg	Charge process
dcg	Discharge process
dehyd	Dehydration
rehyd	Rehydration
cond	Condensation
evap	Evaporation
rct	Reaction
pre	Preheating
id	Ideal
th	Thermal
sto	Stored/storage

Z	(heated) Conveyor screw
A	(additional) Preheater
R	Reactor (series)
L	Condenser
E	Steam generator, evaporator
H	Hydrocyclone
I	Intermediate filter unit
G	Sedimentation column
S	Combined separation series, H+I+G
C	Suspension concentrate storage
O	Process oil storage
W	Process water storage
V	Steam valve

s	Solid
l	Liquid
g	Gaseous
susp	Suspended/suspension

III.   Specific symbols

ω	Stoichiometric water content in boric acid	$\dfrac{M_{H_2O}}{M_{BA}} = 0.29$	$-$
ζ_j^i	Dimensionless mass flow	$\dfrac{\dot{m}_i}{\dot{m}_{CR}^{BA_{chg}}}$; $\quad \zeta_{CR}^{BA,chg} = 1$	$-$
ε_C	Storage void volume	$\left[\dfrac{V_{oil}}{V_{oil} + V_{BA+MB}} \right]_C$	$-$
ε_R	Reactor void volume	$\left[\dfrac{V_{(g)}}{V_{susp}} \right]_R$	$-$
γ_j	Suspension factor (oil to solids)	$\dfrac{\dot{m}_j^{oil}}{\dot{m}_j^{BA+MB}}$	$-$
υ_W	Overstoichiometric water addition	$\dfrac{\dot{m}_{ER,dcg}^{H_2O}}{\dot{m}_{X_{dcg}}^{H_2O}}$	$-$
υ'_W	Water addition factor from water storage	$\dfrac{\dot{m}_{WE,dcg}^{H_2O}}{\dot{m}_{X_{dcg}}^{H_2O}}$	$-$
X_{chg}	Conversion rate (charge process)	$1 - \left[\dfrac{\dot{m}_{in}^{BA}}{\dot{m}_{out}^{BA}} \right]_{R,chg}$	$-$
X_{dcg}	Conversion rate (discharge process)	$1 - \left[\dfrac{\dot{m}_{in}^{MB}}{\dot{m}_{out}^{MB}} \right]_{R,dcg}$	$-$
$r_V^{H_2O}$	Mean volumetric steam release rate (batch)	$\dfrac{\omega m_{CR}^{BA_{chg,batch,id}}}{V_{susp}^{batch} t_{release}^{end}}$	$\dfrac{kg_{H_2O}}{m^3 h}$
η_L	Condenser steam capture rate	$\dfrac{\dot{m}_{RL}^{H_2O_{chg}}}{\dot{m}_{rct}^{H_2O}}$	$-$
η_V	Steam valve steam capture rate	$\dfrac{\dot{m}_{RV}^{H_2O_{dcg}}}{\dot{m}_{ER}^{H_2O_{dcg}} - \dot{m}_{X_{dcg}}^{H_2O}}$	$-$

η_j	Oil separation unit (H, I, G) oil capture	$\dfrac{\dot{m}^{oil}_{j,extracted}}{\dot{m}^{oil}_{RS}}$	–
θ^i_L	Condenser inflow impurity ratio	$\dfrac{\dot{m}^{i}_{RL}}{\dot{m}^{H_2O}_{RL}}$	–
θ^i_V	Steam valve inflow impurity ratio	$\dfrac{\dot{m}^{i}_{RV}}{\dot{m}^{H_2O}_{RV}}$	–
θ^i_j	Oil separation unit (H, I, G) impurity ratio	$\dfrac{\dot{m}^{i}_{j,extracted}}{\dot{m}^{oil}_{j,extracted}}$	–
σ_O	Stored fraction of oil from sedimentation	$\dfrac{\dot{m}^{oil_{chg}}_{GO}}{\dot{m}^{oil_{chg}}_{GO} + \dot{m}^{oil_{chg}}_{GR}}$	–
σ_V	Stored fraction of water from steam valve	$\dfrac{\dot{m}^{H_2O_{dcg}}_{RW}}{\dot{m}^{H_2O_{dcg}}_{RV}}$	–

i… materials: BA, MB, H_2O, oil if not otherwise stated

j… process units

1 Introduction

1.1 Motivation

The role of energy in the civilised world is undisputed. Energy is power, and not only does the warfare in the Middle East and the Ukraine (to name just the most evident aggressions) brutally visualize the world power's craving for energy [1] and the global impact of economic sanctions in the energy sector [2], even the history of our tiny little country would have been written differently if the Soviet Union would not have resisted the Nazi invasion in 1941 [3]. Stabilizing the landscape of energy provision, providing a social and environmental code of ethics, could thus be seen as a peace mission.

There are legions of publications concerned with the development of the global energy sector, and although some scenarios predict a decline in global energy demand, the transition from fossil fuels to renewable sources requires major shifts in energy infrastructures [4].

Throughout the majority of industrial plants, large quantities of waste heat are released into the atmosphere, and the Waste Heat to Power Market is expected to grow [5]. Thermal energy storage (TES) is split into three main pathways: Sensible heat, latent heat (characterized by a phase change), and thermochemical heat storage, each holding its own set of possibilities [6]. Because of higher energy densities and lower heat losses, thermochemical energy storage (TCES) is a research favorite for seasonal and long-term storage among the possible TES methods [7].

1.2 Aim

The aim of this thesis is to consider the apparative and operational requirements for a laboratory-scale plant that enables continuous full-cycle experiments with the TCES system boric acid – metaboric acid – boron oxide, and its basic simulation. So far, experiments have been conducted in small batch reactors under different temperature and pressure profiles to better understand the reaction kinetics; Once these results represent a found empirical knowledge of the novel approach to TCES, i.e., the operation in a suspension of thermal oil, the plant will serve as a platform for observations on heat transfer, conversion, phase separation, convection through different conveying units, cyclic stability, dehydration/rehydration efficiency and byproduct generation. This thesis is limited to theoretical modelling of the basic process steps in the simplified reaction system boric acid - metaboric acid, calculating heat and mass flows as well as visualizing them with Sankey-Diagrams, and designing the experimental plant's basic concepts.

1.3 Methodology of thesis

After conducting a number of batch experiments and gathering practical knowledge about the processes, the first concept for a continuous plant was designed. With thermodynamic data from literature, the material and energy balances were elaborated for this plant under idealized conditions, i.e., complete and stoichiometric conversion both in dehydration and rehydration reactions ($X_{chg} = X_{dcg} = 1$), as well as complete separation scenarios for oil and water.

In a second phase, this "perfect" model was enhanced with non-ideal factors and some phenomena discussed in more detail; Incomplete conversion rates and deviations from ideal separation were introduced, and another set of equations was developed to characterize the emerging mass flows. First calculations for subsequent charge & discharge cycles were conducted, and numerical solutions for a series of eight runs were obtained through application of the equations in Microsoft Excel. That document was designed in a way that future research can utilize it and modify input parameters to fit the model to experimental findings.

Throughout this work, considerations about possibly occurring phenomena are documented, wherever they were of concern to the author.

For both main scenarios, ideal and non-ideal, some parameter variations are discussed, and Sankey-Diagrams were created with e!Sankey (iPoint-systems) to visualize the findings.

2 Theoretical background

2.1 Thermochemical energy storage

In principle, TCES processes can be split in four stages; First, the application of heat to the low-energy material, converting it to the high-energy material (charge process); Second, storage of the high-energy material (charged storage); Third, extraction of heat from the high-energy system, converting it to the low-energy material (discharge process); Fourth, storage of the low-energy material (discharged storage). Depending on reaction characteristics of the used materials, some systems theoretically allow an infinite number of cycles of these four stages; The investigated system boric acid – metaboric acid – boron oxide is among these favorable materials [8].

Ideally, reactions only occur in stages 1 and 3 (charge/discharge, respectively), as potential reactions during storage (stages 2 and 4) would lower cyclic process efficiency. Especially stage 2 represents the key benefit of TCES over other TES systems – the possibility to store chemical energy over prolonged periods, making it a high-potential candidate for seasonal energy storage (heat excess in summer versus heat demand in winter), or comparable long-term heat storage demands.

Chemical reaction systems that are theoretically applicable for TCES are numerous. Key parameters for practical usefulness are storage capacity, specific energy, process efficiency, storage stability over time, and material costs [9]. To limit the scope to materials with favorable properties, Deutsch et. al. [10] developed a search algorithm, highlighting the most promising TCES systems. Especially given its high energy density of up to 2.2 GJ/m³ [11], boric acid was selected for extensive research.

2.2 TCES suspension systems

Currently, fluidized bed reactors are seen as best practice for TCES operations, offering characteristic benefits over fixed bed reactors, for example improved heat and mass transfer and the possibility of continuous operation [12]. Nevertheless, operating the fluidized bed in gas, with intrinsically low viscosity, can lead to undesired agglomeration of the particles, eventually clogging the reactor – leading to reactor downtime for removal of the agglomerates [13]. Thus, a novel approach was developed by F. Winter (ICEBE): Using thermal oil as the suspension medium instead of gas. Since the birth of the idea, research on the behaviour of different materials in such reactor systems was undertaken on the institute. Major requirements for the chemically inert suspension oil, as described by Bürgmayr [14], are high thermal conductivity, low heat capacity, a high flame point, and degradation resistance. Other properties, mainly viscosity, are subject to optimization: On one hand, a higher viscosity than gas poses the initial advantage of the suspension reactor, providing favorable suspension characteristics with slow settling and lower impact energies of particle collisions. On the other hand, higher viscosities also mean slower

removal of the suspended steam formed in dehydration reactions. Generally speaking, the complexity of the processes with their simultaneous presence of solid, liquid, and gas phases requires thorough consideration and elaboration of practical solutions to the many operational challenges, and characterisations of the limiting steps and bottlenecks, of which steam removal was already found to be a crucial task [15].

2.3 Fundamentals: Dehydration and rehydration of boric acid in data

Throughout this thesis, it is assumed that boric acid H_3BO_3 (BA) will not be fully dehydrated to boron oxide, instead, the reaction is considered as complete when monoclinic metaboric acid HBO_2 (MB) is obtained from the incomplete dehydration of boric acid.

Metaboric acid itself is known in three configurations, each resulting of the reaction conditions in the stoichiometrically identical dehydration of boric acid; The following temperatures correspond to ambient pressure.

First, at 80-100°C, orthorhombic metaboric acid is formed, which is a molecular form similar to boric acid itself [16]. Upon further heating, at 130-140°C, a polymeric chain of monoclinic metaboric acid is formed (β-phase), raising both density and melting point [17]. Finally, at 140°C, cubic metaboric acid (γ-phase) is obtained by forming a three-dimensional, high-density tetrahedral network structure [18].

Table 1: Densities and melting points of ortho-/metaboric acid configurations [11, 16]

Property	Orthoboric acid	Metaboric acid: modification III orthorhombic (α)	Metaboric acid: modification II monoclinic (β)	Metaboric acid: modification I cubic (γ)
$\dfrac{\rho}{kg/m^3}$	1435	1789	2045	2487
$\dfrac{T_m}{°C}$	171	176	201	236

Theoretically, cubic $\gamma - HBO_2$ should be achieved at a reaction temperature of 150°C; Nevertheless, to stay on the side of caution by choosing a middle way, the monoclinic phase $\beta - HBO_2$, i.e., modification II, was selected as what is called metaboric acid throughout this work.

The base line for the developed processes are the dehydration and (re-)hydration reaction enthalpies as listed below:

Table 2: Reactions

Reaction		Enthalpy $\Delta_r h_{BA}°$
Dehydration of boric acid	$H_3BO_3^{(s)} \xrightarrow{+\Delta H} HBO_2^{(s)} + H_2O^{(g)}$	$941.3\frac{kJ}{kg_{BA}}$
Hydration of metaboric acid with steam	$HBO_2^{(s)} + H_2O^{(g)} \xrightarrow{-\Delta H} H_3BO_3^{(s)}$	$-941.3\frac{kJ}{kg_{BA}}$
Hydration of metaboric acid with liquid water	$HBO_2^{(s)} + H_2O^{(l)} \xrightarrow{-\Delta H} H_3BO_3^{(s)}$	$-229.7\frac{kJ}{kg_{BA}}$

Molar reaction enthalpies were calculated with standard formation enthalpies $\Delta_f H°$ from the CRC Handbook of chemistry and physics [11, 19] and further targeted at boric acid mass flows (as the educt in dehydration processes and the product in hydration processes). Note that the proposed temperature levels for the reactions differ from standard conditions; Hence, the calculated reaction enthalpies are to be understood as a rough estimate and should be reassessed in future work.

$$\Delta_r H°(dehydration) = \Delta_f H°_{HBO_2^{(s)}}\left(HBO_2^{(s)}\right) + \Delta_f H°(H_2O^{(g)}) - \Delta_f H°\left(H_3BO_3^{(s)}\right)$$

$$= -794.3\frac{kJ}{mol_{HBO_2^{(s)}}} - 241.8\frac{kJ}{mol_{H_2O^{(g)}}} + 1094.3\frac{kJ}{mol_{H_3BO_3^{(s)}}}$$

$$\boldsymbol{\Delta_r H°(dehydration) = 58.2\frac{kJ}{mol}}$$

Eq. 2.1

$$\Delta_r H°(rehydration, steam) = \Delta_f H°\left(H_3BO_3^{(s)}\right) - \Delta_f H°\left(HBO_2^{(s)}\right) - \Delta_f H°(H_2O^{(g)})$$

$$= -1094.3\frac{kJ}{mol_{H_3BO_3^{(s)}}} + 794.3\frac{kJ}{mol_{HBO_2^{(s)}}} + 241.8\frac{kJ}{mol_{H_2O^{(g)}}}$$

$$\boldsymbol{\Delta_r H°(rehydration, steam) = -58.2\frac{kJ}{mol}}$$

Eq. 2.2

$$\Delta_r H°(rehydration, liquid\ water) = \Delta_f H° \left(H_3BO_3^{(s)}\right) - \Delta_f H° \left(HBO_2^{(s)}\right) - \Delta_f H°(H_2O^{(l)})$$

$$= -1094.3 \frac{kJ}{mol_{H_3BO_3^{(s)}}} + 794.3 \frac{kJ}{mol_{HBO_2^{(s)}}} + 285.8 \frac{kJ}{mol_{H_2O^{(l)}}}$$

$$\boldsymbol{\Delta_r H°(rehydration, liquid\ water) = -14.2 \frac{kJ}{mol}}$$

<div align="right">Eq. 2.3</div>

With the molar mass of boric acid $M_{H_3BO_3} = 61.83 \frac{g}{mol}$ [19], specific standard reaction enthalpies are calculated from:

$$\Delta_r h_{BA}° = \frac{\Delta_r H°}{M_{H_3BO_3}}$$

<div align="right">Eq. 2.4</div>

$$\boldsymbol{\Delta_r h_{BA}°(dehydration) = \Delta_{chg} h_{BA}° = 941.3 \frac{kJ}{kg_{BA}}}$$

$$\boldsymbol{\Delta_r h_{BA}°(rehydration, steam) = \Delta_{dcg(g)} h_{BA}° = -941.3 \frac{kJ}{kg_{BA}}}$$

$$\boldsymbol{\Delta_r h_{BA}°(rehydration, liquid\ water) = \Delta_{dcg(l)} h_{BA}° = -229.7 \frac{kJ}{kg_{BA}}}$$

Heat capacities have been calculated as a function of temperature, with the Shomate equation for solid phase heat capacities, for absolute temperature $[T] = K$ and dimensionless parameters from Chase [19]:

$$\frac{c_p°(T)}{J/_{mol*K}} = A + B * \frac{T}{10^3 * K} + C * \left(\frac{T}{10^3 * K}\right)^2 + D * \left(\frac{T}{10^3 * K}\right)^3 + E * \left(\frac{T}{10^3 * K}\right)^{-2}$$

<div align="right">Eq. 2.5</div>

Table 3: Shomate parameters [19]

Compound	A	B	C	D	E	Range
Boric acid	40.82	195.23	-86.65	13.60	-0.92	298K-1500K
Metaboric acid	179.58	-477.66	719.88	-327.84	-3.38	298K-900K

Applying these parameters to the Shomate equation Eq. 2.5 yields the heat capacities of boric acid and metaboric acid at the temperature range of the processes. Heat capacities and densities for the selected process oil, namely FRAGOLTHERM® Q-32-N, were provided upon request by the manufacturer Fragol AG [20]. While the density of the process oil was used as a function of temperature, densities for boric acid and metaboric acid were considered as constant throughout the processes.

Table 4: Temperature dependent material parameters [19, 20]

$\dfrac{T}{°C}$	$\dfrac{c_p^{BA}(T)}{kJ/_{kg * K}}$	$\dfrac{c_p^{MB}(T)}{kJ/_{kg * K}}$	$\dfrac{c_p^{oil}(T)}{kJ/_{kg * K}}$	$\dfrac{\rho_{oil}(T)}{kg/_{m^3}}$
20	1.30	1.20	1.97	871
30	1.33	1.23	2.01	865
40	1.37	1.25	2.05	858
50	1.40	1.27	2.08	853
60	1.43	1.29	2.12	845
70	1.46	1.31	2.16	840
80	1.49	1.32	2.19	833
90	1.52	1.33	2.22	826
100	1.55	1.35	2.26	820
110	1.58	1.36	2.29	815
120	1.60	1.37	2.32	809
130	1.63	1.38	2.36	802
140	2.39	1.65	1.39	795
150	2.43	1.68	1.40	788
160	2.46	1.70	1.41	781

3 The experimental concept

3.1 The experimental process plant in pictures

To give a graphic overview on the developed concept for the process plant, it is introduced at this point, followed by explanations in 3.2, before diving into the calculations. Simplified block schemes were elaborated as well, to aid the understanding of the processes. Microsoft Visio Professional was used as software for the visualisation of the processes.

Black arrows stand for key material flows, i.e., process oil, boric acid or metaboric acid alongside process oil, and water (in RL and LW). Grey arrows are used for instrumentation information and auxiliary flows. Red and blue arrows show thermal oil flows for heating and heat extracting tasks, respectively. The process units are symbolized with a specific letter, and flows between the units are named after the source unit as the first letter and the target unit as the second letter. For some flows, material composition is considered as unchanged, allowing the same nomenclature. The letter S stands for the sum of the oil extraction series, consisting of the three units H, I, and G; For example, the flow RS equals RH, and the sum of recycled oil, consisting of HR, IR and GR is called SR. Key process parameters are stated where they apply.

Cooling and heating was not further specified except than assuming that water will be used for cooling operations, given its high heat capacity and ease of handling (with sufficient flow rates to prevent boiling), and thermal oil for heating purposes. Energy application is controlled by the flow rates and actual energy transport is measured from the rise or drop of temperature under a known flow rate.

Safe operation should provide emergency valves, for cases of problematic pressure increases. The positioning of these valves might be optimized; In the presented concept, they serve more as a reminder that they should be implemented in the plant.
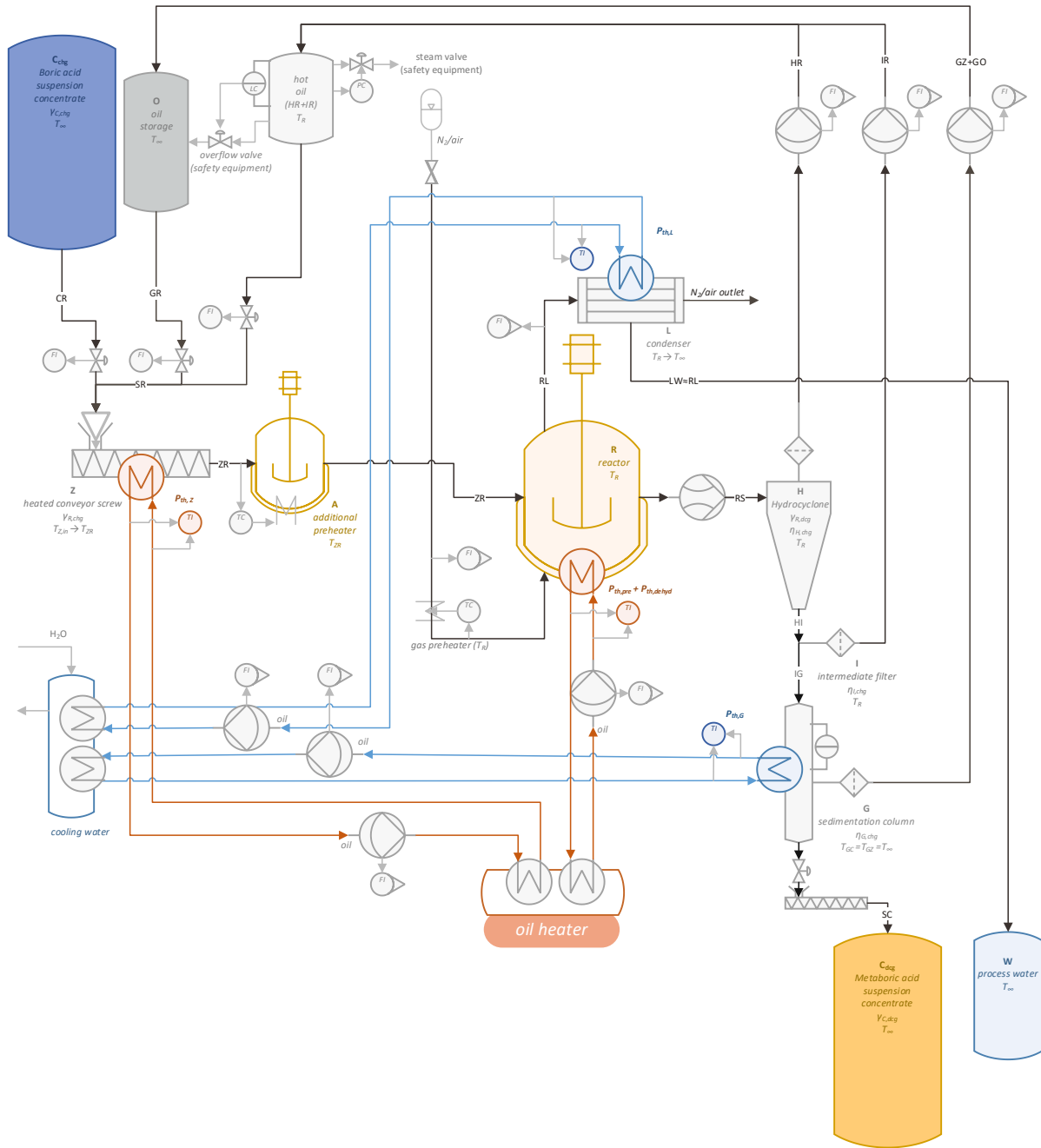
Figure 1: Charge process diagram

experimental concept:
heat discharge mode (with steam)
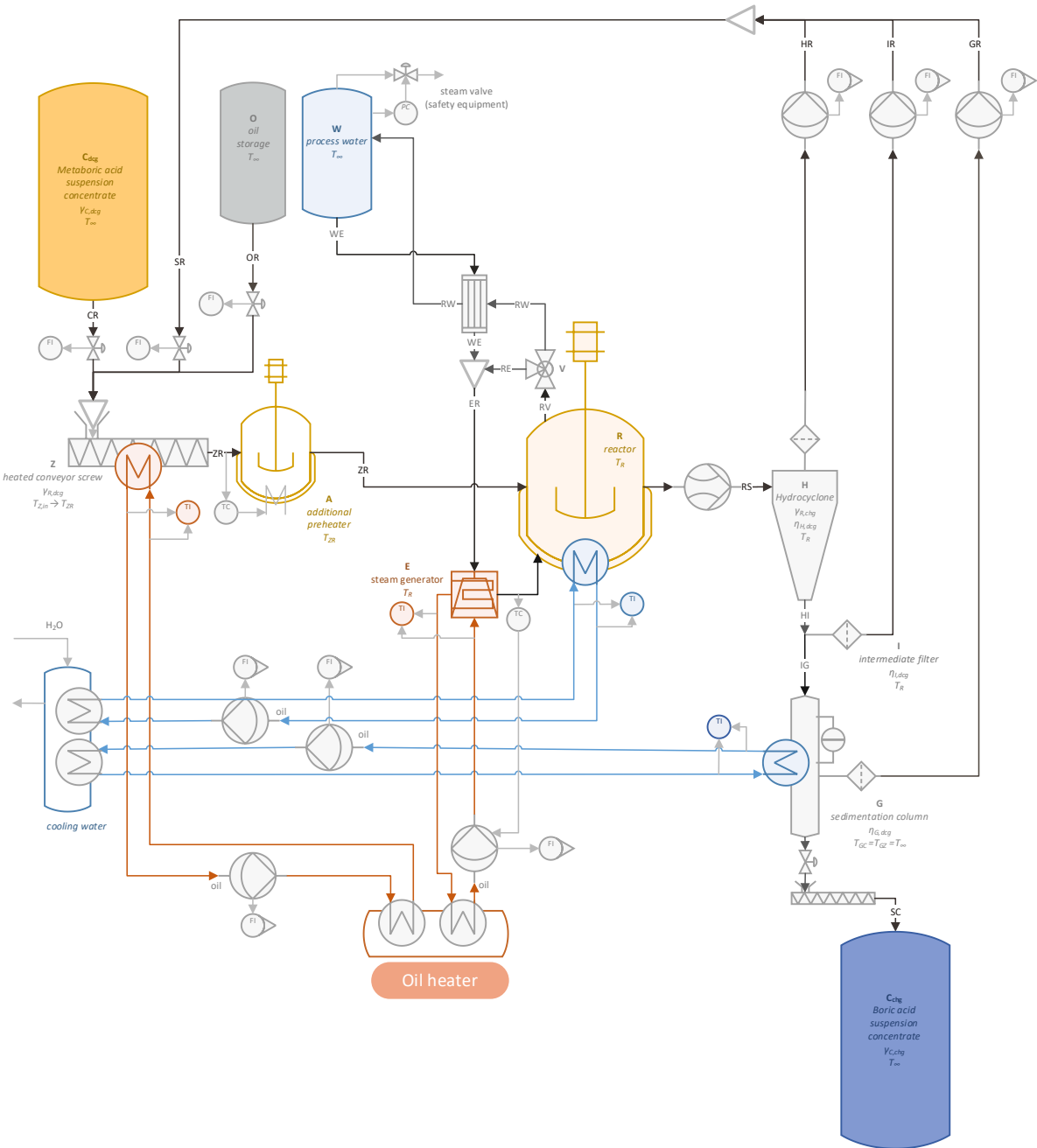
Figure 2: Steam discharge process diagram

While rehydrating with steam is suggested in this thesis, rehydrating with liquid water was considered as an option. This alters above scheme as follows:

experimental concept:
heat discharge mode (with liquid water)
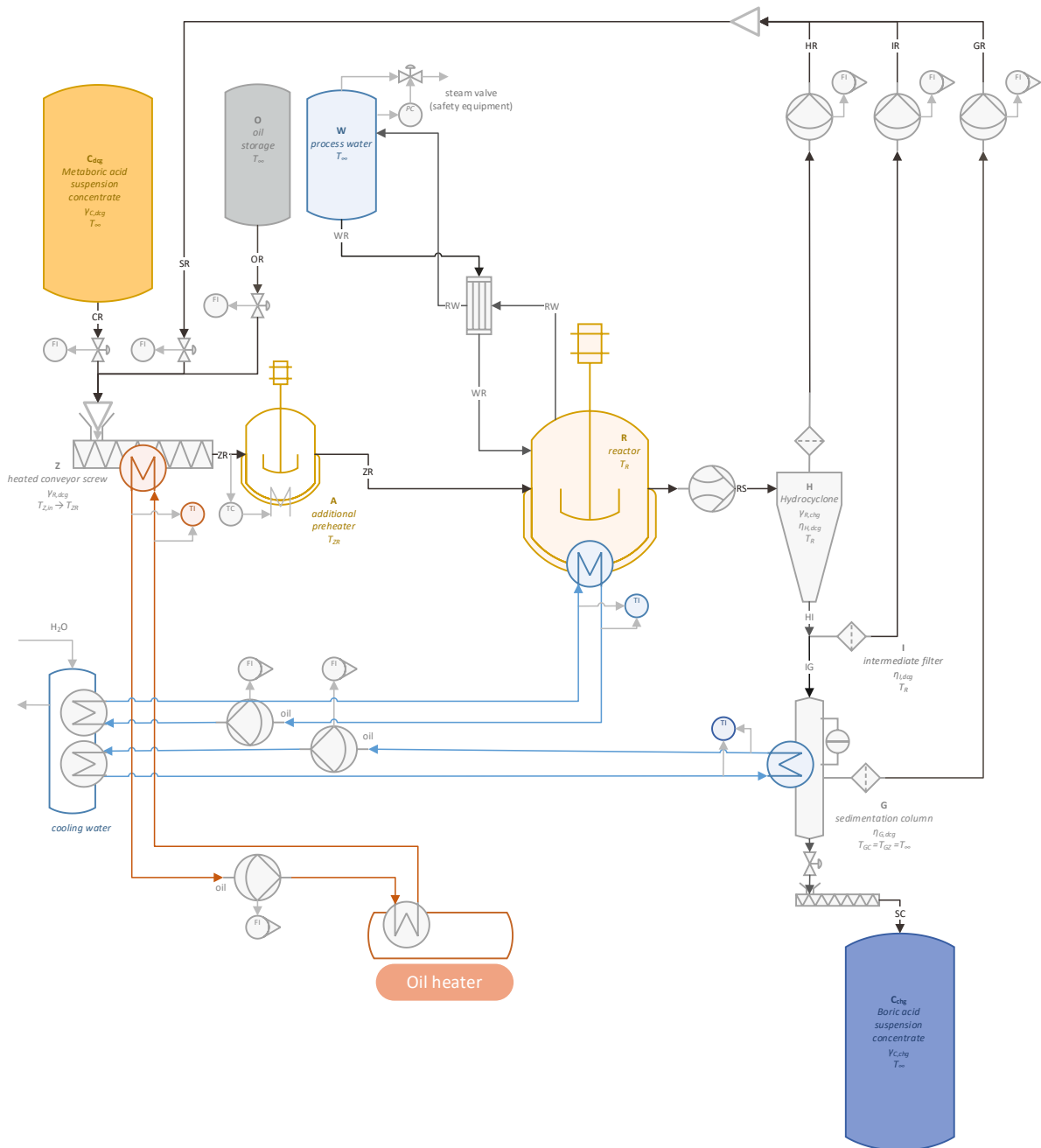
Figure 3: Liquid water discharge process diagram

Simplified block charts were created, for a more intuitive understanding. The conveyor unit Z is no longer shown here to keep the focus on the reactor and oil separation series.

Note that in Figure 5, the oil storage partly lies outside of the separation summary S_{chg}; this is to show that GO is stored while GR is directly recycled and only passes the oil storage tank.

Figure 6 is meant to differentiate internal material flows from material flows entering or leaving the process.

Figure 4: Charge block scheme

Figure 5: Charge oil separation
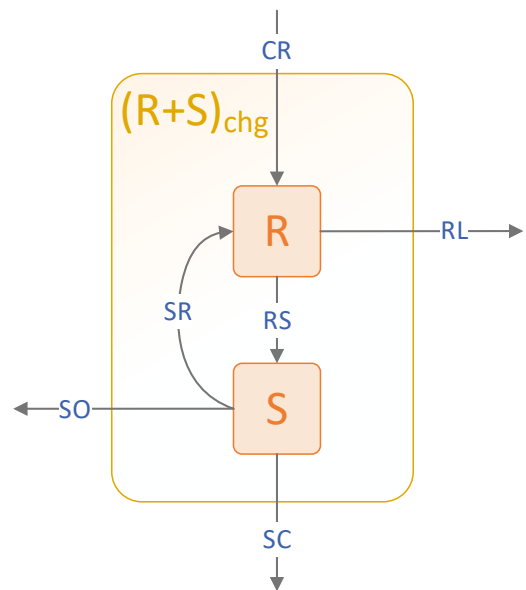
Figure 6: Charge reactor and separation series

The discharge process with steam is shown in the following three figures:

Figure 7: Steam discharge block scheme

Figure 8: Discharge oil separation
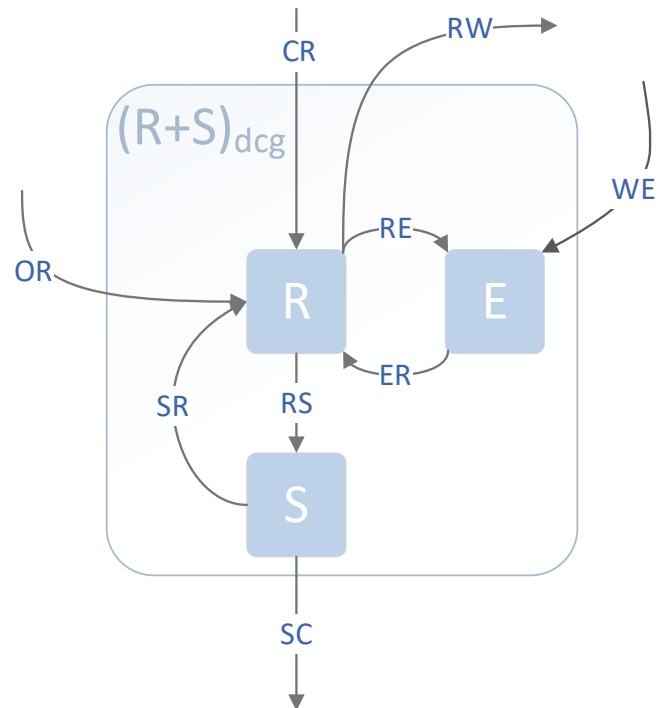
Figure 9: Steam discharge reactor and separation series

For the variant of liquid rehydration, the block schemes involving the reactor are the following (the oil separation series remains unchanged):
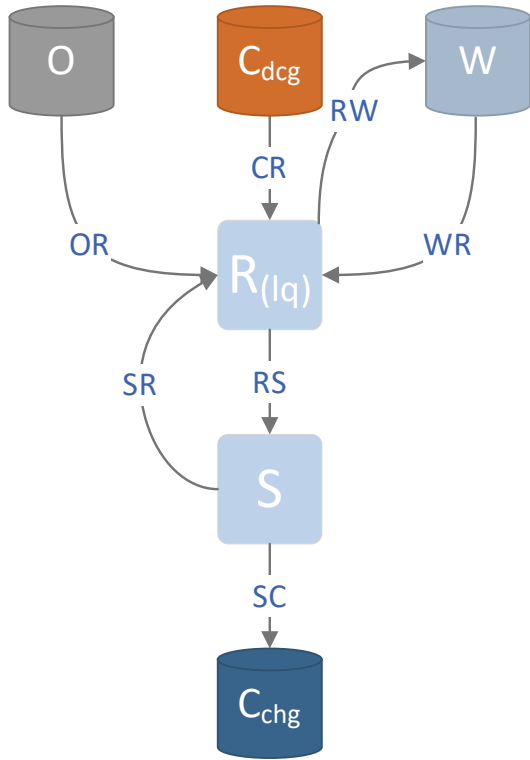
Figure 10: Liquid water discharge block scheme
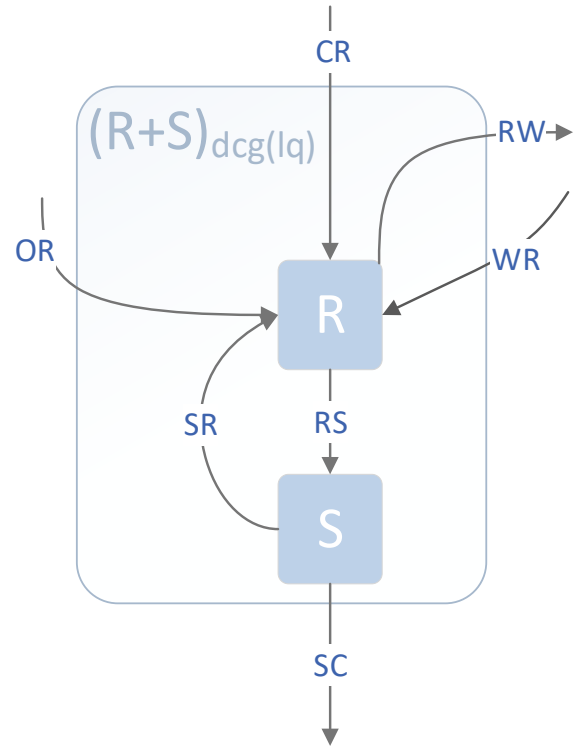
Figure 11: Liquid water discharge reactor and separation series

3.2 The experimental process plant in words

3.2.1 Input flows from tanks

The materials for each process are taken from storage tanks, which cycle between the charge and discharge processes. For the relations between these, check the section on output flows below (3.2.11).

Due to higher density and viscosity, packing densities of suspended particles are expected to be lower than "dry" packing densities of the particles in air, with reasonable settling times. Nevertheless, estimates for packing densities in the tanks are similar to what could be expected from "dry" packing densities, as unnecessary void volume in the storage concentrates needs to be avoided. This may require additional efforts to extract oil and to effectively shorten settling times.

3.2.2 Additional recycled oil

Given that the desired amount of oil in the storage concentrates is substantially lower than a reasonable amount for the process, an internal cycle of process oil was designed, providing a thinner suspension that is easier to stir and turbulent enough for good heat transport, while being thick enough to allow faster removal of suspended steam bubbles by shorter travelling distance to the oil surface. Cycling oil is added to the conveyor screw feeding the reactor, and extracted and recycled after leaving the reactor. The quantity of oil in the reactor, consisting of the oil in the concentrate and the recycled oil, is defined by the input parameter γ_R. The contributions to the flow of recycling oil will be discussed in chapters 4.1.1 and 4.2.1, in the sections about oil handling.

It was assumed that more oil can be extracted after the charge process than after the discharge process, giving reason to an oil storage from which the difference of extracted oil is used in the discharge process. This assumption is discussed in detail in 4.3.6.

3.2.3 Conveyor & preheating

The conveyor screw could be used to preheat the ready mixture, besides mixing and conveying it. Depending on the amounts of water in the suspension and the behaviour of steam in the unit and subsequent piping, its target temperature should not exceed the boiling point of water if considerable steam formation causes problems. The required power is lowered by the hot cycling oil from the Hydrocyclone and the intermediate filter. For the case that it cannot reach the target temperature, a heated stirred tank can do the rest (or all) of the preheating. After that, the suspension is fed into the reactor.

It was expected that, while mixing and preheating the concentrates with additional oil, no reactions and/or changes from the input flow states will occur, other than the desired increase in temperature.

3.2.4 Reactor

As this thesis is more concerned about the peripheral units and processes, what is called "reactor" here should be understood as a reactor system, likely consisting of a series of continuously stirred tank reactors. In the further explanations, however, it is referred to as "reactor".

The temperature dependability of formation enthalpies was neglected in this thesis, using standard formation enthalpies to give a rough estimate on energy flows. Future work needs to be done to obtain more precise energy balances.

3.2.5 Charge reactor

At the proposed reaction temperature of 150°C, boric acid dehydrates to metaboric acid under the release of steam:

$$H_3BO_3^{(s)} \xrightarrow{+\Delta H} HBO_2^{(s)} + H_2O^{(g)}$$

The released water vapor leaves the suspension, aided by a heated purge flow of N_2 and/or air (to inhibit recondensation), and is condensed after leaving the reactor at the top outlet for the gaseous phase. The dry gas is released into the atmosphere and the water is collected in a tank that will be used for rehydration in the discharge step. The remaining suspension, consisting of $HBO_2^{(s)}$ and process oil, passes to the series of oil separation units.

For the calculations carried out in 4.2.1.5, where the idealized reactor is described in a more precise way, an ideal plug flow reactor was proposed as a model, in which the formed steam bubbles instantly leave the suspension. Along the first part of the reactor length, the mixture from the conveyor screw is heated to the reaction temperature; After that, the actual reaction zone follows, where the necessary heat for the reaction is evenly applied, providing a steady steam flow out of the suspension. For the idealized calculations, it is assumed that at the exact time of complete conversion and steam removal, the infinitely small sectional volumes containing a mixture of oil and pure metaboric acid leave the reactor. In the considerations on incomplete conversion rates, no specific attention was given to the reactor concept, and a constant conversion rate was proposed across subsequent cycles.

3.2.6 Discharge reactor

If not otherwise stated, the discharge mode refers to a rehydration with steam, overheated to reaction temperature. Rehydrating with liquid water is explicitly stated as such in some comparisons.

The mixture of oil and metaboric acid enters the reactor, as well as a corresponding stream of water vapor (or liquid water) taken from the water storage tank, so that the metaboric acid is rehydrated to

boric acid under the release of reaction heat:

$$HBO_2^{(s)} + H_2O^{(g/l)} \xrightarrow{-\Delta H} H_3BO_3^{(s)}$$
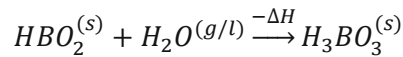
As the dicharge reactor already receives its inflows ZR and ER at reaction temperature, the reaction occurs from $t = 0$ and the residence time τ_R^{dcg} describes the necessary time for rehydration, which is subject to experimental results and further models describing the transport from injected steam bubbles to particles of metaboric acid. In this thesis, a preliminary value for τ_R^{dcg} is guessed in the numerical solution.

Under idealized conditions, the reactor's suspension output flow contains the exact same amount of boric acid that was fed into the prior charge step, and all the water that was collected in the charge step was fully bound by the metaboric acid in the discharge step.

3.2.7 Water condensation and evaporation

Water, as the reaction partner for the rehydration of metaboric acid, and the way it is handled to do so, is of utter importance for the process and must not be underestimated. Its thermophysical properties and the fact that it will be present both in liquid and gaseous state with their distinct set of properties need to be considered thoroughly, especially for the discharge process.

A more in-depth discussion will be held in chapter 4.4.3.

3.2.8 Condenser (charge process)

With water removal as the crucial task in the charge process, the condenser is a unit of special importance, especially considering energy efficiency; About 70% of the necessary energy to remove a molecule of water from a molecule of boric acid are released in the condensation of the water molecule, as shown in 4.1.2.5. Therefore, it is very important to catch as much steam as possible in the condenser and inhibit condensation and backflows within the reactor.

In terms of energy efficiency, it is vital to utilize the heat that can be extracted from the condenser, and a mechanical vapor recompression should be considered, so that the condensation can be performed at reaction temperature to recycle the condensation heat directly to the reactor. This should be understood as a plea for future research. In this thesis, however, the calculations are based on ambient pressure levels.

The condensed water is then stored in the process water tank, which is used as the water source for the discharge process.

3.2.9 Evaporator (discharge process; optional)

As the suggested option, the water for rehydration can be evaporated (and heated to reaction temperature) before injecting it into the suspension volume. This comes with a higher apparative effort, but "outsources" the large evaporation heat intake of the water, which marks the difference between the reaction enthalpies of rehydration with liquid water and steam. It is up to the actual requirements, which route is chosen; In this thesis, steam rehydration was selected as the main option, and a rehydration with liquid water as a variation of the process.

3.2.10 Oil separation series

To recycle the process oil, which is added to the suspension concentrate to facilitate the processes, three units have been considered: A Hydrocyclone, followed by a common tubular membrane filter, and finally a sedimentation column, from which heat can be extracted before releasing the thickened suspension to the storage tank.

3.2.11 Output flows to tanks

The suspension concentrate output flows of the charge process equal the suspension concentrate input flows of the subsequent discharge process and the suspension concentrate output flows of the discharge process equal the suspension concentrate input flows of the following cycle's charge process, plus/minus the changes in composition due to prolonged storage. In the idealized scenario, each cycle equals the other, and because of the pure concentrate outputs (exclusively BA or MB in oil), no changes in composition will occur.

The oil that is assumed to be liberated in the charge process is stored and added again in the discharge process, closing the cycle.

Condensed water from the charge mode is stored and used in the following discharge mode. In the ideal scenario, the charge output flow of water equals the discharge input flow, while in the non-ideal scenario, a loop for overstoichiometric water addition was suggested.

4 Results

Results are split in five sections. Chapters 4.1 and 4.2 describe the idealized charge und discharge processes, respectively, in terms of mass and energy. Chapters 4.3 and 4.4 introduce some non-ideal parameters and investigate their effects on material compositions, and corresponding considerations for the reactor systems are undertaken, to present a numerical example in chapter 4.5.

In principle, the chapters on ideal and non-ideal conditions in this thesis can be read separately; The former, to give a quick introduction into the basic concepts of the proposed experimental plant in this novel approach to TCES as well as some considerations on the reactor; the latter for those who already had a foot (or two) in the field and are using this thesis as a reference on material balances for their own research.

When discussing the process units, not all equations on material flows are commented on all occasions, to reduce reading dead time. If unsure, please read the whole section on the process unit, or the thesis itself.

4.1 Quantifying the ideal charge process

As a first step, boric acid educt flow is set by the reaction enthalpy from Eq. 2.4, which further dictates the required oil addition after choosing the reaction enthalpy output power. After characterizing the mixed flow, consisting of inputs from storage tanks and recycled oil, the necessary heating power for preheating is calculated. Assuming full conversion in the reactor, as well as full extraction of formed water vapor, the resulting mixture of metaboric acid and oil enters the separation series. These three units are also idealized in terms of separation, assuming that only pure oil is extracted, and the metaboric acid entirely passes to the storage tank. After guessing values for the share of extracted oil for the first two units, the third, i.e., the sedimentation column, makes for the difference between priorly extracted oil and stored oil alongside metaboric acid. This share is split up into a recycled flow and a flow to the oil storage tank. Necessary heating input and extractable heat outputs are calculated where applicable, assuming zero losses. In the section concerning the reactor, an orientation value for the reactor volume was estimated, based on the residence time, which consists of a preheating phase and a phase of water vapor extraction.

4.1.1 Developing a framework of equations

4.1.1.1 *Setting the educt flow*

The defining parameter for all mass flows throughout the charging process is the design power input, which dictates the required input mass flow from the concentrate tank C. With $X_{chg,id} = 1$, we obtain:

$$\dot{m}_{CR}^{BA_{chg,id}} = \frac{P_{th,dehyd}^{chg,id}}{\Delta_{chg} h_{BA}{}^{\circ}}$$

Eq. 4.1

4.1.1.2 *Quantifying the oil cycle*

An important set of process variables, γ_j, describes the mass ratio of oil to solids from concentrate in different parts of the process plant. In the charge input concentrate for pure boric acid ($\dot{m}_{CR}^{BA+MB_{chg,id}} = \dot{m}_{CR}^{BA_{chg,id}}$), it can be simplified as:

$$\gamma_C^{chg,id} = \frac{\dot{m}_{CR}^{oil_{chg,id}}}{\dot{m}_{CR}^{BA_{chg,id}}} = \frac{\varepsilon_C^{chg,id} \rho_{oil}}{\left(1 - \varepsilon_C^{chg,id}\right) \rho_{BA}}$$

Eq. 4.2

Herein, $\varepsilon_C^{chg,id}$ presents the void volume, i.e., the oil volume in the particle-containing height, relative to the total volume of the two-phase mix, after complete settling of the suspended particles, and exclusion of the single-phase oil; In that sense, $V_{susp.oil}$ only accounts for the oil suspending the particles, and the excess of oil that floats atop the suspension and does not suspend any particles is not included in V_{susp} anymore:

$$\varepsilon_C^{chg,id} = \lim_{t \to \infty} \frac{V_{susp.oil}(t)}{V_{susp}(t)} = \lim_{t \to \infty} \frac{V_{oil}(t)}{V_{susp.oil}(t) + V_{BA}}$$

$$\varepsilon_C^{chg,id} = \lim_{t \to \infty} \left[\frac{1}{1 + \frac{V_{BA}}{V_{susp.oil}(t)}} \right]_{C,chg,id}$$

Eq. 4.3

For enhanced handling in the reactor, $\gamma_C^{chg,id}$ is then increased to:

$$\gamma_R^{chg,id} = \frac{\dot{m}_{R_{in}}^{oil_{chg,id}}}{\dot{m}_{CR}^{BA_{chg,id}}} = \frac{\dot{m}_{CR}^{oil_{chg,id}} + \dot{m}_{SR}^{oil_{chg,id}}}{\dot{m}_{CR}^{BA_{chg,id}}}$$

Eq. 4.4

From which $\dot{m}_{SR}^{oil_{chg,id}}$ is set, according to the desired $\gamma_R^{chg,id}$.

To understand the distribution of oil flows after the reactor better, see chapter 4.1.1.6 below.

4.1.1.3 Mixing and Preheating

To reduce the required residence time in the reactor, the ready mixture ZR needs to be preheated. Describing the corresponding required power input requires knowledge about the temperatures of the recycled oil streams. In this simplified scenario, it was assumed that the oil flows $\dot{m}_{HR}^{oil_{chg,id}}$ and $\dot{m}_{IR}^{oil_{chg,id}}$ do not decrease in temperature and enter the heated conveyor screw Z at reaction temperature $T_R^{chg,id}$. On the other hand, it was assumed that heat is extracted from the sedimentation tank G until it reaches ambient temperature T_∞, at which both the oil flows $\dot{m}_{GR}^{oil_{chg,id}}$ and $\dot{m}_{GO}^{oil_{chg,id}}$ and the concentrate are released. The temperature of the mixed oil $T_{SR}^{chg,id}$ can then be calculated using the dimensionless separation ratios $\eta_j^{chg,id}$ as:

$$T_{SR}^{chg,id} = T_\infty + \frac{\eta_H^{chg,id} + \eta_I^{chg,id}}{\eta_H^{chg,id} + \eta_I^{chg,id} + (1 - \sigma_O)\eta_G^{chg,id}}\left(T_R^{chg,id} - T_\infty\right)$$

<div align="right">Eq. 4.5</div>

Mixing the flows $SR + CR = ZR$, where $T_{CR}^{chg,id} = T_\infty$, yields yet another (theoretical) temperature $T_{Z_{in}}^{chg,id}$ (as if the flows reached thermal equilibrium at the intake of the conveyor screw, Z_{in}, before being heated to $T_{ZR}^{chg,id}$). For a simplified first estimate, heat capacities were chosen iteratively from a certain temperature close to $T_{Z_{in}}^{chg,id}$:

$$T_{SR}^{chg,id} c_p^{oil,T_{SR}} \dot{m}_{SR}^{oil_{chg,id}} + T_\infty\left(c_p^{oil,T_\infty} \dot{m}_{CR}^{oil_{chg,id}} + c_p^{BA,T_\infty} \dot{m}_{CR}^{BA_{chg,id}}\right)$$
$$= T_{Z_{in}}^{chg,id}\left(c_p^{oil,T_{Z_{in}}} \dot{m}_{ZR}^{oil_{chg,id}} + c_p^{BA,T_{Z_{in}}} \dot{m}_{ZR}^{BA_{chg,id}}\right)$$
$$T_{Z_{in}}^{chg,id} = \frac{T_{SR}^{chg,id} c_p^{oil,T_{SR}} \dot{m}_{SR}^{oil_{chg,id}} + T_\infty\left(c_p^{oil,T_\infty} \dot{m}_{CR}^{oil_{chg,id}} + c_p^{BA,T_\infty} \dot{m}_{CR}^{BA_{chg,id}}\right)}{c_p^{oil,T_{Z_{in}}}\left(\dot{m}_{SR}^{oil_{chg,id}} + \dot{m}_{CR}^{oil_{chg,id}}\right) + c_p^{BA,T_{Z_{in}}} \dot{m}_{CR}^{BA_{chg,id}}}$$

<div align="right">Eq. 4.6</div>

At this point, it should be noted that $\dot{m}_{ZR}^{oil_{chg,id}} = \dot{m}_{SR}^{oil_{chg,id}} + \dot{m}_{CR}^{oil_{chg,id}} = \dot{m}_{R_{in}}^{oil_{chg,id}} = \dot{m}_{R_{out}}^{oil_{chg,id}}$ and $T_{ZR}^{chg,id} = T_{R_{in}}^{chg,id}$.

For the temperature rise in the heated conveyor screw Z, a mean heat capacity $c_p^{i,\bar{T}_Z^{chg,id}}$ was implemented, to obtain the required heating power:

$$P_{th,Z}^{chg,id} = \left(T_{ZR}^{chg,id} - T_{Z_{in}}^{chg,id}\right)\left(c_p^{oil,\bar{T}_Z^{chg,id}} \dot{m}_{R_{in}}^{oil_{chg,id}} + c_p^{BA,\bar{T}_Z^{chg,id}} \dot{m}_{CR}^{BA_{chg,id}}\right)$$

<div align="right">Eq. 4.7</div>

$$\bar{T}_Z^{chg,id} = \frac{T_{ZR}^{chg,id} + T_{Z_{in}}^{chg,id}}{2}$$

<div align="right">Eq. 4.8</div>

4.1.1.4 Reactor

The following considerations are based on the concept of an ideal plug flow reactor, i.e., the suspension does not mix in its flow direction, and leaves the reactor after full conversion and removal of the released water. Obviously, this does not represent any real scenario, but proves to be helpful in understanding the concept of the process. It is further assumed that the reaction suspension is gradually heated to the reaction temperature $T_R^{chg,id}$ across the first part of the reactor length L_{pre}; Assuming a constant sectional velocity $u_R = \frac{\dot{V}_R}{A_R} = const.$, and constant heat application along the reactor length $P(x) = const.$:

$$\frac{P_{th,pre}^{chg,id}}{L_{pre}} = \frac{P_{th,dehyd}^{chg,id}}{L_{dehyd}} \ \Rightarrow \ \frac{P_{th,pre}^{chg,id}}{t_{pre}} = \frac{P_{th,dehyd}^{chg,id}}{t_{dehyd}}$$

Eq. 4.9

While $P_{th,dehyd}^{chg,id}$ was selected as a free variable (that dictates the mass flow of boric acid), $P_{th,pre}^{chg,id}$ is calculated from:

$$P_{th,pre}^{chg,id} = \left(T_R^{chg,id} - T_{ZR}^{chg,id}\right)\left(c_p^{oil,\bar{T}_R^{chg,id}} \dot{m}_{ZR}^{oil_{chg,id}} + c_p^{BA,\bar{T}_R^{chg,id}} \dot{m}_{CR}^{BA_{chg,id}}\right)$$

Eq. 4.10

Where mean heat capacities $c_p^{i,\bar{T}_R^{chg,id}}$ have been used (as in the heated conveyor screw):

$$\bar{T}_R^{chg,id} = \frac{T_R^{chg,id} + T_{ZR}^{chg,id}}{2}$$

Eq. 4.11

Total residence time is thus composed of the explained contribution of the preheating task, and the actual time needed to dehydrate the suspension, which consists of the two tasks dehydration of boric acid and extraction of steam out of the suspension:

$$\tau_R^{chg,id} = t_{pre} + t_{dehyd}$$

Eq. 4.12

$$t_{dehyd} = t_{reaction} + t_{extraction}$$

Eq. 4.13

To solve the equation for residence times, a simplified model was developed in this thesis; data from a batch experiment was used to estimate a rate of steam removal per suspension volume $\left[r_V^{H_2O}\right] = \frac{kg_{H_2O}}{min*m_{susp.}^3}$, together with estimated dimensions of the experimental reactor, which means the numerical value (as shown later) is but a mere orientation value, but the formula can be used for future experiments, with recorded times for complete steam removal. It should be noted that this formula presents a linear release of steam, which may not adequately fit, but serves as a first estimate.

$$r_V^{H_2O} = \frac{m_{RL}^{H_2O_{chg,batch}}}{V_{susp}^{batch} t_{release}^{end}} = \frac{\omega m_{CR}^{BA_{chg,batch,id}}}{V_{susp}^{batch} t_{release}^{end}}$$

Eq. 4.14

The variable ω signifies the water content of boric acid, and as a simplified estimate, only represents the amount of chemically bound water in boric acid:

$$\omega = \frac{M_{H2O}}{M_{BA}} = 0.29$$

<div align="right">Eq. 4.15</div>

With a known $r_V^{H_2O}$, the required residence time for the reaction and steam removal can be calculated from a known suspension volume:

$$t_{dehyd} = \frac{\omega \dot{m}_{CR}^{BA_{chg,id}}}{r_V^{H_2O} \dot{V}_{R,susp}}$$

<div align="right">Eq. 4.16</div>

$$\dot{V}_{R,susp}^{chg,id} = \frac{\dot{m}_{CR}^{BA_{chg,id}}}{\rho_{BA}} + \frac{\dot{m}_{ZR}^{oil_{chg,id}}}{\rho_{oil}^{T_R^{chg,id}}}$$

Herein, $\dot{V}_{R,susp}^{chg,id}$ consists only of the inflows of solid boric acid and liquid oil, which means that a (possibly substantial!) volume increase of the suspension through the formation of (suspended) steam bubbles in a comparatively short time span, as suggested in prior work [15], was not considered and is not depicted in this formula. Applying the findings of Vitiello [15] to the model of the plug flow reactor, the sudden steam release could potentially render the plant useless and pose a safety issue, if not designed accordingly. Further experiments, linking the rate of steam generation into an observed batch suspension volume with a correction term for simultaneously measured emerging steam, are suggested at this point. Understanding the kinetics of steam generation and extraction is vital for more precise reactor design.

Idealizing the comparatively instant reaction followed by a slow steam release in a plug flow reactor, the necessary reaction enthalpy $P_{th,dehyd}^{chg,id}$ is transferred in an infinitely small section where the reaction occurs, and the remaining, unheated and isothermal length of the reactor constantly releases the formed steam, either through a membrane wall or an open surface between the suspension volume (consisting of the three phases oil, suspended gas bubbles, and suspended solids) and the gas volume above. Considering the expanded suspension volume, it may be best to imagine a corresponding sectional expansion of the reactor after the reaction has occurred, which is then gradually decreasing again, according to the release of steam, so that the sectional velocity of the reactor remains constant.

Contrary to that concept, in this thesis, it is imagined that from the point of reaching $T_R^{chg,id}$, from which the remaining reactor length L_{dehyd} is considered isothermal, boric acid is gradually dehydrated through application of $P_{th,dehyd}^{chg,id}$ along L_{dehyd}, and the generated steam instantly leaves the suspension, so that

it does not increase its volume. Also, in the preheating section before, a thermal expansion corresponding to $T_R^{chg,id} - T_{ZR}^{chg,id}$ is neglected.

Assuming full conversion, released water as already used above and formed metaboric acid are:

$$\dot{m}_{released}^{H_2O chg,id} = \omega \dot{m}_{CR}^{BA chg,id} = \dot{m}_{RL}^{H_2O chg,id}$$

Eq. 4.17

$$\dot{m}_{formed}^{MB chg,id} = (1-\omega)\dot{m}_{CR}^{BA chg,id} = \dot{m}_{RS}^{MB chg,id} = \dot{m}_{SC}^{MB chg,id}$$

Eq. 4.18

Note that $[\omega] = \frac{kg_{H_2O}}{kg_{BA}}$ and $[1-\omega] = \frac{kg_{MB}}{kg_{BA}}$, and the terms containing these factors address other materials than what is indicated by the material index in the equation. In above equations, $\omega \dot{m}_{CR}^{BA chg,id}$ represents a water flow and $(1-\omega)\dot{m}_{CR}^{BA chg,id}$ a metaboric acid flow.

The (theoretically) stored energy output rate can be quantified as:

$$P_{sto} = \Delta_{dcg(g)}h_{BA}° \frac{1}{1-\omega} \dot{m}_{SC}^{MB chg,id}$$

Eq. 4.19

As the third variant of the terms addressing other materials than the mentioned mass flow, $\left[\frac{1}{1-\omega}\right] = \frac{kg_{BA}}{kg_{MB}}$ does not address water itself, but the mass flow of boric acid (as product of the rehydration reaction) relative to metaboric acid (as educt of the rehydration reaction).

The reactor volume was estimated as

$$V_R^{chg,id} = (1 + \varepsilon_R)\dot{V}_{R,susp}^{chg,id}\tau_R^{chg,id}$$

Eq. 4.20

To add a safety margin volume for foam development, ε_R was implemented as a dimensionless factor representing the added void volume.

4.1.1.5   Condenser

The released steam from dehydration enters the condenser at $T_R^{chg,id}$, from which it is cooled, condensed, and further cooled to ambient temperature T_∞.

The total condenser heat is composed of three shares:

$$P_{th,L}^{chg,id} = P_{th,T_R \to T_{cond.}}^{chg,id} + P_{th,cond.}^{chg,id} + P_{th,T_{cond.} \to T_\infty}^{chg,id}$$

Eq. 4.21

$$P_{th,L}^{chg,id} = \dot{m}_{RL}^{H_2O chg,id} \left(c_p^{H_2O,\bar{T}_{steam}^{chg,id}} (T_R^{chg,id} - T_{cond.}) + \Delta h_V^{H_2O,100°C} + c_p^{H_2O,\bar{T}_{liquid}^{chg,id}} (T_{cond.} - T_\infty) \right)$$

Eq. 4.22

Where mean heat capacities are based on $\bar{T}_{steam}^{chg,id} = \frac{T_R^{chg,id} + T_{cond.}}{2}$ and $\bar{T}_{liquid}^{chg,id} = \frac{T_{cond.} + T_\infty}{2}$.

4.1.1.6 Oil separation series

The following units represent the means of extraction of oil from the thinner reaction suspension RS at $\gamma_R^{chg,id}$ to the final storage suspension ratio SC at $\gamma_{SC}^{chg,id} = \gamma_C^{dcg,id}$, under the assumption $\gamma_C^{dcg,id} < \gamma_C^{chg,id}$, which will be explained in 4.3.5.

Consisting of three flows,

$$\dot{m}_{SR}^{oil_{chg,id}} = \dot{m}_{HR}^{oil_{chg,id}} + \dot{m}_{IR}^{oil_{chg,id}} + (1 - \sigma_G)\dot{m}_{GR}^{oil_{chg,id}}$$

Eq. 4.23

$\dot{m}_{SR}^{oil_{chg,id}}$ depends on the three separation ratios

$$\eta_j^{chg,id} = \frac{\dot{m}_{j,extracted}^{oil_{chg,id}}}{\dot{m}_{R_{in}}^{oil_{chg,id}}}$$

Eq. 4.24

Where j is either H, I, or G. $\eta_G^{chg,id}$ is directly linked to the final oil-to-solid ratio $\gamma_C^{dcg,id}$ of the product (or $\eta_S^{chg,id}$ for the balance over the separation series $S = H + I + G$)

$$\eta_G^{chg,id} = 1 - \eta_H^{chg,id} - \eta_I^{chg,id} - \frac{\gamma_{SC}^{chg,id} \dot{m}_{SC}^{MB_{chg,id}}}{\dot{m}_{RS}^{oil_{chg,id}}}$$

Eq. 4.25

It was assumed that some oil will be liberated in the charge process (explained in 4.3.5), precisely the share of oil separated in the sedimentation column G that is not required to reach $\gamma_R^{chg,id}$:

$$\dot{m}_{GO}^{oil_{chg,id}} = \dot{m}_{R_{in}}^{oil_{chg,id}} - \dot{m}_{SR}^{oil_{chg,id}} - \dot{m}_{SC}^{oil_{chg,id}}$$

Eq. 4.26

The corresponding ratio is quantified as:

$$\sigma_O = \frac{\dot{m}_{GO}^{oil_{chg,id}}}{\dot{m}_{GO}^{oil_{chg,id}} + \dot{m}_{GR}^{oil_{chg,id}}}$$

Eq. 4.27

While the routes RH & HR, HI & IR, and IG are considered isothermal at $T_R^{chg,id}$, the cooled sedimentation column releases the flows GR, GO and $GC = SC$ at ambient temperature T_∞. The idea behind this is the recycling of sensible heat before storing GO and GC. The idealized exploitation of heat from the column is

$$P_{th,G}^{chg,id} = \left(T_\infty - T_R^{chg,id}\right)\left(c_p^{MB,\bar{T}_{R-\infty}^{chg,id}} \dot{m}_{GC}^{MB chg,id} + c_p^{oil,\bar{T}_{R-\infty}^{chg,id}} \dot{m}_{IG}^{oil chg,id}\right)$$

<div align="right">Eq. 4.28</div>

with $\quad \bar{T}_{R-\infty}^{chg,id} = \frac{T_R^{chg,id}+T_\infty}{2}, \quad \dot{m}_{GC}^{MB chg,id} = (1-\omega)\dot{m}_{CR}^{BA chg,id}$ and $\quad \dot{m}_{IG}^{oil chg,id} = \dot{m}_{GO}^{oil chg,id} + \dot{m}_{GR}^{oil chg,id} + \dot{m}_{GC}^{oil chg,id}$.

Transported exergy in HR and IR from reactor temperature $T_R^{chg,id}$ to ambient temperature T_∞ is calculated as

$$\dot{Ex}_{HR}^{chg,id} = \dot{m}_{HR}^{oil chg,id} c_p^{oil,\bar{T}_{R-\infty}^{chg,id}} \left(T_\infty - T_R^{chg,id}\right)$$

<div align="right">Eq. 4.29</div>

$$\dot{Ex}_{IR}^{chg,id} = \dot{m}_{IR}^{oil chg,id} c_p^{oil,\bar{T}_{R-\infty}^{chg,id}} \left(T_\infty - T_R^{chg,id}\right)$$

<div align="right">Eq. 4.30</div>

After these separation steps, the concentrate from $GC = SC$ is ready to be used in the discharge process, alongside the stored water from RL and the stored oil from $GO = SO$.

4.1.2 Calculation figures for charging at $P_{th,dehyd}^{chg,id} = 1kW$

Setting the following parameters and applying the equations from above chapter 4.1.1 yields a numerical quantification of the ideal charge process.

Table 5: Key input parameters for the ideal charge step

$P_{th,dehyd}^{chg,id}$	$\varepsilon_{C_{chg}}$	$\gamma_R^{chg,id}$	T_{ZR}	T_R	$X_{chg,id}$	η_L	$\varepsilon_{C_{dcg}}$	η_H	η_I
1kW	0.45	1.11	110°C	150°C	1	1	0.50	0.39	0.08

4.1.2.1 Setting the educt flow

For the reaction enthalpy of 941.3 $\frac{kJ}{kg_{BA,in}}$, and a heat input of $P_{th,dehyd}^{chg,id} = 1kW$ for the dehydration of Boric acid, follows with

$$\dot{m}_{CR}^{BA_{chg,id}} = \frac{P_{th,dehyd}^{chg,id}}{\Delta_{chg}h_{BA}°}$$

$$\dot{m}_{CR}^{BA_{chg,id}} = 3.82 \frac{kg_{BA}}{h}$$

4.1.2.2 Quantifying the oil cycle

Estimating $\varepsilon_{C_{chg}} = 0.45$ with $\rho_{oil}^{20°C} = 871 \frac{kg}{m^3}$ and $\rho_{BA} = 1435 \frac{kg}{m^3}$ yields

$$\gamma_C^{chg,id} = \frac{\varepsilon_{C_{chg}}\rho_{oil}}{\left(1 - \varepsilon_{C_{chg}}\right)\rho_{BA}} = \frac{0.45 * 871}{(1 - 0.45) * 1435} \frac{kg_{oil}}{kg_{BA}}$$

$$\gamma_C^{chg,id} = 0.497 \frac{kg_{oil}}{kg_{BA}}$$

and $\dot{m}_{CR}^{oil_{chg,id}} = \gamma_C^{chg,id}\dot{m}_{CR}^{BA_{chg,id}} = 0.497 \frac{kg_{oil}}{kg_{BA}} * 3.82 \frac{kg_{BA}}{h}$

$$\dot{m}_{CR}^{oil_{chg,id}} = 1.90 \frac{kg_{oil}}{h}$$

With $\gamma_R^{chg,id} = \frac{1}{0.9} \frac{kg_{oil}}{kg_{BA}}$, which was found to be a good ratio in experiments with a small stirred batch

reactor, total oil flow to the reactor is

$$\dot{m}_{ZR}^{oil_{chg,id}} = \gamma_R^{chg,id} \dot{m}_{CR}^{BA_{chg,id}} = 1.11\frac{kg_{oil}}{kg_{BA}} * 3.82\frac{kg_{BA}}{h}$$

$$\boldsymbol{\dot{m}_{ZR}^{oil_{chg,id}} = 4.24\frac{kg_{oil}}{h}}$$

Which requires a recycled flow rate from the separation series of

$$\dot{m}_{SR}^{oil_{chg,id}} = \dot{m}_{CR}^{BA_{chg,id}}\left(\gamma_R^{chg,id} - \gamma_C^{chg,id}\right) = 3.82\frac{kg_{BA}}{h} * (1.11 - 0.497)\frac{kg_{oil}}{kg_{BA}}$$

$$\boldsymbol{\dot{m}_{SR}^{oil_{chg,id}} = 2.34\frac{kg_{oil}}{h}}$$

4.1.2.3 Mixing & Preheating

With $T_{SR}^{chg,id} = 404.4K = 131.2°C$ known from chapter 4.1.2.6, the equilibrium temperature $T_{Z_{in}}^{chg,id}$ for the inflows to Z can be iterated from

$$T_{Z_{in}}^{chg,id} = \frac{T_{SR}^{chg,id} c_p^{oil,T_{SR}} \dot{m}_{SR}^{oil_{chg,id}} + T_\infty\left(c_p^{oil,T_\infty} \dot{m}_{CR}^{oil_{chg,id}} + c_p^{BA,T_\infty} \dot{m}_{CR}^{BA_{chg,id}}\right)}{c_p^{oil,T_{Z_{in}}} \dot{m}_{ZR}^{oil_{chg,id}} + c_p^{BA,T_{Z_{in}}} \dot{m}_{CR}^{BA_{chg,id}}}$$

With values for $c_p^{i,T_{Z_{in}}}$ at $T_{Z_{in}}^{chg,id} \approx 60°C$, the closest result finally is

$$T_{Z_{in}}^{chg,id}$$

$$= \frac{404.4K * 2.36\frac{kJ}{kg_{oil}K} * 2.34\frac{kg_{oil}}{h} + 298.15K\left(1.99\frac{kJ}{kg_{oil}K} * 1.90\frac{kg_{oil}}{h} + 1.32\frac{kJ}{kg_{BA}K} * 3.82\frac{kg_{BA}}{h}\right)}{2.12\frac{kJ}{kg_{oil}K} * 4.24\frac{kg_{oil}}{h} + 1.43\frac{kJ}{kg_{BA}K} * 3.82\frac{kg_{BA}}{h}}$$

$$\boldsymbol{T_{Z_{in}}^{chg,id} = 336.6\,K = 63.4\,°C}$$

The heating power $P_{th,Z}^{chg,id}$ that needs to be applied to Z to reach T_{ZR} is calculated with $\bar{T}_Z^{chg,id} = \frac{T_{ZR}^{chg,id} + T_{Z_{in}}^{chg,id}}{2} \approx 90°C$ as

$$P_{th,Z}^{chg,id} = \left(T_{ZR}^{chg,id} - T_{Z_{in}}^{chg,id}\right)\left(c_p^{oil,\bar{T}_Z^{chg,id}} \dot{m}_{ZR}^{oil_{chg,id}} + c_p^{BA,\bar{T}_Z^{chg,id}} \dot{m}_{CR}^{BA_{chg,id}}\right)$$

$$= (110 - 63.4)K * \left(2.22\frac{kJ}{kg_{oil}K} * 4.24\frac{kg_{oil}}{h} + 1.52\frac{kJ}{kg_{BA}K} * 3.82\frac{kg_{BA}}{h}\right) * \frac{1h}{3600s}$$

$$P_{th,Z}^{chg,id} = 0.20\ kW$$

4.1.2.4 Reactor

Beforehand, a steam extraction rate is elaborated. A batch experiment with 250g of Boric acid, suspended in 294g of oil according to $\gamma_R = \frac{1}{0.85}$ yields $V_{susp.}^{batch} = 542ml$ at $\rho_{oil} = 800\frac{g}{ml}$ and $\rho_{BA} = 1435\frac{g}{ml}$. The recorded time for complete steam removal $t_{release}^{end} = 45min$ was considered as a complete dehydration to Metaboric acid, and no further reaction to Boric oxide, because of the proximity of the condensed water volume to the theoretical value $\omega m_{CR}^{BA_{chg,batch,id}} = 0.29\frac{g_{H_2O}}{g_{BA}} * 250g_{BA} = 72.5g_{H_2O}$. Thus,

$$r_V^{H_2O} = \frac{m_{RL}^{H_2O_{chg,batch}}}{V_{susp}^{batch} t_{release}^{end}} = \frac{\omega m_{CR}^{BA_{chg,batch,id}}}{V_{susp}^{batch} t_{release}^{end}} = \frac{72.5\ g_{H_2O}}{542\ ml * 45\ min}$$

$$r_V^{H_2O} = 3.0\ \frac{kg_{H_2O}}{m^3 min}$$

Applying this value to current figures, with

$$\dot{V}_{R,susp}^{chg,id} = \frac{\dot{m}_{CR}^{BA_{chg,id}}}{\rho_{BA}} + \frac{\dot{m}_{ZR}^{oil_{chg,id}}}{\rho_{oil}^{T_R^{chg,id}}} = \frac{3.82}{1.435}\frac{l}{h} + \frac{4.24}{0.788}\frac{l}{h} = 2.7\frac{l}{h} + 5.4\frac{l}{h} = 8.1\frac{l}{h},$$ we obtain the estimated

$$t_{dehyd} = \frac{\omega \dot{m}_{CR}^{BA_{chg,id}}}{r_V^{H_2O}\dot{V}_{R,susp}} = \frac{1.11\frac{kg_{H_2O}}{h}}{3.0\frac{kg_{H_2O}}{m^3 min} * 8.1\frac{l}{h}} = \frac{\frac{1.11}{60}}{\frac{3}{1000} * \frac{8.1}{60}}\ min$$

$$t_{dehyd} = 46\ min$$

Preheating the suspension to $T_R^{chg,id}$, with mean heat capacities at $\bar{T}_R^{chg,id} = \frac{T_R^{chg,id}+T_{ZR}^{chg,id}}{2} = 130°C$, requires the energy input

$$P_{th,pre}^{chg,id} = \left(T_R^{chg,id} - T_{ZR}^{chg,id}\right)\left(c_p^{oil,\bar{T}_R^{chg,id}}\dot{m}_{ZR}^{oil_{chg,id}} + c_p^{BA,\bar{T}_R^{chg,id}}\dot{m}_{CR}^{BA_{chg,id}}\right)$$

$$= (150 - 110)K * \left(2.36\frac{kJ}{kg_{oil}K} * 4.24\frac{kg_{oil}}{h} + 1.63\frac{kJ}{kg_{BA}K} * 3.82\frac{kg_{BA}}{h}\right) * \frac{1h}{3600s}$$

$$P_{th,pre}^{chg,id} = 0.18\ kW$$

From $\frac{P_{th,pre}^{chg,id}}{t_{pre}} = \frac{P_{th,dehyd}^{chg,id}}{t_{dehyd}}$ follows

$$t_{pre} = \frac{P_{th,pre}^{chg,id}}{P_{th,dehyd}^{chg,id}} t_{dehyd} = \frac{0.18}{1.00} * 46min$$

$$\boldsymbol{t_{pre} = 8\ min}$$

Total residence time sums up as

$$\tau_R^{chg,id} = t_{pre} + t_{dehyd} = 8min + 46min$$

$$\boldsymbol{\tau_R^{chg,id} = 54\ min}$$

Therefore, the required reactor volume is calculated (with a void volume of 30% of the reaction suspension volume) as

$$V_R^{chg,id} = (1 + \varepsilon_R)\dot{V}_{R,susp}^{chg,id}\tau_R^{chg,id} = (1 + 0.3) * 8.1\frac{l}{h} * 54min$$

$$\boldsymbol{V_R^{chg,id} = 9.5l}$$

Assuming full conversion $X_{chg,id} = 1$, $\dot{m}_{CR}^{BA_{chg,id}} = 3.82\frac{kg_{BA}}{h}$ yields $\dot{m}_{RS}^{MB_{chg,id}} = (1 - \omega)\dot{m}_{CR}^{BA_{chg,id}} = 0.71\frac{kg_{MB}}{kg_{BA}} * 3.82\frac{kg_{BA}}{h}$

$$\boldsymbol{\dot{m}_{RS}^{MB_{chg,id}} = 2.71\ \frac{kg_{MB}}{h}}$$

And, assuming $\eta_L = 1$, $\dot{m}_{RL}^{H_2O_{chg,id}} = \omega\dot{m}_{CR}^{BA_{chg,id}} = 0.29\frac{kg_{H_2O}}{kg_{BA}} * 3.82\frac{kg_{BA}}{h}$

$$\boldsymbol{\dot{m}_{RL}^{H_2O_{chg,id}} = 1.11\ \frac{kg_{H_2O}}{h}}$$

The rate of thermochemically stored energy then is

$$P_{sto} = \Delta_{dcg(g)}h_{BA}°\frac{1}{1 - \omega}\dot{m}_{SC}^{MB_{chg,id}} = -941.3\ \frac{kJ}{kg_{BA}} * \frac{1\ kg_{BA\ rehydrated}}{0.71\ kg_{MB\ input}} * 2.71\frac{kg_{MB}}{h} * \frac{1h}{3600s}$$

$$P_{sto} = -1.00kW = P_{th,rehyd}^{dcg,id} = -P_{th,dehyd}^{chg,id}$$

Which underlines the ideal scenario of full conversion and zero energy losses.

4.1.2.5 Condenser

With $\Delta h_V^{H_2O,100°C} = 2256 \frac{kJ}{kg_{H_2O}}$, $c_p^{H_2O,\bar{T}_{steam}^{chg,id}} = 2.00 \frac{kJ}{kg_{H_2O(g)}K} \approx const.(T)$ [21] and $c_p^{H_2O,\bar{T}_{liquid}^{chg,id}} =$

$4.19 \frac{kJ}{kg_{H_2O(l)}K} \approx const.(T)$ [22], we obtain

$$P_{th,L}^{chg,id} = \dot{m}_{RL}^{H_2O_{chg,id}} \left(c_p^{H_2O,\bar{T}_{steam}^{chg,id}} \left(T_{cond.} - T_R^{chg,id} \right) - \Delta h_V^{H_2O,100°C} + c_p^{H_2O,\bar{T}_{liquid}^{chg,id}} \left(T_\infty - T_{cond.} \right) \right)$$

$$= 1.11 \frac{kg_{H_2O}}{h} \left(2.00 \frac{kJ}{kg_{H_2O(g)}K} * (100 - 150)K - 2256 \frac{kJ}{kg_{H_2O}} + 4.19 \frac{kJ}{kg_{H_2O(l)}K} (25 - 100)K \right)$$

$$P_{th,L}^{chg,id} = 1.11 \frac{kg_{H_2O}}{h} * \frac{1h}{3600s} * \left(-100 \frac{kJ}{kg_{H_2O(g)}} - 2256 \frac{kJ}{kg_{H_2O}} - 314 \frac{kJ}{kg_{H_2O(l)}} \right)$$

$$\boldsymbol{P_{th,L}^{chg,id} = -0.82 \; kW}$$

To emphasize the share of the condensation enthalpy,

$$P_{th,L,cond.}^{chg,id} = -2256 \frac{kJ}{kg_{H_2O}} * 1.11 \frac{kg_{H_2O}}{h} * \frac{1h}{3600s} = 0.70 kW$$

$$\frac{P_{th,L,cond.}^{chg,id}}{P_{th,L}^{chg,id}} = \frac{0.70 kW}{0.82 kW} = 85\%$$

This is to underline the potential of mechanical vapor recompression for heat recovery at T_R.

4.1.2.6 Oil separation series

With an estimated $\varepsilon_{C_{dcg}} = 0.50$ and $\rho_{oil}^{25°C} = 868 \frac{kg}{m^3}$ and $\rho_{MB} = 2045 \frac{kg}{m^3}$ follows $\gamma_{SC}^{chg,id} = \gamma_C^{dcg,id} =$

$\frac{\varepsilon_{C_{dcg}} \rho_{oil}}{(1 - \varepsilon_{C_{dcg}}) \rho_{MB}} = \frac{868}{2045}$

$$\boldsymbol{\gamma_{SC}^{chg,id} = 0.42 \; \frac{kg_{oil}}{kg_{MB}}}$$

The density shift alters the input value $\gamma_R^{chg,id} = \frac{4.24 \, kg_{oil}}{3.82 \, kg_{BA}}$ to $\gamma_{RS}^{chg,id} = \frac{4.24 \, kg_{oil}}{2.71 \, kg_{MB}}$

$$\boldsymbol{\gamma_{RS}^{chg,id} = 1.56 \; \frac{kg_{oil}}{kg_{MB}}}$$

and leaves the extractable oil stream $\dot{m}_{SR}^{oil_{chg,id}} + \dot{m}_{SO}^{oil_{chg,id}} = \dot{m}_{RS}^{MB_{chg,id}} \left(\gamma_{RS}^{chg,id} - \gamma_{SC}^{chg,id} \right) =$

$$2.71 \frac{kg_{MB}}{h} * (1.56 - 0.42) \frac{kg_{oil}}{kg_{BA}} = 3.09 \frac{kg_{oil}}{h}, \quad \text{where} \quad \dot{m}_{RS}^{MB_{chg,id}} = \dot{m}_{SC}^{MB_{chg,id}} \quad \text{and} \quad \dot{m}_{SR}^{oil_{chg,id}} =$$

$$2.34 \frac{kg_{oil}}{h} \Rightarrow \dot{m}_{SO}^{oil_{chg,id}} = 3.09 \frac{kg_{oil}}{h} - 2.34 \frac{kg_{oil}}{h}$$

$$\dot{m}_{SO}^{oil_{chg,id}} = 0.75 \frac{kg_{oil}}{h}$$

The remaining oil is stored alongside the metaboric acid as $\dot{m}_{SC}^{oil_{chg,id}} = \gamma_{SC}^{chg,id} \dot{m}_{SC}^{MB_{chg,id}} = 0.42 \frac{kg_{oil}}{kg_{MB}} *$

$$2.71 \frac{kg_{MB}}{h}$$

$$\dot{m}_{SC}^{oil_{chg,id}} = 1.14 \frac{kg_{oil}}{h}$$

For the three separation units, values for $\eta_j = \frac{\dot{m}_{j,extracted}^{oil_{chg,id}}}{\dot{m}_{RS}^{oil_{chg,id}}}$ have been guessed, fulfilling

$$\eta_H^{chg,id} + \eta_I^{chg,id} + \eta_G^{chg,id} + \frac{\dot{m}_{SC}^{oil_{chg,id}}}{\dot{m}_{RS}^{oil_{chg,id}}} = 1 \text{ and } \dot{m}_{IG}^{oil_{chg,id}} > \dot{m}_{SC}^{oil_{chg,id}}; \text{ These values lead to}$$

$$\dot{m}_{HR}^{oil_{chg,id}} = \eta_H \dot{m}_{RS}^{oil_{chg,id}} = 0.39 * 4.24 \frac{kg_{oil}}{h}$$

$$\dot{m}_{HR}^{oil_{chg,id}} = 1.65 \frac{kg_{oil}}{h}$$

Approximating $c_p^{i,\bar{T}_{R-\infty}^{chg,id}}$ at $\bar{T}_{R-\infty}^{chg,id} = \frac{T_R^{chg,id} + T_\infty}{2} \approx 90°C$, exergy flows $\dot{Ex}$ follow as

$$\dot{Ex}_{HR}^{chg,id} = \dot{m}_{HR}^{oil_{chg,id}} c_p^{oil,\bar{T}_{R-\infty}^{chg,id}} (T_\infty - T_R^{chg,id}) = 1.65 \frac{kg_{oil}}{h} * \frac{1h}{3600s} * 2.22 \frac{kJ}{kg_{oil}K} * (25 - 150)K$$

$$\dot{Ex}_{HR}^{chg,id} = -0.13 \ kW$$

$$\dot{m}_{IR}^{oil_{chg,id}} = \eta_I \dot{m}_{RS}^{oil_{chg,id}} = 0.08 * 4.24 \frac{kg_{oil}}{h}$$

$$\dot{m}_{IR}^{oil_{chg,id}} = 0.34 \frac{kg_{oil}}{h}$$

$$\dot{Ex}_{IR}^{chg,id} = \dot{m}_{IR}^{oil_{chg,id}} c_p^{oil,\bar{T}_{R-\infty}^{chg,id}} (T_\infty - T_R^{chg,id}) = 0.34 \frac{kg_{oil}}{h} * \frac{1h}{3600s} * 2.22 \frac{kJ}{kg_{oil}K} * (25 - 150)K$$

$$\dot{Ex}_{IR}^{chg,id} = -0.03 \ kW$$

Leaving the last oil separation factor subject to the known values

$$\eta_G^{chg,id} = 1 - \eta_H^{chg,id} - \eta_I^{chg,id} - \frac{\gamma_{SC}^{chg,id} \dot{m}_{SC}^{MB_{chg,id}}}{\dot{m}_{RS}^{oil_{chg,id}}} = 1 - 0.39 - 0.08 - \frac{0.42 * 2.71}{4.24}$$

$$\boldsymbol{\eta_G^{chg,id} = 0.26}$$

Thus, $\dot{m}_{G(R,O)}^{oil_{chg,id}} = \dot{m}_{GR}^{oil_{chg,id}} + \dot{m}_{GO}^{oil_{chg,id}} = \eta_G \dot{m}_{RS}^{oil_{chg,id}} = 0.26 * 4.24 \frac{kg_{oil}}{h}$

$$\boldsymbol{\dot{m}_{G(R,O)}^{oil_{chg,id}} = 1.10 \frac{kg_{oil}}{h}}$$

Of which $\dot{m}_{GR}^{oil_{chg,id}}$ is determined by:

$$\dot{m}_{SR}^{oil_{chg,id}} = \dot{m}_{HR}^{oil_{chg,id}} + \dot{m}_{IR}^{oil_{chg,id}} + \dot{m}_{GR}^{oil_{chg,id}} \Rightarrow \dot{m}_{GR}^{oil_{chg,id}} = \dot{m}_{SR}^{oil_{chg,id}} - \dot{m}_{HR}^{oil_{chg,id}} - \dot{m}_{IR}^{oil_{chg,id}}$$

$$= (2.34 - 1.65 - 0.34) \frac{kg_{oil}}{h}$$

$$\boldsymbol{\dot{m}_{GR}^{oil_{chg,id}} = 0.35 \frac{kg_{oil}}{h}}$$

Which matches $\dot{m}_{GO}^{oil_{chg,id}} = \dot{m}_{G(R,O)}^{oil_{chg,id}} - \dot{m}_{GR}^{oil_{chg,id}} = 1.10 \frac{kg_{oil}}{h} - 0.35 \frac{kg_{oil}}{h} = \dot{m}_{SO}^{oil_{chg,id}} = 0.75 \frac{kg_{oil}}{h}$

from above. With these values, the oil storage share of sedimentation extract is:

$$\sigma_O = \frac{\dot{m}_{GO}^{oil_{chg,id}}}{\dot{m}_{G(R,O)}^{oil_{chg,id}}} = \frac{0.75}{1.10}$$

$$\boldsymbol{\sigma_O = 0.68}$$

The equilibrium temperature $T_{SR}^{chg,id}$ for the recycled oil flow SR is

$$T_{SR}^{chg,id} = T_\infty + \frac{\eta_H^{chg,id} + \eta_I^{chg,id}}{\eta_H^{chg,id} + \eta_I^{chg,id} + (1 - \sigma_O)\eta_G^{chg,id}} \left(T_R^{chg,id} - T_\infty \right)$$

$$= 298.15 K + \frac{0.39 + 0.08}{0.39 + 0.08 + (1 - 0.68) * 0.26} (150 - 25) K$$

$$\boldsymbol{T_{SR}^{chg,id} = 404.4 \, K = 131.2 \, °C}$$

With $\dot{m}_{IG}^{oil_{chg,id}} = \dot{m}_{RS}^{oil_{chg,id}} - \dot{m}_{HR}^{oil_{chg,id}} - \dot{m}_{IR}^{oil_{chg,id}} = (4.25 - 1.66 - 0.34)\frac{kg_{oil}}{h} = 2.25\frac{kg_{oil}}{h}$, we

obtain the theoretically extractable heat from the sedimentation column as:

$$P_{th,G}^{chg,id} = \left(T_\infty - T_R^{chg,id}\right)\left(c_p^{MB,\bar{T}_{R-\infty}^{chg,id}}\,\dot{m}_{GC}^{MB_{chg,id}} + c_p^{oil,\bar{T}_{R-\infty}^{chg,id}}\,\dot{m}_{IG}^{oil_{chg,id}}\right)$$

$$= (25 - 150)K * \left(1.33\frac{kJ}{kg_{MB}K} * 2.71\frac{kg_{MB}}{h} + 2.22\frac{kJ}{kg_{oil}K} * 2.25\frac{kg_{oil}}{h}\right) * \frac{1h}{3600s}$$

$$\boldsymbol{P_{th,G}^{chg,id} = -0.30\ kW}$$

4.2 Quantifying the ideal discharge process

The calculations in this chapter are developed around the variant of steam rehydration, with the variant of liquid water rehydration as a considerable option mentioned at points of interest.

Again, the baseline of the calculations is the reaction enthalpy from Eq. 2.4, dictating the metaboric acid input flow for a desired output power. Addition of oil from the oil storage tank and the oil recycling flows are obtained from the selected oil-to-solid suspension ratio in the reactor. The temperature of the mixed flow of metaboric acid and process oil, determined by the chosen suspension ratio, leads to the necessary preheating power. With the assumption of full conversion and stoichiometric water addition, pure boric acid leaves the reactor together with the process oil, which is extracted in the same three units as in the charge mode. Again, values for oil extraction shares of the first two units are guessed, leaving the extraction share of the sedimentation column subject to the final oil-to-solid suspension ratio of the product concentrate (boric acid and process oil). All three oil extraction units are idealized in that sense that only pure oil is extracted, without any traces of boric acid. Heat input requirements and output potential was calculated where applicable, assuming zero losses. The reactor volume was calculated based on a preliminary guess for the necessary residence time.

4.2.1 Developing a framework of equations

4.2.1.1 Setting the educt flow

Given the theoretical reversibility of the reactions, i.e., dehydration and hydration, the discharge step with steam under ideal conditions is characterized by $\Delta_{dcg(g)} h_{BA}° = -\Delta_{chg} h_{BA}°$. In words, the reaction enthalpy needed to dehydrate one kilogram of Boric acid is exactly the released enthalpy to form one kilogram of Boric acid when Metaboric acid is rehydrated with steam. For a stoichiometric rehydration at full conversion $X_{dcg,id} = 1$ follows

$$\dot{m}_{CR}^{MB_{dcg,id}} = \frac{P_{th,rehyd.}^{dcg,id}}{\Delta_{dcg(g)} h_{BA}° \frac{1}{1-\omega}}$$

Eq. 4.31

In case of a rehydration with liquid water, the energy needed to heat and evaporate the water inflow would have to be provided by the rehydration enthalpy, decreasing the extractable heat from the reactor. For better comparability of the charge and discharge processes and some other considerations, this option is not elaborated in this thesis. For an in-depth argumentation of this decision, see chapter 4.4.3.

4.2.1.2 Quantifying the oil cycle

As already introduced in the charge process, oil-to-solid ratios γ_j characterize the suspension in different sections of the discharge plant. With full conversion rates, their definition reference (total solids from discharge concentrate inflow) simplifies to $\dot{m}_{CR}^{BA+MB_{dcg,id}} = \dot{m}_{CR}^{MB_{dcg,id}}$.

$$\gamma_C^{dcg,id} = \frac{\dot{m}_{CR}^{oil_{dcg,id}}}{\dot{m}_{CR}^{MB_{dcg,id}}} = \frac{\varepsilon_C^{dcg,id}\rho_{oil}}{(1 - \varepsilon_C^{dcg,id})\rho_{MB}}$$

Eq. 4.32

$$\varepsilon_C^{dcg,id} = \lim_{t\to\infty}\left[\frac{1}{1 + \frac{V_{MB}}{V_{susp.oil}(t)}}\right]_{C,dcg,id}$$

Eq. 4.33

With the mentioned assumption of $\gamma_C^{chg,id} > \gamma_C^{dcg,id}$ and the resulting difference in required suspension oil, the released oil from the charge process $\dot{m}_{SO}^{oil_{chg,id}} = \dot{m}_{OR}^{oil_{dcg,id}}$ is now added to the discharge process, while all the oil extracted in the separation series is recycled as $\dot{m}_{SR}^{oil_{dcg,id}}$:

$$\gamma_R^{dcg,id} = \frac{\dot{m}_{R_{in}}^{oil_{dcg,id}}}{\dot{m}_{CR}^{MB_{dcg,id}}} = \frac{\dot{m}_{CR}^{oil_{dcg,id}} + \dot{m}_{SR}^{oil_{dcg,id}} + \dot{m}_{OR}^{oil_{dcg,id}}}{\dot{m}_{CR}^{MB_{dcg,id}}}$$

Eq. 4.34

To understand the distribution of oil flows after the reactor better, see chapter 4.2.1.6.

4.2.1.3 Mixing & Preheating

The mixed flow $Z_{in} = CR + OR + SR$ into the conveyor screw Z equals the flow ZR (from Z to the reactor R) in composition, while it is gradually heated.

As no reaction of pure Metaboric acid in oil is to be expected without the addition of water, the preheating of Z_{in} is performed to $T_{ZR}^{dcg,id} = T_R^{dcg,id}$. With CR and OR coming in at ambient temperature T_∞ and SR at

$$T_{SR}^{dcg,id} = T_\infty + \frac{\eta_H^{dcg,id} + \eta_I^{dcg,id}}{\eta_H^{dcg,id} + \eta_I^{dcg,id} + \eta_G^{dcg,id}}(T_R^{dcg,id} - T_\infty)$$

Eq. 4.35

Which can be solved after calculating the three values $\eta_j^{dcg,id}$ for the oil extraction (as in 4.2.1.6); As

the next step, the equilibrium temperature $T_{Z_{in}}^{dcg,id}$ is iterated from

$$T_{Z_{in}}^{dcg,id} = \frac{T_{SR}^{dcg,id} c_p^{oil,T_{SR}} \dot{m}_{SR}^{oil_{dcg,id}} + T_\infty \left(c_p^{oil,T_\infty} \left(\dot{m}_{CR}^{oil_{dcg,id}} + \dot{m}_{OR}^{oil_{dcg,id}} \right) + c_p^{MB,T_\infty} \dot{m}_{CR}^{MB_{dcg,id}} \right)}{c_p^{oil,T_{Z_{in}}} \dot{m}_{ZR}^{oil_{dcg,id}} + c_p^{MB,T_{Z_{in}}} \dot{m}_{CR}^{MB_{dcg,id}}}$$

<div align="right">Eq. 4.36</div>

Heating the discharge suspension from $T_{Z_{in}}^{dcg,id}$ to $T_{ZR}^{dcg,id}$ requires the following power input:

$$P_{th,Z}^{dcg,id} = \left(T_{ZR}^{dcg,id} - T_{Z_{in}}^{dcg,id} \right) \left(c_p^{oil,\bar{T}_Z^{dcg,id}} \dot{m}_{ZR}^{oil_{dcg,id}} + c_p^{MB,\bar{T}_Z^{dcg,id}} \dot{m}_{CR}^{MB_{chg,id}} \right)$$

<div align="right">Eq. 4.37</div>

Heat capacities for oil and Metaboric acid are taken at $\bar{T}_Z^{dcg,id} = \frac{T_{ZR}^{dcg,id} + T_{Z_{in}}^{dcg,id}}{2}$

4.2.1.4 Evaporator

Evaporating $\dot{m}_{WE}^{H_2O(l)_{dcg,id}} = \dot{m}_{ER}^{H_2O(g)_{dcg,id}}$ and heating it up to $T_R^{dcg,id}$ requires a significant input of energy:

$$P_{th,E}^{dcg,id} = \dot{m}_{WE}^{H_2O(l)_{dcg,id}} \left(c_p^{H_2O,\bar{T}_{liquid}^{dcg,id}} (T_b - T_\infty) + \Delta h_V^{H_2O,T_b=100°C} + c_p^{H_2O,\bar{T}_{steam}^{chg,id}} \left(T_R^{dcg,id} - T_b \right) \right)$$

<div align="right">Eq. 4.38</div>

4.2.1.5 Reactor

A complete rehydration ($X_{dcg,id} = 1$) with stoichiometric inflows and ideal separation yields:

$$\dot{m}_{formed}^{BA_{dcg,id}} = \dot{m}_{CR}^{MB_{dcg,id}} + \dot{m}_{ER}^{H_2O_{dcg,id}} = \frac{1}{1-\omega} \dot{m}_{CR}^{MB_{dcg,id}} = \frac{1}{\omega} \dot{m}_{ER}^{H_2O_{dcg,id}} = \dot{m}_{SC}^{BA_{dcg,id}}$$

<div align="right">Eq. 4.39</div>

The reactor volume is calculated with:

$$V_R^{dcg,id} = (1 + \varepsilon_R) \dot{V}_{R,susp}^{dcg,id} \tau_R^{dcg,id}$$

<div align="right">Eq. 4.40</div>

4.2.1.6 Oil separation series & oil addition from storage

As in the charge process, the three units for oil extraction H, I and G after the reactor follow the target to reduce the oil suspension ratio from $\gamma_R^{dcg,id}$ to $\gamma_{SC}^{dcg,id} = \gamma_C^{chg,id}$, again assuming $\gamma_C^{dcg,id} < \gamma_C^{chg,id}$. In contrast to the charge series, no oil from separation is stored, but some is added to the reaction suspension from the oil storage O in order to achieve $\gamma_R^{dcg,id}$.

$$\dot{m}_{SR}^{oil_{dcg,id}} = \dot{m}_{HR}^{oil_{dcg,id}} + \dot{m}_{IR}^{oil_{chg,id}} + \dot{m}_{GR}^{oil_{dcg,id}}$$

<div align="right">Eq. 4.41</div>

Two of the three separation ratios $\eta_j^{dcg,id} = \dfrac{\dot{m}_{jR}^{oil_{dcg,id}}}{\dot{m}_{R_{in}}^{oil_{dcg,id}}}$, namely $\eta_H^{dcg,id}$ and $\eta_I^{dcg,id}$, are set as estimates

again, and $\eta_G^{dcg,id}$ is then deducted with the estimated $\gamma_{SC}^{dcg,id}\left(\varepsilon_{C_{chg}}\right)$ as

$$\eta_G^{dcg,id} = 1 - \eta_H^{dcg,id} - \eta_I^{dcg,id} - \frac{\gamma_{SC}^{dcg,id}\dot{m}_{SC}^{BA_{dcg,id}}}{\dot{m}_{RS}^{oil_{dcg,id}}}$$

<div align="right">Eq. 4.42</div>

Before storing GC, heat is recovered from G as in the charge process, assuming isothermal flows RH & HR, HI & IR, and IG at $T_R^{chg,id}$, while G is cooled to ambient temperature T_∞ at which GR and $GC = SC$, i.e., the final Boric acid suspension concentrate, are released.

$$P_{th,G}^{dcg,id} = \left(T_\infty - T_R^{dcg,id}\right)\left(c_p^{BA,\bar{T}_G^{dcg,id}}\dot{m}_{GC}^{BA_{dcg,id}} + c_p^{oil,\bar{T}_G^{dcg,id}}\dot{m}_{IG}^{oil_{dcg,id}}\right)$$

<div align="right">Eq. 4.43</div>

$$\dot{m}_{IG}^{oil_{dcg,id}} = \dot{m}_{ZR}^{oil_{dcg,id}} - \dot{m}_{HR}^{oil_{dcg,id}} - \dot{m}_{IR}^{oil_{dcg,id}}$$

<div align="right">Eq. 4.44</div>

$$\bar{T}_G^{dcg,id} = \frac{T_R^{dcg,id} + T_\infty}{2}$$

<div align="right">Eq. 4.45</div>

Transported exergy in HR and IR from initial temperature $T_R^{dcg,id}$ to ambient temperature T_∞ is calculated as

$$\dot{Ex}_{HR}^{dcg,id} = \dot{m}_{HR}^{oil_{dcg,id}}c_p^{oil,\bar{T}_{R-\infty}^{dcg,id}}\left(T_\infty - T_R^{dcg,id}\right)$$

<div align="right">Eq. 4.46</div>

$$\dot{Ex}_{IR}^{dcg,id} = \dot{m}_{IR}^{oil_{dcg,id}}c_p^{oil,\bar{T}_{R-\infty}^{dcg,id}}\left(T_\infty - T_R^{dcg,id}\right)$$

<div align="right">Eq. 4.47</div>

$$\bar{T}_{R-\infty}^{dcg,id} = \frac{T_R^{dcg,id} + T_\infty}{2}$$

<div align="right">Eq. 4.48</div>

4.2.2 Calculation figures for discharging at $P_{th,rehyd}^{chg,id} = -1kW$

Table 6: Key parameters for the ideal discharge step

$P_{th,rehyd}^{dcg,id}$	$\varepsilon_{C_{dcg}}$	$\gamma_R^{chg,id}$	T_{ZR}	T_R	$X_{dcg,id}$	$\varepsilon_{C_{chg}}$	η_H	η_I
-1kW	0.50	1.57	130°C	130°C	1	0.45	0.20	0.12

4.2.2.1 Setting the educt flow

With a set value of $P_{th,rehyd}^{dcg,id} = -1kW$, we obtain

$$\dot{m}_{CR}^{MB_{dcg,id}} = \frac{P_{th,rehyd.}^{dcg,id}}{\Delta_{dcg(g)}h_{BA}° \frac{1}{1-\omega}}$$

$$= \frac{-1kW}{-941.3 \frac{kJ}{kg_{BA,out}}} * 0.71 \frac{kg_{MB,in}}{kg_{BA,out}} * \frac{3600s}{1h}$$

$$\dot{m}_{CR}^{MB_{dcg,id}} = 2.71 \frac{kg_{MB}}{h}$$

Which underlines the theoretical reversibility of the reaction; The product of the discharge process equals the educt of the charge process, and vice versa.

4.2.2.2 Quantifying the oil cycle

For densities at T_∞,

$$\gamma_C^{dcg,id} = \frac{\dot{m}_{CR}^{oil_{dcg,id}}}{\dot{m}_{CR}^{MB_{dcg,id}}} = \frac{\varepsilon_{C_{dcg}}\rho_{oil}}{\left(1 - \varepsilon_{C_{dcg}}\right)\rho_{MB}} = \frac{868}{2045}$$

$$\gamma_C^{dcg,id} = 0.42 \frac{kg_{oil}}{kg_{MB}}$$

$$\dot{m}_{CR}^{oil_{dcg,id}} = \gamma_C^{dcg,id} \dot{m}_{CR}^{MB_{dcg,id}} = 0.42 \frac{kg_{oil}}{kg_{MB}} * 2.71 \frac{kg_{MB}}{h}$$

$$\dot{m}_{CR}^{oil_{dcg,id}} = 1.14 \frac{kg_{oil}}{h}$$

As already calculated in the charge step, confirming $CR_{dcg} = SC_{chg}$. Also, the discharge reactor input oil-to-solid ratio equals the charge reactor output oil-to-solid ratio,

$$\gamma_R^{dcg,id} = \frac{\dot{m}_{R_{in}}^{oil_{dcg,id}}}{\dot{m}_{CR}^{MB_{dcg,id}}} = \frac{\dot{m}_{CR}^{oil_{dcg,id}} + \dot{m}_{SR}^{oil_{dcg,id}} + \dot{m}_{OR}^{oil_{dcg,id}}}{\dot{m}_{CR}^{MB_{dcg,id}}}$$

$$\boldsymbol{\gamma_R^{dcg,id} = 1.56}$$

From which we obtain $\dot{m}_{R_{in}}^{oil_{dcg,id}} = \gamma_R^{dcg,id} \dot{m}_{CR}^{MB_{dcg,id}} = 1.56 \frac{kg_{oil}}{kg_{MB}} * 2.71 \frac{kg_{MB}}{h}$

$$\boldsymbol{\dot{m}_{R_{in}}^{oil_{dcg,id}} = 4.24 \frac{kg_{oil}}{h}}$$

Which also equals the charge reactor oil input $\dot{m}_{R_{in}}^{oil_{chg,id}}$, leaving $\dot{m}_{SR}^{oil_{dcg,id}} + \dot{m}_{OR}^{oil_{dcg,id}} = \dot{m}_{R_{in}}^{oil_{dcg,id}} - \dot{m}_{CR}^{oil_{dcg,id}} = 4.24 \frac{kg_{oil}}{h} - 1.14 \frac{kg_{oil}}{h} = 3.10 \frac{kg_{oil}}{h}$, and when setting

$$\boldsymbol{\dot{m}_{OR}^{oil_{dcg,id}} = \dot{m}_{SO}^{oil_{chg,id}} = 0.75 \frac{kg_{oil}}{h}}$$

$$\dot{m}_{SR}^{oil_{dcg,id}} = \dot{m}_{R_{in}}^{oil_{dcg,id}} - \dot{m}_{CR}^{oil_{dcg,id}} - \dot{m}_{OR}^{oil_{dcg,id}} = 4.24 \frac{kg_{oil}}{h} - 1.14 \frac{kg_{oil}}{h} - 0.75 \frac{kg_{oil}}{h}$$

$$\boldsymbol{\dot{m}_{SR}^{oil_{dcg,id}} = 2.34 \frac{kg_{oil}}{h}}$$

Having confirmed now that $\dot{m}_{SR}^{oil_{dcg,id}} = \dot{m}_{SR}^{oil_{chg,id}}$, the discharge process oil input relates to the charge process oil input in the following manner:

$$\dot{m}_{R_{in}}^{oil_{dcg,id}} = \dot{m}_{CR}^{oil_{dcg,id}} + \dot{m}_{SR}^{oil_{dcg,id}} + \dot{m}_{OR}^{oil_{dcg,id}} = \dot{m}_{R_{in}}^{oil_{chg,id}} = \dot{m}_{CR}^{oil_{chg,id}} + \dot{m}_{SR}^{oil_{chg,id}}$$

$$\dot{m}_{CR}^{oil_{dcg,id}} + \dot{m}_{SR}^{oil_{dcg,id}} + \dot{m}_{OR}^{oil_{dcg,id}} = \dot{m}_{CR}^{oil_{chg,id}} + \dot{m}_{SR}^{oil_{chg,id}}$$

$$\dot{m}_{CR}^{oil_{chg,id}} - \dot{m}_{CR}^{oil_{dcg,id}} = \dot{m}_{OR}^{oil_{dcg,id}} = \dot{m}_{SO}^{oil_{chg,id}}$$

4.2.2.3 Mixing & Preheating

With $\eta_G^{dcg,id} = 0.23$ after setting $\eta_H^{dcg,id} = 0.20$ and $\eta_I^{dcg,id} = 0.12$ (see 4.2.2.6),

$$T_{SR}^{dcg,id} = T_\infty + \frac{\eta_H^{dcg,id} + \eta_I^{dcg,id}}{\eta_H^{dcg,id} + \eta_I^{dcg,id} + \eta_G^{dcg,id}} \left(T_R^{dcg,id} - T_\infty\right)$$

$$= 25°C + \frac{0.20 + 0.12}{0.20 + 0.12 + 0.23}(130°C - 25°C)$$

$$\boldsymbol{T_{SR}^{dcg,id} = 359.24K = 86.1°C}$$

$$T_{Z_{in}}^{dcg,id} = \frac{T_{SR}^{dcg,id} c_p^{oil,T_{SR}} \dot{m}_{SR}^{oil_{dcg,id}} + T_\infty \left(c_p^{oil,T_\infty}\left(\dot{m}_{CR}^{oil_{dcg,id}} + \dot{m}_{OR}^{oil_{dcg,id}}\right) + c_p^{MB,T_\infty} \dot{m}_{CR}^{MB_{dcg,id}}\right)}{c_p^{oil,T_{Z_{in}}} \dot{m}_{ZR}^{oil_{dcg,id}} + c_p^{MB,T_{Z_{in}}} \dot{m}_{CR}^{MB_{dcg,id}}}$$

Iterating this formula for equilibrium temperature of the inflows to Z comes to the closest result with heat capacities for $T_{Z_{in}}^{dcg,id} \approx 50°C$:

$$T_{Z_{in}}^{dcg,id}$$

$$= \frac{358.15K * 2.21\frac{kJ}{kg_{oil}K} * 2.34\frac{kg_{oil}}{h} + 298.15K\left(1.99\frac{kJ}{kg_{oil}K}(1.15 + 0.75)\frac{kg_{oil}}{h} + 1.21\frac{kJ}{kg_{MB}K} * 2.71\frac{kg_{MB}}{h}\right)}{2.08\frac{kJ}{kg_{oil}K} * 4.24\frac{kg_{oil}}{h} + 1.27\frac{kJ}{kg_{MB}K} * 2.71\frac{kg_{MB}}{h}}$$

$$\boldsymbol{T_{Z_{in}}^{dcg,id} = 322.74K = 49.6°C}$$

Knowing the input flow composition and temperature, the heating power to reach $T_{ZR}^{dcg,id} = T_R^{dcg,id}$ is then calculated with heat capacities from Table 4 at $\bar{T}_Z^{dcg,id} = \frac{T_R^{dcg,id} + T_{Z_{in}}^{dcg,id}}{2} = \frac{130°C + 49.6°C}{2} \approx 90°C$.

$$P_{th,Z}^{dcg,id} = \left(T_R^{dcg,id} - T_{Z_{in}}^{dcg,id}\right)\left(c_p^{oil,\bar{T}_Z^{dcg,id}} \dot{m}_{ZR}^{oil_{dcg,id}} + c_p^{MB,\bar{T}_Z^{dcg,id}} \dot{m}_{CR}^{MB_{chg,id}}\right)$$

$$= (130 - 49.6)K * \left(2.22\frac{kJ}{kg_{oil}K} * 4.24\frac{kg_{oil}}{h} + 1.33\frac{kJ}{kg_{MB}K} * 2.71\frac{kg_{MB}}{h}\right) * \frac{1h}{3600s}$$

$$\boldsymbol{P_{th,Z}^{dcg,id} = 0.29kW}$$

4.2.2.4 Evaporator

The required heating for evaporating $\dot{m}_{WE}^{H_2O(l)dcg,id}$ and overheating the steam to $T_R^{dcg,id} = 130°C$ is calculated using approximate constant heat capacities both for liquid water and steam:

$$P_{th,E}^{dcg,id} = \dot{m}_{WE}^{H_2O(l)dcg,id} \left(c_p^{H_2O,\bar{T}_{liquid}^{dcg,id}} (T_b - T_\infty) + \Delta h_V^{H_2O,T_b=100°C} + c_p^{H_2O,\bar{T}_{steam}^{chg,id}} (T_R^{dcg,id} - T_b) \right)$$

$$= 1.11 \frac{kg_{H_2O}}{h} * \frac{1h}{3600s} \left(4.19 \frac{kJ}{kg_{H_2O(l)}K} (100 - 25)K + 2256 \frac{kJ}{kg_{H_2O}} \right.$$

$$\left. + 2.00 \frac{kJ}{kg_{H_2O(g)}K} (130 - 100)K \right)$$

$$\boldsymbol{P_{th,E}^{dcg,id} = 0.81 kW}$$

Note that $-P_{th,L}^{chg,id} = 0.82kW$ is slightly higher in the share of overheated steam due to $T_R^{chg,id} - T_R^{dcg,id} = 20°C$.

4.2.2.5 Reactor

Formed Boric acid from stoichiometrically rehydrating Metaboric acid at $X_{dcg,id} = 1$ is quantified as

$$\dot{m}_{formed}^{BA_{dcg,id}} = \dot{m}_{CR}^{MB_{dcg,id}} + \dot{m}_{ER}^{H_2O_{dcg,id}} = \frac{1}{1-\omega} \dot{m}_{CR}^{MB_{dcg,id}} = \frac{1}{\omega} \dot{m}_{ER}^{H_2O_{dcg,id}} = \dot{m}_{SC}^{BA_{dcg,id}}$$

$$\dot{m}_{SC}^{BA_{dcg,id}} = \frac{1\ kg_{BA}}{0.71\ kg_{MB}} * 2.71 \frac{kg_{MB}}{h} = \frac{1\ kg_{BA}}{0.29\ kg_{H_2O}} * 1.11 \frac{kg_{H_2O}}{h}$$

$$\dot{m}_{SC}^{BA_{dcg,id}} = 3.82 \frac{kg_{BA}}{h}$$

After the reaction, the initial $\gamma_R^{dcg,id} = \frac{4.24 \frac{kg_{oil}}{h}}{2.71 \frac{kg_{MB}}{h}} = 1.56 \frac{kg_{oil}}{kg_{MB}}$ drops back to $\gamma_{RS}^{dcg,id} = \frac{4.24 \frac{kg_{oil}}{h}}{3.82 \frac{kg_{BA}}{h}} = \gamma_R^{chg,id} = 1.11 \frac{kg_{oil}}{kg_{BA}}$.

The suspension volume flow is calculated as:

$$\dot{V}_{R,susp}^{dcg,id} = \frac{\dot{m}_{CR}^{MB_{dcg,id}}}{\rho_{BA}} + \frac{\dot{m}_{ZR}^{oil_{dcg,id}}}{\rho_{oil}^{T_R^{dcg,id}}} = \frac{2.71}{2.045}\frac{l}{h} + \frac{4.24}{0.802}\frac{l}{h}$$

$$\dot{V}_{R,susp}^{dcg,id} = 6.6\frac{l}{h}$$

With an estimate of $\tau_R^{dcg,id} = 15min$, the reactor volume is calculated as:

$$V_R^{dcg,id} = (1 + \varepsilon_R)\dot{V}_{R,susp}^{dcg,id}\tau_R^{dcg,id} = (1 + 0.3) * 6.6\frac{l}{h} * 15min$$

$$V_R^{dcg,id} = 2.1l$$

4.2.2.6 Oil separation series

Setting $\eta_H^{dcg,id} = 0.20$ and $\eta_I^{dcg,id} = 0.12$,

$$\dot{m}_{HR}^{oil_{dcg,id}} = \eta_H^{dcg,id}\dot{m}_{RS}^{oil_{dcg,id}} = 0.20 * 4.24\frac{kg_{oil}}{h}$$

$$\dot{m}_{HR}^{oil_{dcg,id}} = 0.85\frac{kg_{oil}}{h}$$

With $\bar{T}_{R-\infty}^{dcg,id} = \frac{T_R^{dcg,id}+T_\infty}{2} \approx 80°C$, exergy flows follow as

$$\dot{Ex}_{HR}^{dcg,id} = \dot{m}_{HR}^{oil_{dcg,id}}c_p^{oil,\bar{T}_{R-\infty}^{dcg,id}}\left(T_\infty - T_R^{dcg,id}\right) = 0.85\frac{kg_{oil}}{h} * \frac{1h}{3600s} * 2.19\frac{kJ}{kg_{oil}K} * (25 - 130)K$$

$$\dot{Ex}_{HR}^{dcg,id} = -0.05kW$$

$$\dot{m}_{IR}^{oil_{dcg,id}} = \eta_I^{dcg,id}\dot{m}_{RS}^{oil_{dcg,id}} = 0.12 * 4.24\frac{kg_{oil}}{h}$$

$$\dot{m}_{IR}^{oil_{dcg,id}} = 0.51\frac{kg_{oil}}{h}$$

$$\dot{Ex}_{IR}^{dcg,id} = \dot{m}_{IR}^{oil_{dcg,id}}c_p^{oil,T_R^{dcg,id}}\left(T_\infty - T_R^{dcg,id}\right) = 0.51\frac{kg_{oil}}{h} * \frac{1h}{3600s} * 2.19\frac{kJ}{kg_{oil}K} * (25 - 130)K$$

$$\dot{Ex}_{IR}^{dcg,id} = -0.03kW$$

Solving $\dot{m}_{SR}^{oil_{dcg,id}} = \dot{m}_{HR}^{oil_{dcg,id}} + \dot{m}_{IR}^{oil_{chg,id}} + \dot{m}_{GR}^{oil_{dcg,id}}$ for $\dot{m}_{GR}^{oil_{dcg,id}}$ yields

$$\dot{m}_{GR}^{oil_{dcg,id}} = \dot{m}_{SR}^{oil_{dcg,id}} - \dot{m}_{HR}^{oil_{dcg,id}} - \dot{m}_{IR}^{oil_{chg,id}} = (2.34 - 0.85 - 0.51)\frac{kg_{oil}}{h}$$

$$\dot{m}_{GR}^{oil_{dcg,id}} = 0.98 \frac{kg_{oil}}{h}$$

And subsequently,

$$\eta_G^{dcg,id} = \frac{\dot{m}_{GR}^{oil_{dcg,id}}}{\dot{m}_{RS}^{oil_{dcg,id}}} = \frac{0.98}{4.24}$$

$$\eta_G^{dcg,id} = 0.23$$

The remaining oil stored in the concentrate is

$$\dot{m}_{SC}^{oil_{dcg,id}} = \dot{m}_{RS}^{oil_{dcg,id}}\left(1 - \eta_H^{dcg,id} - \eta_I^{dcg,id} - \eta_G^{dcg,id}\right) = 4.24\frac{kg_{oil}}{h} * (1 - 0.20 - 0.12 - 0.23)$$

$$= \gamma_C^{chg,id}\dot{m}_{SC}^{BA_{dcg,id}} = 0.497 \frac{kg_{oil}}{kg_{BA}} * 3.82 \frac{kg_{BA}}{h}$$

$$\dot{m}_{SC}^{oil_{dcg,id}} = 1.90 \frac{kg_{oil}}{h}$$

For the heat extraction of the sedimentation column G, we first solve

$$\dot{m}_{IG}^{oil_{dcg,id}} = \dot{m}_{RS}^{oil_{dcg,id}} - \dot{m}_{HR}^{oil_{dcg,id}} - \dot{m}_{IR}^{oil_{dcg,id}} = (4.24 - 0.85 - 0.51)\frac{kg_{oil}}{h} = 2.88\frac{kg_{oil}}{h}$$

Which leads to

$$P_{th,G}^{dcg,id} = \left(T_\infty - T_R^{dcg,id}\right)\left(c_p^{BA,\bar{T}_{R-\infty}^{dcg,id}} \dot{m}_{GC}^{BA_{dcg,id}} + c_p^{oil,\bar{T}_{R-\infty}^{dcg,id}} \dot{m}_{IG}^{oil_{dcg,id}}\right)$$

$$P_{th,G}^{dcg,id} = (25 - 130)K * \left(1.49 \frac{kJ}{kg_{BA}K} * 3.82 \frac{kg_{BA}}{h} + 2.19 \frac{kJ}{kg_{oil}K} 2.88 \frac{kg_{oil}}{h}\right) * \frac{1h}{3600s}$$

$$P_{th,G}^{dcg,id} = -0.35 kW$$

4.3 Conversion profiling of the charge process

4.3.1 Input from suspension concentrate

Based on the target value for heat generation P_{th}^{chg} and the expected conversion rate X_{chg},

$$\dot{m}_{CR}^{BA_{chg}} = \frac{P_{th,dehyd}^{chg}}{\Delta_{chg} h_{BA}° X_{chg}}$$

Eq. 4.49

As the first mass flow that is considered, $\dot{m}_{CR}^{BA_{chg}}$ serves as the base for all subsequent dimensionless mass flows ζ_j^i. The conversion factor $\frac{1}{\dot{m}_{CR}^{BA_{chg}}}$ for dimensionless forms is used for all equations throughout this thesis expressing ζ and will not be explicitly stated, for better readability.

The precise definition (other than the simplified Eq. 4.2) of the oil-to-solid mass ratio of the concentrate γ_C^{dcg} is:

$$\gamma_C^{chg} = \frac{\dot{m}_{CR}^{oil_{chg}}}{\dot{m}_{CR}^{(BA+MB)_{chg}}} = \frac{\varepsilon_C^{chg} \rho_{oil}}{\left(1 - \varepsilon_C^{chg}\right)\rho_{BA+MB}}$$

Eq. 4.50

To account for the presence of both boric acid and metaboric acid, a mean density was defined as:

$$\rho_{BA+MB} = \rho_{BA} + (\rho_{MB} - \rho_{BA})\frac{m_{MB}}{m_{BA} + m_{MB}}$$

Eq. 4.51

The same needs to be applied to modify $\varepsilon_C^{chg,id}$ from Eq. 4.3 to ε_C^{dcg}:

$$\varepsilon_C^{chg} = \lim_{t\to\infty}\left[\frac{V_{susp.oil}(t)}{V_{susp}(t)}\right]_{C,chg} = \lim_{t\to\infty}\left[\frac{V_{oil}(t)}{V_{susp.oil}(t) + V_{BA+MB}}\right]_{C,chg}$$

$$\varepsilon_C^{chg} = \lim_{t\to\infty}\left[\frac{1}{1 + \frac{V_{BA+MB}}{V_{susp.oil}(t)}}\right]_{C,chg}$$

Eq. 4.52

Note that, while the volume was adjusted (from pure boric acid in Eq. 4.3), it was still assumed here that the suspension will reach its maximum density; In practice, to cut costs by shortening the sedimentation time, ε_C will likely be higher than what is presented in this thesis.

4.3.2 Conveyor & preheating

No changes in composition were considered during the tasks of mixing and preheating the flows.

Increasing the suspension ratio for the reaction suspension is one of the key targets for the conveyor unit. The suspension ratio for the reaction suspension is defined as:

$$\gamma_R^{chg} = \frac{\dot{m}_{ZR}^{oil_{chg}}}{\dot{m}_{CR}^{(BA+MB)_{chg}}} = \frac{\dot{m}_{CR}^{oil_{chg}} + \dot{m}_{SR}^{oil_{chg}}}{\dot{m}_{CR}^{(BA+MB)_{chg}}}$$

Eq. 4.53

4.3.3 Reactor

The preheated suspension is heated to reaction temperature and releases chemically bound water from the Boric acid. The following conversion rate is used to quantify the changes in the reactor:

$$X_{chg} = 1 - \left[\frac{\dot{m}_{in}^{BA}}{\dot{m}_{out}^{BA}}\right]_{R,chg}$$

Eq. 4.54

With the assumptions that will follow, it can be simplified to:

$$X_{chg} \approx 1 - \frac{\dot{m}_{CR}^{BA_{chg}}}{\dot{m}_{R_{out}}^{BA_{chg}}}$$

Eq. 4.55

4.3.3.1 Boric acid

The material balance for boric acid in the charge reactor is composed of the following contributions:

$$\dot{m}_{ZR}^{BA_{chg}} - \dot{m}_{X_{chg}}^{BA} - \dot{m}_{R_{out}}^{BA_{chg}} = 0$$

Eq. 4.56

The flow of boric acid into the reactor consists of the input from concentrate and residual boric acid from the oil cycle:

$$\dot{m}_{ZR}^{BA_{chg}} = \dot{m}_{CR}^{BA_{chg}} + \dot{m}_{SR}^{BA_{chg}}$$

Eq. 4.57

After the reaction, the unreacted boric acid is mostly passed on to the separation series, and a small fraction is expected to enter the condenser:

$$\dot{m}_{R_{out}}^{BA_{chg}} = \dot{m}_{RS}^{BA_{chg}} + \dot{m}_{RL}^{BA_{chg}}$$

Eq. 4.58

In the charge reaction, boric acid is consumed:

$$\dot{m}_{X_{chg}}^{BA} = \left(\dot{m}_{CR}^{BA_{chg}} + \dot{m}_{SR}^{BA_{chg}}\right) X_{chg}$$

Eq. 4.59

Altogether, the boric acid material balance over the charge reactor is:

$$\dot{m}_{CR}^{BA_{chg}} + \dot{m}_{SR}^{BA_{chg}} = \dot{m}_{RS}^{BA_{chg}} + \dot{m}_{RL}^{BA_{chg}} + \left(\dot{m}_{CR}^{BA_{chg}} + \dot{m}_{SR}^{BA_{chg}}\right) X_{chg}$$

$$\Rightarrow$$

$$\left(\dot{m}_{CR}^{BA_{chg}} + \dot{m}_{SR}^{BA_{chg}}\right)\left(1 - X_{chg}\right) - \dot{m}_{RS}^{BA_{chg}} - \dot{m}_{RL}^{BA_{chg}} = 0$$

To introduce a dimensionless form of the equations in this chapter 4.3 and the following, 4.4, with $\dot{m}_{CR}^{BA_{chg}}$ selected as the base , as it is the initial target mass flow.

Thus,

$$\left(\dot{m}_{CR}^{BA_{chg}} + \dot{m}_{SR}^{BA_{chg}}\right)\left(1 - X_{chg}\right) - \dot{m}_{RS}^{BA_{chg}} - \dot{m}_{RL}^{BA_{chg}} = 0 \qquad \Big| * \frac{1}{\dot{m}_{CR}^{BA_{chg}}} \Rightarrow$$

$$\left(1 + \zeta_{SR}^{BA_{chg}}\right)\left(1 - X_{chg}\right) - \zeta_{RS}^{BA_{chg}} - \zeta_{RL}^{BA_{chg}} = 0$$

<div align="right">Eq. 4.60</div>

Compared to the boric acid input from concentrate, the traces permeating the filter membranes of the separation units are negligibly small:

$$\dot{m}_{CR}^{BA_{chg}} \gg \dot{m}_{SR}^{BA_{chg}}$$

This yields the simplified material balance of boric acid over the charge reactor:

$$\dot{m}_{CR}^{BA_{chg}}\left(1 - X_{chg}\right) - \dot{m}_{RS}^{BA_{chg}} - \dot{m}_{RL}^{BA_{chg}} \approx 0$$

$$1 - X_{chg} - \zeta_{RS}^{BA_{chg}} - \zeta_{RL}^{BA_{chg}} \approx 0$$

<div align="right">Eq. 4.61</div>

4.3.3.2   Metaboric acid

The material balance of metaboric acid over the charge reactor is

$$\dot{m}_{ZR}^{MB_{chg}} + \dot{m}_{X_{chg}}^{MB} - \dot{m}_{R_{out}}^{MB_{dcg}} = 0$$

<div align="right">Eq. 4.62</div>

The inflow is composed of:

$$\dot{m}_{ZR}^{MB_{chg}} = \dot{m}_{CR}^{MB_{chg}} + \dot{m}_{SR}^{MB_{chg}}$$

<div align="right">Eq. 4.63</div>

The outflow is composed of:

$$\dot{m}_{R_{out}}^{MB_{dcg}} = \dot{m}_{RS}^{MB_{chg}} + \dot{m}_{RL}^{MB_{chg}}$$

Eq. 4.64

Formed boric acid is quantified as:

$$\dot{m}_{X_{chg}}^{MB} = (1 - \omega)\left(\dot{m}_{CR}^{BA_{chg}} + \dot{m}_{SR}^{BA_{chg}}\right)X_{chg}$$

Eq. 4.65

Altogether,

$$(1 - \omega)\left(\dot{m}_{CR}^{BA_{chg}} + \dot{m}_{SR}^{BA_{chg}}\right)X_{chg} + \dot{m}_{CR}^{MB_{chg}} + \dot{m}_{SR}^{MB_{chg}} - \dot{m}_{RS}^{MB_{chg}} - \dot{m}_{RL}^{MB_{chg}} = 0$$

$$(1 - \omega)\left(1 + \zeta_{SR}^{BA_{chg}}\right)X_{chg} + \zeta_{CR}^{MB_{chg}} + \zeta_{SR}^{MB_{chg}} - \zeta_{RS}^{MB_{chg}} - \zeta_{RL}^{MB_{chg}} = 0$$

Eq. 4.66

It was assumed that possible traces of metaboric acid leaving the reaction suspension in the gas phase are spontaneously rehydrated to boric acid, rendering the metaboric outflow to the condenser zero:

$$\dot{m}_{RL}^{MB_{chg}} = 0$$

Compared to the formed metaboric acid in the reaction, its traces permeating the filter membranes of the separation units are negligibly small:

$$(1 - \omega)\dot{m}_{CR}^{BA_{chg}}X_{chg} \gg \dot{m}_{SR}^{MB_{chg}}$$

These two assumptions and $\dot{m}_{CR}^{BA_{chg}} \gg \dot{m}_{SR}^{BA_{chg}}$ (4.3.3.1) yield the simplified material balance of metaboric acid over the charge reactor:

$$(1 - \omega)\dot{m}_{CR}^{BA_{chg}}X_{chg} + \dot{m}_{CR}^{MB_{chg}} - \dot{m}_{RS}^{MB_{chg}} \approx 0$$

$$(1 - \omega)X_{chg} + \zeta_{CR}^{MB_{chg}} - \zeta_{RS}^{MB_{chg}} \approx 0$$

Eq. 4.67

4.3.3.3 Water

The balance for water in the discharge reactor is composed of the following contributions:

$$\dot{m}_{ZR}^{H_2O_{chg}} + \dot{m}_{X_{dcg}}^{H_2O} - \dot{m}_{R_{out}}^{H_2O_{chg}} = 0$$

Eq. 4.68

As explained for the previous materials, the contained terms are:

$$\dot{m}_{ZR}^{H_2O_{chg}} = \dot{m}_{CR}^{H_2O_{chg}} + \dot{m}_{SR}^{H_2O_{chg}}$$

Eq. 4.69

$$\dot{m}_{R_{out}}^{H_2O_{chg}} = \dot{m}_{RS}^{H_2O_{chg}} + \dot{m}_{RL}^{H_2O_{chg}}$$

Eq. 4.70

$$\dot{m}_{X_{chg}}^{H_2O} = \omega \left(\dot{m}_{CR}^{BA_{chg}} + \dot{m}_{SR}^{BA_{chg}} \right) X_{chg}$$

Eq. 4.71

In the charge reactor, the amounts of water entering the reactor are considered negligible compared to the formed steam:

$$\dot{m}_{ZR}^{H_2O_{chg}} \ll \dot{m}_{R_{out}}^{H_2O_{chg}}$$

The mass balance of water over the charge reactor is

$$\omega \left(\dot{m}_{CR}^{BA_{chg}} + \dot{m}_{SR}^{BA_{chg}} \right) X_{chg} + \dot{m}_{CR}^{H_2O_{chg}} + \dot{m}_{SR}^{H_2O_{chg}} - \dot{m}_{RS}^{H_2O_{chg}} - \dot{m}_{RL}^{H_2O_{chg}} = 0$$

$$\omega \left(1 + \zeta_{SR}^{BA_{chg}} \right) X_{chg} + \zeta_{CR}^{H_2O_{chg}} + \zeta_{SR}^{H_2O_{chg}} - \zeta_{RS}^{H_2O_{chg}} - \zeta_{RL}^{H_2O_{chg}} = 0$$

Eq. 4.72

Given that the specific volume of steam ($1694 \frac{m^3}{kg}$ at 1 bar [21]) is substantially higher than that of liquid water, and high volumetric steam contents in the suspension outlet of the reactor are undesired, the mass content of water entering and leaving the oil separation series is considered negligibly small:

$$\dot{m}_{RS}^{H_2O_{chg}} \ll \omega \dot{m}_{CR}^{BA_{chg}} X_{chg}$$

$$\dot{m}_{SR}^{H_2O_{chg}} \ll \omega \dot{m}_{CR}^{BA_{chg}} X_{chg}$$

Together with $\dot{m}_{CR}^{BA_{chg}} \gg \dot{m}_{SR}^{BA_{chg}}$ (4.3.3.1), the simplified material balance of water over the charge reactor is

$$\omega \dot{m}_{CR}^{BA_{chg}} X_{chg} + \dot{m}_{CR}^{H_2O_{chg}} - \dot{m}_{RL}^{H_2O_{chg}} \approx 0$$

$$\omega X_{chg} + \zeta_{CR}^{H_2O_{chg}} - \zeta_{RL}^{H_2O_{chg}} \approx 0$$

Eq. 4.73

It is explicitly notable that although some flows of water are negligible in terms of mass, the corresponding volume flows are to be considered thoroughly, given that these flows will be steam under the current design. Because of this, although $\dot{m}_{RS}^{H_2O_{chg}}$ and $\dot{m}_{SR}^{H_2O_{chg}}$ were neglected for the reactor mass balance, the possibly high corresponding volume flow of $\dot{m}_{RS}^{H_2O_{chg}}$ justifies its calculation.

As a first estimate for $\dot{m}_{RS}^{H_2O_{chg}}$, the following equations are used:

$$\omega \dot{m}_{CR}^{BA_{chg}} X_{chg} + \dot{m}_{CR}^{H_2O_{chg}} - \dot{m}_{RL}^{H_2O_{chg}} - \dot{m}_{RS}^{H_2O_{chg}} \approx 0$$

$$\omega X_{chg} + \zeta_{CR}^{H_2O_{chg}} - \zeta_{RL}^{H_2O_{chg}} - \zeta_{RS}^{H_2O_{chg}} \approx 0$$

<div align="right">Eq. 4.74</div>

Put in words, the two water flows out of the reactor RL and RS are composed of the water residues fed from the storage tank into the reactor CR, and formed water based on the dehydration of boric acid only from the storage tank, neglecting the dehydration of recycled boric acid through the process.

4.3.4   Condenser

To quantify the amount of water caught in the condenser relative to the amount of water released by the reaction, another factor was introduced:

$$\eta_L = \frac{\dot{m}_{RL}^{H_2O}}{\dot{m}_{rct}^{H_2O}}$$

<div align="right">Eq. 4.75</div>

While in this thesis, $\dot{m}_{rct}^{H_2O} = \omega \dot{m}_{ZR}^{BA_{chg}} X_{chg}$ with ω only accounting for chemically bound water, the amount of released water during the reaction could be higher due to absorbed water. Also, traces of water entering the reactor and not originating from the reaction have an influence, and η_L could exceed 1, especially when overstoichiometric quantities of water are used in the discharge process. Nevertheless, $\dot{m}_{rct}^{H_2O}$ seems to be the most reasonable reference value for steam extraction, as the amount of adsorbed water and its sorption energy on the particle surface is not known at this point.

$$\dot{m}_{RL}^{H_2O} = \eta_L X_{chg} \omega \dot{m}_{ZR}^{BA_{chg}}$$

<div align="right">Eq. 4.76</div>

With 4.3.3.1,

$$\dot{m}_{RL}^{H_2O} \approx \eta_L X_{chg} \omega \dot{m}_{CR}^{BA_{chg}}$$

<div align="right">Eq. 4.77</div>

To allow a quantification of oil and boric acid carried away from the reactor through the condensing route, auxiliary factors relative to the mass flow of condensed water are introduced as follows:

$$\theta_L^i = \frac{\dot{m}_{RL}^i}{\dot{m}_{RL}^{H_2O}}$$

$$i \ldots BA, oil$$

<div align="right">Eq. 4.78</div>

It was assumed that all mass flows entering the condenser ($i \ldots BA, oil, H_2O$) will end up in the water

storage tank unchanged in composition and without debris buildup in the condensator:

$$\dot{m}_{RL}^i = \dot{m}_{LW}^i$$

The purge gas flow is not included in the calculations and should be considered zero in terms of mass.

4.3.5 Oil separation units, storage and recycling of oil

As introduced above, the oil added to the concentrate for a manageable suspension in the reactor is provided by three separate units: A Hydrocyclone ($j = H$), an intermediate tubular membrane filter ($j = I$), and a sedimentation column ($j = G$), For each of them, oil extraction efficiencies were introduced, and the formation of a sum ($j = S$) is also possible:

$$\eta_j = \frac{\dot{m}_{j,extracted}^{oil}}{\dot{m}_{RS}^{oil}}$$

<div align="right">Eq. 4.79</div>

$\dot{m}_{j,extracted}^{oil}$ represents the extracted oil flows of the separation units, on the routes HR, IR, and GO+GR.

Factors quantifying the amounts of solids and water carried away from the units are defined as

$$\theta_j^i = \frac{\dot{m}_{j,extracted}^i}{\dot{m}_{j,extracted}^{oil}}$$

$$i \dots H_2O, BA + MB$$

<div align="right">Eq. 4.80</div>

For the latter of above indexes, $BA + MB$ signifies that the membrane was considered to be non-selective between boric acid and metaboric acid. As a theoretical example, with

$$\dot{m}_{j,in}^{BA} = 0.8\frac{kg}{h}; \dot{m}_{j,in}^{MB} = 3\frac{kg}{h}; \dot{m}_{j,extracted}^{oil} = 1\frac{kg}{h}; \theta_j^{BA+MB} = 0.01$$

the total of $BA + MB$ extracted would be

$$\dot{m}_{j,extracted}^{BA+MB} = 1\frac{kg_{oil}}{h} * 0.01 = 0.01\frac{kg_{BA+MB}}{h}$$

and the contents of boric acid and metaboric acid would be

$$\dot{m}_{j,extracted}^{BA} = \dot{m}_{j,extracted}^{BA+MB}\frac{\dot{m}_{j,in}^{BA}}{\dot{m}_{j,in}^{BA} + \dot{m}_{j,in}^{MB}} = 0.01 * \frac{0.8}{0.8 + 3} = 0.0021\frac{kg_{BA}}{h}$$

$$\dot{m}_{j,extracted}^{MB} = \dot{m}_{j,extracted}^{BA+MB}\frac{\dot{m}_{j,in}^{MB}}{\dot{m}_{j,in}^{BA} + \dot{m}_{j,in}^{MB}} = 0.01 * \frac{3}{0.8 + 3} = 0.0079\frac{kg_{MB}}{h}$$

In a first estimation, η_j and θ_j^i are considered as constant through subsequent process runs, while two sets of variables were set – one for charge, another for discharge processes.

Extracting the chemically bound water from boric acid raises the solid density of the remaining metaboric acid, leading to the assumption that the lowered volume of solid matter releases a certain amount of process oil that exceeds the desired γ_R. In other words, applied to the charge and discharge process, required values for γ change with the content of metaboric acid relative to boric acid, and γ_C^{dcg} as well as γ_R^{dcg} are lower than γ_C^{chg} and γ_R^{chg} when held at the same ratio $\frac{V_{oil}}{V_{BA+MB}}$. Consequently, process oil is released and stored during the charge process, and later added to the discharge process to compensate the particle volume increase caused by fixation of water in metaboric acid particles, i.e., the formation of boric acid. This prevents an undesired thickening of the discharge suspension.

The variable σ_O presents the amount of oil extracted at the sedimentation column in the charge process that is held in the oil storage tank, so that only the required amount of oil set by γ_R^{chg} is recycled to the reactor. This variable uses the sum of boric acid and metaboric acid flows in CR as a base.

$$\dot{m}_{ZR}^{oil_{chg}} = \gamma_R^{chg} \dot{m}_{CR}^{(BA+MB)_{chg}}$$

<div align="right">Eq. 4.81</div>

$$\dot{m}_{CR}^{(BA+MB)_{chg}} = \dot{m}_{CR}^{BA_{chg}} + \dot{m}_{CR}^{MB_{chg}}$$

The recycled fraction of oil extracted in the sedimentation column G is:

$$\dot{m}_{GR}^{oil_{chg}} = \dot{m}_{R_{in}}^{oil_{chg}} - \dot{m}_{CR}^{oil_{chg}} - \dot{m}_{HR}^{oil_{chg}} - \dot{m}_{IR}^{oil_{chg}}$$

<div align="right">Eq. 4.82</div>

Whereas the stored amount is:

$$\dot{m}_{GO}^{oil_{chg}} = \eta_G \dot{m}_{RH}^{oil_{chg}} - \dot{m}_{GR}^{oil_{chg}}$$

<div align="right">Eq. 4.83</div>

A factor to quantify the stored oil based on the oil extracted in the sedimentation column G was be defined as:

$$\sigma_O = \frac{\dot{m}_{GO}^{oil_{chg}}}{\dot{m}_{GO}^{oil_{chg}} + \dot{m}_{GR}^{oil_{chg}}}$$

<div align="right">Eq. 4.84</div>

The following equations summarize the flows in and out of the separation series:

$$\dot{m}_{RS}^{i_{chg}} - \dot{m}_{SC}^{i_{chg}} - \dot{m}_{SR}^{i_{chg}} - \dot{m}_{SO}^{i_{chg}} = 0$$

$$\zeta_{RS}^{i_{chg}} - \zeta_{SC}^{i_{chg}} - \zeta_{SR}^{i_{chg}} - \zeta_{SO}^{i_{chg}} = 0$$

<div align="right">Eq. 4.85</div>

4.3.6 Reactor + oil separation series

This chapter presents the material balances over the combination of the charge reactor and the following oil separation series.

4.3.6.1 Boric acid

The material balance of boric acid over the combination of the charge reactor and the following oil separation series is:

$$\dot{m}_{CR}^{BA_{chg}} - \left(\dot{m}_{CR}^{BA_{chg}} + \dot{m}_{SR}^{BA_{chg}}\right)X_{chg} - \dot{m}_{RL}^{BA_{chg}} - \dot{m}_{SO}^{BA_{chg}} - \dot{m}_{SC}^{BA_{chg}} = 0$$

$$1 - \left(1 + \zeta_{SR}^{BA_{chg}}\right)X_{chg} - \zeta_{RL}^{BA_{chg}} - \zeta_{SO}^{BA_{chg}} - \zeta_{SC}^{BA_{chg}} = 0$$

Eq. 4.86

Analog to the simplification introduced in 4.3.3.1, $\dot{m}_{CR}^{BA_{chg}}$ was considered large enough to neglect all the other flows, except the output flow to the concentrate storage tank $\dot{m}_{SC}^{BA_{chg}}$:

$$\dot{m}_{CR}^{BA_{chg}} \gg \dot{m}_{SR}^{BA_{chg}} + \dot{m}_{RL}^{BA_{chg}} + \dot{m}_{SO}^{BA_{chg}} \Rightarrow$$

$$\dot{m}_{CR}^{BA_{chg}}\left(1 - X_{chg}\right) - \dot{m}_{SC}^{BA_{chg}} \approx 0$$

$$1 - X_{chg} - \zeta_{SC}^{BA_{chg}} \approx 0$$

Eq. 4.87

4.3.6.2 Metaboric acid

The material balance of metaboric acid over the combination of the charge reactor and the following oil separation series is:

$$\dot{m}_{CR}^{MB_{chg}} + (1 - \omega)\left(\dot{m}_{CR}^{BA_{chg}} + \dot{m}_{SR}^{BA_{chg}}\right)X_{chg} - \dot{m}_{RL}^{MB_{chg}} - \dot{m}_{SO}^{MB_{chg}} - \dot{m}_{SC}^{MB_{chg}} = 0$$

$$\zeta_{CR}^{MB_{chg}} + (1 - \omega)\left(\zeta_{CR}^{BA_{chg}} + \zeta_{SR}^{BA_{chg}}\right)X_{chg} - \zeta_{RL}^{MB_{chg}} - \zeta_{SO}^{MB_{chg}} - \zeta_{SC}^{MB_{chg}} = 0$$

Eq. 4.88

With the simplifications $\dot{m}_{CR}^{BA_{chg}} \gg \dot{m}_{SR}^{BA_{chg}}$; $\dot{m}_{RL}^{MB_{chg}} \approx 0$ (as introduced in 4.3.3.1 and 4.3.3.2), and assuming a negligible trace of metaboric acid stored in the oil tank:

$$\dot{m}_{SC}^{MB_{chg}} \gg \dot{m}_{SO}^{MB_{chg}}$$

We obtain the simplified material balance of metaboric acid over the combination of the charge reactor and the following oil separation series:

$$\dot{m}_{CR}^{MB_{chg}} + (1 - \omega)\dot{m}_{CR}^{BA_{chg}}X_{chg} - \dot{m}_{SC}^{MB_{chg}} \approx 0$$

$$\zeta_{CR}^{MB_{chg}} + (1 - \omega)\zeta_{CR}^{BA_{chg}} X_{chg} - \zeta_{SC}^{MB_{chg}} \approx 0$$

<div align="right">Eq. 4.89</div>

4.3.6.3 Water

The material balance of water over the combination of the charge reactor and the following oil separation series is

$$\dot{m}_{CR}^{H_2O_{chg}} + \omega \left(\dot{m}_{CR}^{BA_{chg}} + \dot{m}_{SR}^{BA_{chg}} \right) X_{chg} - \dot{m}_{RL}^{H_2O_{chg}} - \dot{m}_{SO}^{H_2O_{chg}} - \dot{m}_{SC}^{H_2O_{chg}} = 0$$

$$\zeta_{CR}^{H_2O_{chg}} + \omega \left(\zeta_{CR}^{BA_{chg}} + \zeta_{SR}^{BA_{chg}} \right) X_{chg} - \zeta_{RL}^{H_2O_{chg}} - \zeta_{SO}^{H_2O_{chg}} - \zeta_{SC}^{H_2O_{chg}} = 0$$

<div align="right">Eq. 4.90</div>

With the simplification $\dot{m}_{CR}^{BA_{chg}} \gg \dot{m}_{SR}^{BA_{chg}}$ (4.3.3.1), and assuming $\dot{m}_{RL}^{H_2O_{chg}} \gg \dot{m}_{SO}^{H_2O_{chg}} + \dot{m}_{SC}^{H_2O_{chg}}$ based on the considerations of 4.3.3.3, we obtain the simplified material balance of water over the combination of the charge reactor and the following oil separation series:

$$\dot{m}_{CR}^{H_2O_{chg}} + \omega \dot{m}_{CR}^{BA_{chg}} X_{chg} - \dot{m}_{RL}^{H_2O_{chg}} \approx 0$$

$$\zeta_{CR}^{H_2O_{chg}} + \omega \zeta_{CR}^{BA_{chg}} X_{chg} - \zeta_{RL}^{H_2O_{chg}} \approx 0$$

<div align="right">Eq. 4.91</div>

4.3.6.4 Oil

The material balance of oil over the combination of the charge reactor and the following oil separation series is

$$\dot{m}_{CR}^{oil_{chg}} - \dot{m}_{RL}^{oil_{chg}} - \dot{m}_{SO}^{oil_{chg}} - \dot{m}_{SC}^{oil_{chg}} = 0$$

$$\zeta_{CR}^{oil_{chg}} - \zeta_{RL}^{oil_{chg}} - \zeta_{SO}^{oil_{chg}} - \zeta_{SC}^{oil_{chg}} = 0$$

<div align="right">Eq. 4.92</div>

By neglecting the flow of oil to the condenser,

$$\dot{m}_{CR}^{oil_{chg}} \gg \dot{m}_{RL}^{oil_{chg}}$$

We obtain the simplified material balance of oil over the combination of the charge reactor and the following oil separation series:

$$\dot{m}_{CR}^{oil_{chg}} - \dot{m}_{SO}^{oil_{chg}} - \dot{m}_{SC}^{oil_{chg}} = 0$$

$$\zeta_{CR}^{oil_{chg}} - \zeta_{SO}^{oil_{chg}} - \zeta_{SC}^{oil_{chg}} = 0$$

<div align="right">Eq. 4.93</div>

4.3.7 Suspension concentrate (process end)

It was assumed that all residual process water, collected in the suspension concentrate, will react with the stoichiometric excess of metaboric acid and form boric acid again, given a typical storage duration. Another simplifying assumption was that boric acid will be formed until the limiting component is depleted, i.e., all available reaction pairs find each other. In the case of the process output SC to C_{dcg}, i.e., the concentrate after the charging process, it is safe to say that metaboric acid will be in stoichiometric excess and water the limiting factor.

In the calculations presented in this thesis, the amounts of water caught in the concentrate tank after charging is negligible compared to the flow to the condenser; Nevertheless, a mathematical description of the assumed (undesired) rehydration to boric acid might be necessary especially in the discharge process under overstoichiometric water addition, and for the case that the condenser does not collect the amounts of water assumed in this thesis.

4.3.7.1 Boric acid

The "effective" mass flow to the concentrate storage tank, i.e., assuming that residual water will react with metaboric acid during prolonged storage times, is quantified as:

$$\dot{m}_{SC}^{BA_{effective,chg}} = \dot{m}_{SC}^{BA_{chg}} + \left(1 + \frac{1-\omega}{\omega}\right)\dot{m}_{SC}^{H_2O_{chg}}$$

$$\zeta_{SC}^{BA_{effective,chg}} = \zeta_{SC}^{BA_{chg}} + \left(1 + \frac{1-\omega}{\omega}\right)\zeta_{SC}^{H_2O_{chg}}$$

Eq. 4.94

Thus, the "effective" mass flow of boric acid increases when $\dot{m}_{SC}^{H_2O_{chg}} > 0$:

$$\dot{m}_{SC}^{BA_{effective,chg}} \geq \dot{m}_{SC}^{BA_{chg}}$$

4.3.7.2 Metaboric acid

Metaboric acid is partly consumed in the storage rehydration:

$$\dot{m}_{SC}^{MB_{effective,chg}} = \dot{m}_{SC}^{MB_{chg}} - \left(\frac{1-\omega}{\omega}\right)\dot{m}_{SC}^{H_2O_{chg}}$$

$$\zeta_{SC}^{MB_{effective,chg}} = \zeta_{SC}^{MB_{chg}} - \left(\frac{1-\omega}{\omega}\right)\zeta_{SC}^{H_2O_{chg}}$$

Eq. 4.95

$$\dot{m}_{SC}^{MB_{effective,chg}} \leq \dot{m}_{SC}^{MB_{chg}}$$

4.3.7.3   Water

Given that metaboric acid is the target product and water an undesired residue, it is safe to say that all the water stored alongside the metaboric acid concentrate will be consumed, under the stated assumption of full rehydration during prolonged storage times:

$$\dot{m}_{SC}^{H_2O_{effective,chg}} = 0$$

$$\zeta_{SC}^{H_2O_{effective,chg}} = 0$$

Eq. 4.96

4.4 Conversion profiling of the discharge process

4.4.1 Input from suspension concentrate

For improved understanding of the process flows, the discharge concentrate input flows to the discharge reactor $\dot{m}_{CR}^{i_{dcg}}$ are set as the charge product concentrate after storage, i.e., after rehydration of metaboric acid with the water residue (until water is depleted):

$$\dot{m}_{CR}^{i_{dcg(n)}} = \dot{m}_{SC}^{i_{effective,chg(n)}}$$

<div align="right">Eq. 4.97</div>

The index n represents the charge-discharge cycle, $n = 1, 2, ...$

Unlike the ideal scenario, where the oil-to-solid ratio at the sedimentation column outlet to the charge product concentrate already equals the oil-to-solid ratio of the following discharge process, $\gamma_C^{dcg,id} = \frac{\dot{m}_{CR}^{oil_{dcg,id}}}{\dot{m}_{CR}^{(BA+MB)_{dcg,id}}} = \frac{\dot{m}_{CR}^{oil_{dcg,id}}}{\dot{m}_{CR}^{MB_{dcg,id}}} = \frac{\dot{m}_{SC}^{oil_{chg,id}}}{\dot{m}_{SC}^{MB_{chg,id}}}$, in the non-ideal scenario, changes in composition during prolonged storage need to be considered.

Analog to 4.3.1, the oil to solid ration of the discharge concentrate, and the contained terms, are:

$$\gamma_C^{dcg} = \frac{\dot{m}_{CR}^{oil_{dcg}}}{\dot{m}_{CR}^{(BA+MB)_{dcg}}} = \frac{\varepsilon_C^{dcg}\rho_{oil}}{\left(1 - \varepsilon_C^{dcg}\right)\rho_{BA+MB}}$$

<div align="right">Eq. 4.98</div>

$$\rho_{BA+MB} = \rho_{BA} + (\rho_{MB} - \rho_{BA})\frac{m_{MB}}{m_{BA} + m_{MB}}$$

$$\varepsilon_C^{dcg} = \lim_{t \to \infty}\left[\frac{1}{1 + \frac{V_{BA+MB}}{V_{susp.oil}(t)}}\right]_{C,dcg}$$

<div align="right">Eq. 4.99</div>

Note that, while the volume was adjusted (from pure boric acid in 4.1.1.1 to $BA + MB$), it was still assumed here that the suspension will reach its theoretical maximum density; In practice, to cut costs by shortening the sedimentation time, ε_C will likely be higher than presented in this thesis, reducing the volumetric energy density of the suspension.

4.4.2 Conveyor & preheating

The same units as in the charge step are used in the discharge process for the task of mixing, conveying and preheating the reactor inflow ZR. The increased suspension ratio for the reaction is:

$$\gamma_R^{dcg} = \frac{\dot{m}_{ZR}^{oil_{dcg}}}{\dot{m}_{CR}^{(BA+MB)_{dcg}}} = \frac{\dot{m}_{CR}^{oil_{dcg}} + \dot{m}_{SR}^{oil_{dcg}} + \dot{m}_{OR}^{oil_{dcg}}}{\dot{m}_{CR}^{(BA+MB)_{dcg}}}$$

<div align="right">Eq. 4.100</div>

4.4.3   Water addition, recycling and storage

The goal of the discharge step is to have as much of the metaboric acid, contained in the concentrate tank, react with water. To achieve higher conversion, an overstoichiometric excess of water could be added. On the other hand, excess water in the discharge product suspension needs to be extracted in the following charge run, so it is advisable to keep a balance between lower conversion and lower energy efficiency in the follow-up charge. As it is unlikely that the process plant will be used only for experiments with stoichiometric rehydration, a model including water excess is proposed in this thesis.

Option (a): steam rehydration

Water is added from priorly stored condensed water and/or an external source. It passes through an evaporator and the steam is fed homogenously into the reactor bottom along a gassing zone, ideally to promote turbulence and a large phase contact area. Steam that already passed the suspension is led to the evaporator from an outlet in the reactor head; This is to ensure constant steam input conditions and prevent condensation in the piping (another approach would be to directly recycle the steam and eventually heat the corresponding piping at least before stationary conditions are established). To minimize steam leaving the reactor at the suspension outlet, proper reactor design should ensure that the suspension outlet is positioned in a zone of the reactor where the low-density steam will be at minimum concentrations, which could be achieved by reactor elements that enable a separate gassing zone and a zone in which sufficient residence time allows the steam to leave the suspension while suspension with lowest steam concentration is extracted at the bottom; Or, in a series of reactors, adding steam only at the beginning of the cascade, extracting steam all along the cascade, and extracting the suspension only at the end.

Option (b): liquid water rehydration

The process could also be run without the evaporator, adding the water in liquid phase. This would lower the achievable discharge energy output by a factor of around 4-5, as the energy needed to evaporate the water and overheat the steam would be provided by the discharge reaction itself. Both options should be considered, but the calculations in this thesis are focussed on the case of steam addition to keep the reaction enthalpy of charge and discharge modes constant, which makes the two processes more comparable. Thus, using steam in the discharge reaction will keep the reactor input/output power on the same level, while handling the same mass flows and assuming the same conversion rate in both processes, which might not necessarily be the target, but makes for a more comprehensible depiction of the processes.

A mentionable point of the liquid option is that the evaporation of water inside of the reactor would lead to a considerable increase of reactor pressure. This could be a desired effect, as experiments with

dehydration under vacuum in a Rotavapor led to a drop of the required reaction temperature, and rehydration under raised pressure levels might show benefits as well; Also, the raised pressure could be utilized for transport purposes. Maintaining the elevated pressure requires adequate pressure equipment to prevent backflows out of the reactor, and shortcomings on safety. Another option for steam handling would be to let the steam leave the reactor head and enter a condenser unit, from which it is recycled into the reactor (or stored, not further discussed here).

The following considerations are based on option (a), i.e., steam rehydration.

Water addition is based on the content of metaboric acid in the discharge input suspension concentrate, and calculations concerning water flows are neglecting peripheral water contributions to the reactor, based on the assumptions $\dot{m}_{ER}^{H_2O\,dcg} \gg \dot{m}_{OR}^{H_2O\,dcg} + \dot{m}_{SR}^{H_2O\,dcg}$ and $\dot{m}_{CR}^{H_2O\,dcg} = 0$.

The mass flow of water being leaving the evaporator to the reactor is phrased as:

$$\dot{m}_{ER}^{H_2O\,dcg} = v_W \dot{m}_{X_{dcg}}^{H_2O}$$

<div align="right">Eq. 4.101</div>

Where v_W is the factor for overstoichiometric water addition.

The term $\dot{m}_{X_{dcg}}^{H_2O}$ describes stoichiometric water addition ($v_W = 1$) according to the conversion rate X_{dcg}, and is expressed as:

$$\dot{m}_{X_{dcg}}^{H_2O} = \frac{\omega}{1-\omega} \dot{m}_{CR}^{MB_{dcg}} X_{dcg}$$

<div align="right">Eq. 4.102</div>

Water addition to the reactor consists of the input from the water storage $\dot{m}_{WE}^{H_2O\,dcg}$ and the recycled steam fraction $\dot{m}_{RE}^{H_2O\,dcg}$:

$$\dot{m}_{ER}^{H_2O\,dcg} = \dot{m}_{WE}^{H_2O\,dcg} + \dot{m}_{RE}^{H_2O\,dcg}$$

<div align="right">Eq. 4.103</div>

It is assumed that the flow composition to the evaporator is not altered in the evaporation:

$$\dot{m}_{ER}^{i_{dcg}} = \dot{m}_{WE}^{i_{dcg}} + \dot{m}_{RE}^{i_{dcg}}$$

$\dot{m}_{WE}^{H_2O\,dcg}$ can be set according to desired process parameters, with v'_W being freely selected:

$$\dot{m}_{WE}^{H_2O\,dcg} = v'_W \dot{m}_{X_{dcg}}^{H_2O}$$

<div align="right">Eq. 4.104</div>

This way, $\dot{m}_{RE}^{H_2O\,dcg}$ is the subordinate contribution to reactor water input and is set by a valve (described below) to reach $\dot{m}_{ER}^{H_2O\,dcg}$.

Similar to the condenser route in 4.3.4, no metaboric acid content is to be expected in the steam flow:

$$\dot{m}_{RE}^{MB_{dcg}} = \dot{m}_{WE}^{MB_{dcg}} = 0$$

Neglecting traces of water in the oil storage $\dot{m}_{OR}^{H_2O_{dcg}} \approx 0$ and the oil cycle $\dot{m}_{SR}^{H_2O_{dcg}} \approx 0$, as well as assuming $\dot{m}_{CR}^{H_2O_{dcg}} = 0$, simplifies total water input to:

$$\dot{m}_{R_{in}}^{H_2O_{dcg}} \approx \dot{m}_{ER}^{H_2O_{dcg}}$$

<div align="right">Eq. 4.105</div>

The reactor's steam outlet $\dot{m}_{RV}^{H_2O_{dcg}}$ transports the recycled steam fraction $\dot{m}_{RE}^{H_2O_{dcg}}$ as well as the steam fraction $\dot{m}_{RW}^{H_2O_{dcg}}$ that preheats $\dot{m}_{WE}^{H_2O_{dcg}}$ before entering the water storage in liquid state:

$$\dot{m}_{RV}^{H_2O_{dcg}} = \dot{m}_{RE}^{H_2O_{dcg}} + \dot{m}_{RW}^{H_2O_{dcg}}$$

<div align="right">Eq. 4.106</div>

Similar to other extraction units, η_V describes the steam extraction efficiency; $\eta_V = 1$ would be the ideal case in which unreacted water does not leave the reactor via the oil suspension ($\dot{m}_{RS}^{H_2O_{dcg}} = 0$).

$$\eta_V = \frac{\dot{m}_{RV}^{H_2O_{dcg}}}{\dot{m}_{ER}^{H_2O_{dcg}} - \dot{m}_{X_{dcg}}^{H_2O}}$$

<div align="right">Eq. 4.107</div>

This way, η_V is proportional to the remaining water that is not being bound in the formation of boric acid during the reactor residence time (expressed as $\dot{m}_{X_{dcg}}^{H_2O}$).

As in previously described units, θ is the dimensionless factor for the collection of undesired components:

$$\theta_V^i = \frac{\dot{m}_{RV}^i}{\dot{m}_{RV}^{H_2O}}$$

$$i \dots BA, H_2O$$

<div align="right">Eq. 4.108</div>

The valve V regulates the recycled steam $\dot{m}_{RE}^{H_2O_{dcg}}$ relative to the stored amount of steam $\dot{m}_{RW}^{H_2O_{dcg}}$, which is condensed while preheating $\dot{m}_{WE}^{H_2O_{dcg}}$, and then fed into the water storage W (from which it is eventually recycled in its liquid state). As long as Eq. 4.35 is fulfilled, the valve parameter can be set according to desired process conditions. Similar to the oil storage parameter σ_O in the charge process, the water valve parameter is called σ_V and defined as

$$\sigma_V = \frac{\dot{m}_{RW}^{H_2O_{dcg}}}{\dot{m}_{RV}^{H_2O_{dcg}}}$$

<div align="right">Eq. 4.109</div>

The remaining steam that was not extracted from the suspension leaves the reactor at the bottom suspension outlet:

$$(1 - \eta_V) = \frac{\dot{m}_{RS}^{H_2O_{dcg}}}{\dot{m}_{ER}^{H_2O_{dcg}} - \dot{m}_{X_{dcg}}^{H_2O}}$$

<div align="right">Eq. 4.110</div>

These equations fulfil the reactor's mass balance for water:

$$\dot{m}_{ER}^{H_2O_{dcg}} - \dot{m}_{RV}^{H_2O_{dcg}} - \dot{m}_{RS}^{H_2O_{dcg}} - \dot{m}_{X_{dcg}}^{H_2O} = 0$$

<div align="right">Eq. 4.111</div>

4.4.4 Reactor

The conversion rate of the discharge process was defined as:

$$X_{dcg} = 1 - \left[\frac{\dot{m}_{in}^{MB}}{\dot{m}_{out}^{MB}}\right]_{R,dcg}$$

<div align="right">Eq. 4.112</div>

Or, in its simplified form:

$$X_{dcg} \approx 1 - \frac{\dot{m}_{CR}^{MB_{dcg}}}{\dot{m}_{RS}^{MB_{dcg}}}$$

<div align="right">Eq. 4.113</div>

4.4.4.1 Boric acid

The balance for boric acid in the discharge reactor is composed of the following contributions:

$$\dot{m}_{R_{in}}^{BA_{dcg}} + \dot{m}_{X_{dcg}}^{BA} - \dot{m}_{R_{out}}^{BA_{dcg}} = 0$$

<div align="right">Eq. 4.114</div>

$$\dot{m}_{R_{in}}^{BA_{dcg}} = \dot{m}_{CR}^{BA_{dcg}} + \dot{m}_{OR}^{BA_{dcg}} + \dot{m}_{SR}^{BA_{dcg}} + \dot{m}_{ER}^{BA_{dcg}}$$

<div align="right">Eq. 4.115</div>

$$\dot{m}_{R_{out}}^{BA_{dcg}} = \dot{m}_{RS}^{BA_{dcg}} + \dot{m}_{RE}^{BA_{dcg}} + \dot{m}_{RW}^{BA_{dcg}}$$

<div align="right">Eq. 4.116</div>

$$\dot{m}_{X_{dcg}}^{BA} = \left(\dot{m}_{CR}^{MB_{dcg}} + \dot{m}_{OR}^{MB_{dcg}} + \dot{m}_{SR}^{MB_{dcg}}\right)\frac{1}{1 - \omega}X_{dcg}$$

<div align="right">Eq. 4.117</div>

Combining these equations yields the material balance for boric acid in the discharge reactor:

$$\dot{m}_{CR}^{BA_{dcg}} + \dot{m}_{OR}^{BA_{dcg}} + \dot{m}_{SR}^{BA_{dcg}} + \dot{m}_{WE}^{BA_{dcg}} + \left(\dot{m}_{CR}^{MB_{dcg}} + \dot{m}_{OR}^{MB_{dcg}} + \dot{m}_{SR}^{MB_{dcg}}\right)\frac{1}{1 - \omega}X_{dcg} - \dot{m}_{RS}^{BA_{dcg}}$$
$$- \dot{m}_{RE}^{BA_{dcg}} - \dot{m}_{RW}^{BA_{dcg}} = 0$$

$$\zeta_{CR}^{BA_{dcg}} + \zeta_{OR}^{BA_{dcg}} + \zeta_{SR}^{BA_{dcg}} + \zeta_{WE}^{BA_{dcg}} + \left(\zeta_{CR}^{MB_{dcg}} + \zeta_{OR}^{MB_{dcg}} + \zeta_{SR}^{MB_{dcg}}\right)\frac{1}{1 - \omega}X_{dcg} - \zeta_{RS}^{BA_{dcg}} - \zeta_{RE}^{BA_{dcg}}$$
$$- \zeta_{RW}^{BA_{dcg}} = 0$$

<div align="right">Eq. 4.118</div>

Some material flows can be neglected, based on assumptions as already discussed in chapter 4.3:

$$\dot{m}_{CR}^{BA_{dcg}} \gg \dot{m}_{OR}^{BA_{dcg}} + \dot{m}_{SR}^{BA_{dcg}} + \dot{m}_{WE}^{BA_{dcg}} + \dot{m}_{RE}^{BA_{dcg}} + \dot{m}_{RW}^{BA_{dcg}}$$

$$\dot{m}_{CR}^{MB_{dcg}} \gg \dot{m}_{OR}^{MB_{dcg}} + \dot{m}_{SR}^{MB_{dcg}}$$

Applying these simplifications yields the simplified material balance for boric acid in the discharge reactor:

$$\dot{m}_{CR}^{BA_{dcg}} + \dot{m}_{CR}^{MB_{dcg}} \left(\frac{1}{1-\omega} \right) X_{dcg} - \dot{m}_{RS}^{BA_{dcg}} \approx 0$$

$$\zeta_{CR}^{BA_{dcg}} + \zeta_{CR}^{MB_{dcg}} \left(\frac{1}{1-\omega} \right) X_{dcg} - \zeta_{RS}^{BA_{dcg}} \approx 0$$

Eq. 4.119

4.4.4.2 Metaboric acid

The balance for metaboric acid in the discharge reactor is composed of the following contributions:

$$\dot{m}_{R_{in}}^{MB_{dcg}} - \dot{m}_{X_{dcg}}^{MB} - \dot{m}_{R_{out}}^{MB_{dcg}} = 0$$

Eq. 4.120

$$\dot{m}_{R_{in}}^{MB_{dcg}} = \dot{m}_{CR}^{MB_{dcg}} + \dot{m}_{OR}^{MB_{dcg}} + \dot{m}_{SR}^{MB_{dcg}}$$

Eq. 4.121

$$\dot{m}_{R_{out}}^{MB_{dcg}} = \dot{m}_{RS}^{MB_{dcg}}$$

Eq. 4.122

$$\dot{m}_{X_{dcg}}^{MB} = X_{dcg} \left(\dot{m}_{CR}^{MB_{dcg}} + \dot{m}_{OR}^{MB_{dcg}} + \dot{m}_{SR}^{MB_{dcg}} \right)$$

Eq. 4.123

Combining these equations yields the material balance for metaboric acid in the discharge reactor:

$$\left(\dot{m}_{CR}^{MB_{dcg}} + \dot{m}_{OR}^{MB_{dcg}} + \dot{m}_{SR}^{MB_{dcg}} \right) \left(1 - X_{dcg} \right) - \dot{m}_{RS}^{MB_{dcg}} = 0$$

$$\left(\zeta_{CR}^{MB_{dcg}} + \zeta_{OR}^{MB_{dcg}} + \zeta_{SR}^{MB_{dcg}} \right) \left(1 - X_{dcg} \right) - \zeta_{RS}^{MB_{dcg}} = 0$$

Eq. 4.124

Some flows can be neglected:

$$\dot{m}_{CR}^{MB_{dcg}} \gg \dot{m}_{OR}^{MB_{dcg}} + \dot{m}_{SR}^{MB_{dcg}}$$

Applying this simplification yields the simplified material balance for metaboric acid in the discharge reactor:

$$\dot{m}_{CR}^{MB_{dcg}} \left(1 - X_{dcg} \right) - \dot{m}_{RS}^{MB_{dcg}} = 0$$

$$\zeta_{CR}^{MB_{dcg}} \left(1 - X_{dcg} \right) - \zeta_{RS}^{MB_{dcg}} = 0$$

Eq. 4.125

4.4.4.3 Water

The balance for water in the discharge reactor is composed of the following contributions:

$$\dot{m}_{R_{in}}^{H_2O_{dcg}} - \dot{m}_{X_{dcg}}^{H_2O} - \dot{m}_{R_{out}}^{H_2O_{dcg}} = 0$$

Eq. 4.126

$$\dot{m}_{R_{in}}^{H_2O_{dcg}} = \dot{m}_{CR}^{H_2O_{dcg}} + \dot{m}_{OR}^{H_2O_{dcg}} + \dot{m}_{SR}^{H_2O_{dcg}} + \dot{m}_{ER}^{H_2O_{dcg}}$$

Eq. 4.127

$$\dot{m}_{R_{out}}^{H_2O} = \dot{m}_{RS}^{H_2O_{dcg}} + \dot{m}_{RV}^{H_2O_{dcg}}$$

Eq. 4.128

$$\dot{m}_{X_{dcg}}^{H_2O} = \frac{\omega}{1-\omega}\dot{m}_{CR}^{MB_{dcg}}X_{dcg}$$

Eq. 4.129

The assumption from 4.4.1 is picked up again:

$$\dot{m}_{CR}^{H_2O_{dcg}} = 0$$

These equations yield the material balance for water in the discharge reactor:

$$\dot{m}_{OR}^{H_2O_{dcg}} + \dot{m}_{SR}^{H_2O_{dcg}} + \dot{m}_{WE}^{H_2O_{dcg}} - \frac{\omega}{1-\omega}\left(\dot{m}_{CR}^{MB_{dcg}} + \dot{m}_{OR}^{MB_{dcg}} + \dot{m}_{SR}^{MB_{dcg}}\right)X_{dcg} - \dot{m}_{RS}^{H_2O_{dcg}} - \dot{m}_{RW}^{H_2O_{dcg}}$$
$$= 0$$

$$\zeta_{OR}^{H_2O_{dcg}} + \zeta_{SR}^{H_2O_{dcg}} + \zeta_{WE}^{H_2O_{dcg}} - \frac{\omega}{1-\omega}\left(\zeta_{CR}^{MB_{dcg}} + \zeta_{OR}^{MB_{dcg}} + \zeta_{SR}^{MB_{dcg}}\right)X_{dcg} - \zeta_{RS}^{H_2O_{dcg}} - \zeta_{RW}^{H_2O_{dcg}} = 0$$

Eq. 4.130

Some flows can be neglected:

$$\dot{m}_{WE}^{H_2O_{dcg}} \gg \dot{m}_{OR}^{H_2O_{dcg}} + \dot{m}_{SR}^{H_2O_{dcg}}$$

$$\dot{m}_{CR}^{MB_{dcg}} \gg \dot{m}_{OR}^{MB_{dcg}} + \dot{m}_{SR}^{MB_{dcg}}$$

Applying these simplifications yields the simplified material balance for water in the discharge reactor:

$$\dot{m}_{WE}^{H_2O_{dcg}} - \frac{\omega}{1-\omega}\dot{m}_{CR}^{MB_{dcg}}X_{dcg} - \dot{m}_{RS}^{H_2O_{dcg}} - \dot{m}_{RW}^{H_2O_{dcg}} \approx 0$$

$$\zeta_{WE}^{H_2O_{dcg}} - \frac{\omega}{1-\omega}\zeta_{CR}^{MB_{dcg}}X_{dcg} - \zeta_{RS}^{H_2O_{dcg}} - \zeta_{RW}^{H_2O_{dcg}} \approx 0$$

Eq. 4.131

4.4.5 Oil separation units, oil addition

In principle, the oil separation series for the discharge step is proposed as the same sequence as in the charge step. In contrast, based on the already stated assumption that the discharge step consumes the liberated oil from the charge step with its increased solid volume flow, all extracted oil flows from the discharge oil separation series are directly recycled to the conveyor screw.

Model parameters for the separate units are defined as already explained in the corresponding chapter of the charge process 4.3.5:

$$\eta_j = \frac{\dot{m}_{j,extracted}^{oil}}{\dot{m}_{RS}^{oil}}$$

$$j \dots H, I, G, S$$

<div align="right">Eq. 4.132</div>

$$\theta_j^i = \frac{\dot{m}_{j,extracted}^i}{\dot{m}_{j,extracted}^{oil}}$$

$$i \dots H_2O, BA + MB; \quad j \dots H, I, G, S$$

<div align="right">Eq. 4.133</div>

The balance for each material i over the series is:

$$\dot{m}_{RS,chg}^i - \dot{m}_{SC,chg}^i - \dot{m}_{SR,chg}^i = 0$$

$$\zeta_{RS,chg}^i - \zeta_{SC,chg}^i - \zeta_{SR,chg}^i = 0$$

<div align="right">Eq. 4.134</div>

4.4.6 Reactor + oil separation series

This chapter presents the material balances over the combination of the discharge reactor and the following oil separation series.

4.4.6.1 Boric acid

The material balance of boric acid over the combination of the discharge reactor and the following oil separation series is:

$$\dot{m}_{CR}^{BA_{dcg}} + \dot{m}_{OR}^{BA_{dcg}} + \dot{m}_{WE}^{BA_{dcg}} + \frac{1}{1-\omega}\left(\dot{m}_{CR}^{MB_{dcg}} + \dot{m}_{OR}^{MB_{dcg}} + \dot{m}_{WE}^{MB_{dcg}}\right)X_{dcg} - \dot{m}_{RW}^{BA_{dcg}} - \dot{m}_{SC}^{BA_{dcg}} = 0$$

$$\zeta_{CR}^{BA_{dcg}} + \zeta_{OR}^{BA_{dcg}} + \zeta_{WE}^{BA_{dcg}} + \frac{1}{1-\omega}\left(\zeta_{CR}^{MB_{dcg}} + \zeta_{OR}^{MB_{dcg}} + \zeta_{WE}^{MB_{dcg}}\right)X_{dcg} - \zeta_{RW}^{BA_{dcg}} - \zeta_{SC}^{BA_{dcg}} = 0$$

<div align="right">Eq. 4.135</div>

With the aforementioned assumptions,

$$\dot{m}_{CR}^{MB_{dcg}} \gg \dot{m}_{OR}^{MB_{dcg}}; \quad \dot{m}_{WE}^{MB_{dcg}} = 0; \quad \dot{m}_{CR}^{BA_{dcg}} \gg \dot{m}_{OR}^{BA_{dcg}} + \dot{m}_{WE}^{BA_{dcg}}; \quad \dot{m}_{SC}^{BA_{dcg}} \gg \dot{m}_{RW}^{BA_{dcg}}$$

We obtain the simplified material balance of boric acid over the combination of the discharge reactor and the following oil separation series:

$$\dot{m}_{CR}^{BA_{dcg}} + \frac{1}{1-\omega}\dot{m}_{CR}^{MB_{dcg}}X_{dcg} - \dot{m}_{SC}^{BA_{dcg}} \approx 0$$

$$\zeta_{CR}^{BA_{dcg}} + \frac{1}{1-\omega}\zeta_{CR}^{MB_{dcg}}X_{dcg} - \zeta_{SC}^{BA_{dcg}} \approx 0$$

<div align="right">Eq. 4.136</div>

4.4.6.2 Metaboric acid

The material balance of metaboric acid over the combination of the discharge reactor and the following oil separation series is:

$$\left(\dot{m}_{CR}^{MB_{dcg}} + \dot{m}_{OR}^{MB_{dcg}} + \dot{m}_{WE}^{MB_{dcg}}\right)\left(1 - X_{dcg}\right) - \dot{m}_{RW}^{MB_{dcg}} - \dot{m}_{SC}^{MB_{dcg}} = 0$$

$$\left(\zeta_{CR}^{MB_{dcg}} + \zeta_{OR}^{MB_{dcg}} + \zeta_{WE}^{MB_{dcg}}\right)\left(1 - X_{dcg}\right) - \zeta_{RW}^{MB_{dcg}} - \zeta_{SC}^{MB_{dcg}} = 0$$

<div align="right">Eq. 4.137</div>

With the aforementioned assumptions,

$$\dot{m}_{CR}^{MB_{dcg}} \gg \dot{m}_{OR}^{MB_{dcg}}; \ \dot{m}_{WE}^{MB_{dcg}} = \dot{m}_{RW}^{MB_{dcg}} = 0$$

We obtain the simplified material balance of metaboric acid over the combination of the discharge reactor and the following oil separation series:

$$\dot{m}_{CR}^{MB_{dcg}}\left(1 - X_{dcg}\right) - \dot{m}_{SC}^{MB_{dcg}} \approx 0$$

$$\zeta_{CR}^{MB_{dcg}}\left(1 - X_{dcg}\right) - \zeta_{SC}^{MB_{dcg}} \approx 0$$

<div align="right">Eq. 4.138</div>

4.4.6.3 Water

The material balance of water over the combination of the discharge reactor and the following oil separation series is:

$$\dot{m}_{CR}^{H_2O_{dcg}} + \dot{m}_{OR}^{H_2O_{dcg}} + \dot{m}_{WE}^{H_2O_{dcg}} - \frac{\omega}{1-\omega}\left(\dot{m}_{CR}^{MB_{dcg}} + \dot{m}_{OR}^{MB_{dcg}} + \dot{m}_{WE}^{MB_{dcg}}\right)X_{dcg} - \dot{m}_{RW}^{H_2O_{dcg}} - \dot{m}_{SC}^{H_2O_{dcg}}$$
$$= 0$$

$$\zeta_{CR}^{H_2O_{dcg}} + \zeta_{OR}^{H_2O_{dcg}} + \zeta_{WE}^{H_2O_{dcg}} - \frac{\omega}{1-\omega}\left(\zeta_{CR}^{MB_{dcg}} + \zeta_{OR}^{MB_{dcg}} + \zeta_{WE}^{MB_{dcg}}\right)X_{dcg} - \zeta_{RW}^{H_2O_{dcg}} - \zeta_{SC}^{H_2O_{dcg}} = 0$$

<div align="right">Eq. 4.139</div>

With the aforementioned assumptions,

$$\dot{m}_{WE}^{H_2O dcg} \gg \dot{m}_{OR}^{H_2O dcg}; \quad \dot{m}_{CR}^{H_2O dcg} = 0; \quad \dot{m}_{CR}^{MB dcg} \gg \dot{m}_{OR}^{MB dcg} + \dot{m}_{WE}^{BA dcg} \Rightarrow$$

We obtain the simplified material balance of metaboric acid over the combination of the discharge reactor and the following oil separation series:

$$\dot{m}_{WE}^{H_2O dcg} - \frac{\omega}{1-\omega} \dot{m}_{CR}^{MB dcg} X_{dcg} - \dot{m}_{RW}^{H_2O dcg} - \dot{m}_{SC}^{H_2O dcg} = 0$$

$$\zeta_{WE}^{H_2O dcg} - \frac{\omega}{1-\omega} \zeta_{CR}^{MB dcg} X_{dcg} - \zeta_{RW}^{H_2O dcg} - \zeta_{SC}^{H_2O dcg} = 0$$

Eq. 4.140

4.4.7 Suspension concentrate (process end)

For charging as well as discharging, the assumption was made that residual water will react with metaboric acid during prolonged storage times. Unlike the charge process, it is not clear yet whether metaboric acid or water will be the limiting component, hence both options have been considered, whereas the second option $\dot{n}_{SC}^{MB} < \dot{n}_{SC}^{H_2O}$ would only be the case for very high conversion rates and/or high residual water contents, more likely to occur in a scenario of liquid water addition as steam does not contain that much water in terms of mass, compared to the residual metaboric acid from the full conversion scenario $X_{dcg} < 1$.

4.4.7.1 Boric acid

The amount of boric acid will increase, until the limiting component, to which the two pathways refer, is depleted:

$$\dot{m}_{SC}^{BA_{effective,dcg}} = \dot{m}_{SC}^{BA dcg} + \begin{cases} \dot{n}_{SC}^{MB} \geq \dot{n}_{SC}^{H_2O} : \left(1 + \dfrac{1-\omega}{\omega}\right) \dot{m}_{SC}^{H_2O dcg} \\ \dot{n}_{SC}^{MB} \leq \dot{n}_{SC}^{H_2O} : \left(1 + \dfrac{\omega}{1-\omega}\right) \dot{m}_{SC}^{MB dcg} \end{cases}$$

$$\zeta_{SC}^{BA_{effective,dcg}} = \zeta_{SC}^{BA dcg} + \begin{cases} \dot{n}_{SC}^{MB} \geq \dot{n}_{SC}^{H_2O} : \left(1 + \dfrac{1-\omega}{\omega}\right) \zeta_{SC}^{H_2O dcg} \\ \dot{n}_{SC}^{MB} \leq \dot{n}_{SC}^{H_2O} : \left(1 + \dfrac{\omega}{1-\omega}\right) \zeta_{SC}^{MB dcg} \end{cases}$$

Eq. 4.141

4.4.7.2 Metaboric acid

With metaboric acid as the limiting component, it will be entirely consumed in the reaction; In the more likely case of water as the limiting factor, metaboric acid is stoichiometrically rehydrated until water is depleted:

$$
\dot{m}_{SC}^{MB_{effective,dcg}} = \begin{cases} \dot{n}_{SC}^{MB} \geq \dot{n}_{SC}^{H_2O}: \dot{m}_{SC}^{MB_{dcg}} - \dfrac{1-\omega}{\omega}\dot{m}_{SC}^{H_2O_{dcg}} \\ \dot{n}_{SC}^{MB} \leq \dot{n}_{SC}^{H_2O}: 0 \end{cases}
$$

$$
\zeta_{SC}^{MB_{effective,dcg}} = \begin{cases} \dot{n}_{SC}^{MB} \geq \dot{n}_{SC}^{H_2O}: \zeta_{SC}^{MB_{dcg}} - \dfrac{1-\omega}{\omega}\zeta_{SC}^{H_2O_{dcg}} \\ \dot{n}_{SC}^{MB} \leq \dot{n}_{SC}^{H_2O}: 0 \end{cases}
$$

<div align="right">Eq. 4.142</div>

4.4.7.3 Water

The reaction of water occurs under the opposite principles of the rehydration of metaboric acid. With an excess of metaboric acid, all of the water will be consumed:

$$
\dot{m}_{SC}^{H_2O_{effective,dcg}} = \begin{cases} \dot{n}_{SC}^{MB} \geq \dot{n}_{SC}^{H_2O}: 0 \\ \dot{n}_{SC}^{MB} \leq \dot{n}_{SC}^{H_2O}: \dot{m}_{SC}^{H_2O_{dcg}} - \dfrac{\omega}{1-\omega}\dot{m}_{SC}^{MB_{dcg}} \end{cases}
$$

$$
\zeta_{SC}^{H_2O_{effective,dcg}} = \begin{cases} \dot{n}_{SC}^{MB} \geq \dot{n}_{SC}^{H_2O}: 0 \\ \dot{n}_{SC}^{MB} \leq \dot{n}_{SC}^{H_2O}: \zeta_{SC}^{H_2O_{dcg}} - \dfrac{\omega}{1-\omega}\zeta_{SC}^{MB_{dcg}} \end{cases}
$$

<div align="right">Eq. 4.143</div>

4.5 Numerical application of incomplete conversion in cycles

To estimate conversion profiles for multiple cycles, a calculation sheet was created with Microsoft Excel. The equations from chapters 4.3 and 4.4 were used to obtain numeric results for a set value of pure boric acid input in the first cycle. Initial parameters are used as fixed references. The charge output of one cycle is referenced as the discharge input of the same cycle (including the calculations on conversion during storage), and the discharge output of one cycle as the charge input of the next cycle, for a total of n=8 cycles. The results are listed on the following pages, from Table 8 to Table 23, in a form that can be linked to the simplified block diagrams (Figure 4 to Figure 9)

Table 7: Conversion profiling reference parameters

Parameter	Charge process	Discharge process
γ_C	0.5	0.33[a]
γ_R	1.1	1.5
υ_W	-	1.4
υ'_W	-	1.1
X	0.8	
chg: η_L; dcg: η_V	0.9975	0.99
chg: $\theta_{L,BA}$; dcg: $\theta_{V,BA}$	$5 * 10^{-3}$	10^{-3}
chg: $\theta_{L,oil}$; dcg: $\theta_{V,oil}$	$2.5 * 10^{-3}$	$2 * 10^{-3}$
η_H	0.20	0.15
η_I	0.20	0.15
η_G	0.37	0.30
sum: η_S	0.77[a]	0.60[a]
$\theta_{H,BA+MB}$	$2 * 10^{-2}$	
θ_{H,H_2O}	10^{-3}	
$\theta_{I,BA+MB}$	10^{-2}	
θ_{I,H_2O}	10^{-4}	
$\theta_{G,BA+MB}$	10^{-2}	
θ_{G,H_2O}	10^{-4}	

a) Output variable

Table 8: Flow compositions, charge process, n=1

CHARGE, n=1

C_chg (n=1):
$\dot{m}_{BA}$	4,000
$\dot{m}_{MB}$	0,000
$\dot{m}_{H2O}$	0,000
$\dot{m}_{Oil}$	2,000

CR:
ξ_{BA}	1,000
ξ_{MB}	0,000
ξ_{H2O}	0,000
ξ_{Oil}	0,500

SR=HR+IR+GR:
$\dot{m}_{BA}$	0,009	ξ_{BA}	0,002
$\dot{m}_{MB}$	0,024	ξ_{MB}	0,006
$\dot{m}_{H2O}$	0,001	ξ_{H2O}	0,0003
$\dot{m}_{Oil}$	2,400	ξ_{Oil}	0,600

ZR:
$\dot{m}_{BA}$	4,009	ξ_{BA}	1,002
$\dot{m}_{MB}$	0,024	ξ_{MB}	0,006
$\dot{m}_{H2O}$	0,001	ξ_{H2O}	0,000
$\dot{m}_{Oil}$	4,400	ξ_{Oil}	1,100

RL:
$\dot{m}_{BA}$	0,005	ξ_{BA}	0,001
$\dot{m}_{MB}$	0,000	ξ_{MB}	0,000
$\dot{m}_{H2O}$	0,926	ξ_{H2O}	0,231
$\dot{m}_{Oil}$	0,002	ξ_{Oil}	0,001

R_chg / RS=RH:
$\dot{m}_{BA}$	0,795	ξ_{BA}	0,199
$\dot{m}_{MB}$	2,272	ξ_{MB}	0,568
$\dot{m}_{H2O}$	0,0232	ξ_{H2O}	0,00058
$\dot{m}_{Oil}$	4,398	ξ_{Oil}	1,099

S (chg)

H / HI:
$\dot{m}_{BA}$	0,791	ξ_{BA}	0,198
$\dot{m}_{MB}$	2,259	ξ_{MB}	0,565
$\dot{m}_{H2O}$	0,00144	ξ_{H2O}	0,000
$\dot{m}_{Oil}$	3,518	ξ_{Oil}	0,880

HR:
$\dot{m}_{BA}$	0,005	ξ_{BA}	0,001
$\dot{m}_{MB}$	0,013	ξ_{MB}	0,003
$\dot{m}_{H2O}$	0,00088	ξ_{H2O}	0,0002
$\dot{m}_{Oil}$	0,880	ξ_{Oil}	0,220

I / IG:
$\dot{m}_{BA}$	0,789	ξ_{BA}	0,197
$\dot{m}_{MB}$	2,252	ξ_{MB}	0,563
$\dot{m}_{H2O}$	0,00135	ξ_{H2O}	0,000
$\dot{m}_{Oil}$	2,639	ξ_{Oil}	0,660

IR:
$\dot{m}_{BA}$	0,002	ξ_{BA}	0,001
$\dot{m}_{MB}$	0,007	ξ_{MB}	0,002
$\dot{m}_{H2O}$	0,00009	ξ_{H2O}	0,000
$\dot{m}_{Oil}$	0,880	ξ_{Oil}	0,220

G / GC:
$\dot{m}_{BA}$	0,787	ξ_{BA}	0,197
$\dot{m}_{MB}$	2,248	ξ_{MB}	0,562
$\dot{m}_{H2O}$	0,00129	ξ_{H2O}	0,0003
$\dot{m}_{Oil}$	1,011	ξ_{Oil}	0,253

GO:
$\dot{m}_{BA}$	0,003	ξ_{BA}	0,001
$\dot{m}_{MB}$	0,007	ξ_{MB}	0,002
$\dot{m}_{H2O}$	0,00010	ξ_{H2O}	0,000
$\dot{m}_{Oil}$	0,986	ξ_{Oil}	0,247

GR:
$\dot{m}_{BA}$	0,002	ξ_{BA}	0,000
$\dot{m}_{MB}$	0,005	ξ_{MB}	0,001
$\dot{m}_{H2O}$	0,00006	ξ_{H2O}	0,000
$\dot{m}_{Oil}$	0,641	ξ_{Oil}	0,160

W

C_dis (n=1)

Table 9: Flow compositions, discharge process, n=1

Table 10: Flow compositions, charge process, n=2

CHARGE, n=2

CR
		ξ	
$\dot{m}_{BA}$	3.297	ξ_{BA}	0.824
$\dot{m}_{MB}$	0.440	ξ_{MB}	0.110
$\dot{m}_{H2O}$	0.00000	ξ_{H2O}	0.000
$\dot{m}_{Oil}$	1.821	ξ_{Oil}	0.455

ZR
		ξ	
$\dot{m}_{BA}$	3.304	ξ_{BA}	0.826
$\dot{m}_{MB}$	0.464	ξ_{MB}	0.116
$\dot{m}_{H2O}$	0.001	ξ_{H2O}	0.000
$\dot{m}_{Oil}$	4.111	ξ_{Oil}	1.028

SR=HR+IR+GR
		ξ	
$\dot{m}_{BA}$	0.007	ξ_{BA}	0.002
$\dot{m}_{MB}$	0.024	ξ_{MB}	0.006
$\dot{m}_{H2O}$	0.001	ξ_{H2O}	0.0002
$\dot{m}_{Oil}$	2.290	ξ_{Oil}	0.572

RL
		ξ	
$\dot{m}_{BA}$	0.004	ξ_{BA}	0.001
$\dot{m}_{MB}$	0.000	ξ_{MB}	0.000
$\dot{m}_{H2O}$	0.763	ξ_{H2O}	0.191
$\dot{m}_{Oil}$	0.002	ξ_{Oil}	0.000

RS=RH
		ξ	
$\dot{m}_{BA}$	0.656	ξ_{BA}	0.164
$\dot{m}_{MB}$	2.313	ξ_{MB}	0.578
$\dot{m}_{H2O}$	0.00191	ξ_{H2O}	0.00048
$\dot{m}_{Oil}$	4.109	ξ_{Oil}	1.027

H
		ξ	
$\dot{m}_{BA}$	0.652	ξ_{BA}	0.163
$\dot{m}_{MB}$	2.300	ξ_{MB}	0.575
$\dot{m}_{H2O}$	0.00109	ξ_{H2O}	0.000
$\dot{m}_{Oil}$	3.287	ξ_{Oil}	0.822

HR
		ξ	
$\dot{m}_{BA}$	0.004	ξ_{BA}	0.001
$\dot{m}_{MB}$	0.013	ξ_{MB}	0.003
$\dot{m}_{H2O}$	0.00082	ξ_{H2O}	0.0002
$\dot{m}_{Oil}$	0.822	ξ_{Oil}	0.205

I
		ξ	
$\dot{m}_{BA}$	0.650	ξ_{BA}	0.163
$\dot{m}_{MB}$	2.294	ξ_{MB}	0.573
$\dot{m}_{H2O}$	0.00101	ξ_{H2O}	0.000
$\dot{m}_{Oil}$	2.465	ξ_{Oil}	0.616

IR
		ξ	
$\dot{m}_{BA}$	0.002	ξ_{BA}	0.000
$\dot{m}_{MB}$	0.006	ξ_{MB}	0.002
$\dot{m}_{H2O}$	0.00008	ξ_{H2O}	0.000
$\dot{m}_{Oil}$	0.822	ξ_{Oil}	0.205

G
		ξ	
$\dot{m}_{BA}$	0.649	ξ_{BA}	0.162
$\dot{m}_{MB}$	2.288	ξ_{MB}	0.572
$\dot{m}_{H2O}$	0.001	ξ_{H2O}	0.0002
$\dot{m}_{Oil}$	0.945	ξ_{Oil}	0.236

GO
		ξ	
$\dot{m}_{BA}$	0.002	ξ_{BA}	0.000
$\dot{m}_{MB}$	0.007	ξ_{MB}	0.002
$\dot{m}_{H2O}$	0.00009	ξ_{H2O}	0.000
$\dot{m}_{Oil}$	0.874	ξ_{Oil}	0.219

GR
		ξ	
$\dot{m}_{BA}$	0.001	ξ_{BA}	0.000
$\dot{m}_{MB}$	0.005	ξ_{MB}	0.001
$\dot{m}_{H2O}$	0.00006	ξ_{H2O}	0.000
$\dot{m}_{Oil}$	0.646	ξ_{Oil}	0.162

Labels: $C_{chg}(n=2)$, W, S(chg), SR, R=ZR, R=RL, S=HI+GO, O, W=RL+GR, S=IG+GC

71

Table 11: Flow compositions, discharge process, n=2

DISCHARGE, n=2

VALVE V

Reaction:
$\dot{m}_{BA,formed}$	2,576
$\dot{m}_{H2O,converted}$	1,829
$\dot{m}_{H2O,remaining}$	0,747
	0,299

Table 12: Flow compositions, charge process, n=3

CHARGE, n=3

CR

	$\dot{m}$		ξ
$\dot{m}_{BA}$ / ξ_{BA}	3,206		0,802
$\dot{m}_{MB}$ / ξ_{MB}	0,448		0,112
$\dot{m}_{H2O}$ / ξ_{H2O}	0,00000		0,000
$\dot{m}_{Oil}$ / ξ_{Oil}	1,763		0,441

SR=HR+GR

	$\dot{m}$		ξ
$\dot{m}_{BA}$ / ξ_{BA}	0,007		0,002
$\dot{m}_{MB}$ / ξ_{MB}	0,024		0,006
$\dot{m}_{H2O}$ / ξ_{H2O}	0,001		0,0002
$\dot{m}_{Oil}$ / ξ_{Oil}	2,257		0,564

ZR

	$\dot{m}$		ξ
$\dot{m}_{BA}$ / ξ_{BA}	3,213		0,803
$\dot{m}_{MB}$ / ξ_{MB}	0,472		0,118
$\dot{m}_{H2O}$ / ξ_{H2O}	0,001		0,000
$\dot{m}_{Oil}$ / ξ_{Oil}	4,020		1,005

RL

	$\dot{m}$		ξ
$\dot{m}_{BA}$ / ξ_{BA}	0,004		0,001
$\dot{m}_{MB}$ / ξ_{MB}	0,000		0,000
$\dot{m}_{H2O}$ / ξ_{H2O}	0,742		0,186
$\dot{m}_{Oil}$ / ξ_{Oil}	0,002		0,000

RS=RH

	$\dot{m}$		ξ
$\dot{m}_{BA}$ / ξ_{BA}	0,159		0,159
$\dot{m}_{MB}$ / ξ_{MB}	2,269		0,567
$\dot{m}_{H2O}$ / ξ_{H2O}	0,00186		0,00046
$\dot{m}_{Oil}$ / ξ_{Oil}	4,018		1,004

H

	$\dot{m}$
$\dot{m}_{BA}$	0,638
$\dot{m}_{MB}$	2,269
$\dot{m}_{H2O}$	0,00186
$\dot{m}_{Oil}$	4,018

HI

	$\dot{m}$		ξ
$\dot{m}_{BA}$ / ξ_{BA}	0,634		0,159
$\dot{m}_{MB}$ / ξ_{MB}	2,257		0,564
$\dot{m}_{H2O}$ / ξ_{H2O}	0,00106		0,000
$\dot{m}_{Oil}$ / ξ_{Oil}	3,214		0,804

HR

	$\dot{m}$		ξ
$\dot{m}_{BA}$ / ξ_{BA}	0,004		0,001
$\dot{m}_{MB}$ / ξ_{MB}	0,013		0,003
$\dot{m}_{H2O}$ / ξ_{H2O}	0,00080		0,0002
$\dot{m}_{Oil}$ / ξ_{Oil}	0,804		0,201

IG

	$\dot{m}$		ξ
$\dot{m}_{BA}$ / ξ_{BA}	0,632		0,158
$\dot{m}_{MB}$ / ξ_{MB}	2,250		0,563
$\dot{m}_{H2O}$ / ξ_{H2O}	0,00098		0,000
$\dot{m}_{Oil}$ / ξ_{Oil}	2,411		0,603

IR

	$\dot{m}$		ξ
$\dot{m}_{BA}$ / ξ_{BA}	0,002		0,000
$\dot{m}_{MB}$ / ξ_{MB}	0,006		0,002
$\dot{m}_{H2O}$ / ξ_{H2O}	0,00008		0,000
$\dot{m}_{Oil}$ / ξ_{Oil}	0,804		0,201

GC

	$\dot{m}$		ξ
$\dot{m}_{BA}$ / ξ_{BA}	0,631		0,158
$\dot{m}_{MB}$ / ξ_{MB}	2,245		0,561
$\dot{m}_{H2O}$ / ξ_{H2O}	0,00091		0,0002
$\dot{m}_{Oil}$ / ξ_{Oil}	0,924		0,231

GO

	$\dot{m}$		ξ
$\dot{m}_{BA}$ / ξ_{BA}	0,002		0,000
$\dot{m}_{MB}$ / ξ_{MB}	0,007		0,002
$\dot{m}_{H2O}$ / ξ_{H2O}	0,00008		0,000
$\dot{m}_{Oil}$ / ξ_{Oil}	0,837		0,209

GR

	$\dot{m}$		ξ
$\dot{m}_{BA}$ / ξ_{BA}	0,001		0,000
$\dot{m}_{MB}$ / ξ_{MB}	0,005		0,001
$\dot{m}_{H2O}$ / ξ_{H2O}	0,00006		0,000
$\dot{m}_{Oil}$ / ξ_{Oil}	0,650		0,162

Table 13: Flow compositions, discharge process, n=3

Table 14: Flow compositions, charge process, n=4

CHARGE, n=4

C_chg (n=4)

CR

		ξ_BA	0,002
ṁ_BA	3,140	ξ_BA	0,785
ṁ_MB	0,439	ξ_MB	0,110
ṁ_H2O	0,00000	ξ_H2O	0,000
ṁ_Oil	1,726	ξ_Oil	0,431

ZR

ṁ_BA	3,147	ξ_BA	0,787
ṁ_MB	0,463	ξ_MB	0,116
ṁ_H2O	0,001	ξ_H2O	0,000
ṁ_Oil	3,938	ξ_Oil	0,984

SR=HR+GR

ṁ_BA	0,007	ξ_BA	0,002
ṁ_MB	0,023	ξ_MB	0,006
ṁ_H2O	0,001	ξ_H2O	0,0002
ṁ_Oil	2,212	ξ_Oil	0,553

R_chg

RS=RH

ṁ_BA	0,156	ξ_BA	0,156
ṁ_MB	2,223	ξ_MB	0,556
ṁ_H2O	0,00182	ξ_H2O	0,00046
ṁ_Oil	3,936	ξ_Oil	0,984

RL

ṁ_BA	0,004	ξ_BA	0,001
ṁ_MB	0,000	ξ_MB	0,000
ṁ_H2O	0,727	ξ_H2O	0,182
ṁ_Oil	0,002	ξ_Oil	0,000

H

HI

ṁ_BA	0,621	ξ_BA	0,155
ṁ_MB	2,211	ξ_MB	0,553
ṁ_H2O	0,00103	ξ_H2O	0,000
ṁ_Oil	3,149	ξ_Oil	0,787

HR

ṁ_BA	0,003	ξ_BA	0,001
ṁ_MB	0,012	ξ_MB	0,003
ṁ_H2O	0,00079	ξ_H2O	0,0002
ṁ_Oil	0,787	ξ_Oil	0,197

I

IG

ṁ_BA	0,619	ξ_BA	0,155
ṁ_MB	2,205	ξ_MB	0,551
ṁ_H2O	0,00096	ξ_H2O	0,000
ṁ_Oil	2,362	ξ_Oil	0,590

IR

ṁ_BA	0,002	ξ_BA	0,002
ṁ_MB	0,006	ξ_MB	0,006
ṁ_H2O	0,00008	ξ_H2O	0,000
ṁ_Oil	0,787	ξ_Oil	0,197

G

GC

ṁ_BA	0,618	ξ_BA	0,154
ṁ_MB	2,200	ξ_MB	0,550
ṁ_H2O	0,00089	ξ_H2O	0,0002
ṁ_Oil	0,905	ξ_Oil	0,226

GO

ṁ_BA	0,002	ξ_BA	0,000
ṁ_MB	0,006	ξ_MB	0,002
ṁ_H2O	0,00008	ξ_H2O	0,000
ṁ_Oil	0,819	ξ_Oil	0,205

GR

ṁ_BA	0,001	ξ_BA	0,000
ṁ_MB	0,005	ξ_MB	0,001
ṁ_H2O	0,00006	ξ_H2O	0,000
ṁ_Oil	0,637	ξ_Oil	0,159

S (chg)

W

C_chg (n=4)

Table 15: Flow compositions, discharge process, n=4

DISCHARGE, n=4

RE=RR		
ξ_{BA}	0,000	
ξ_{WB}	0,000	
ξ_{H2O}	**0,054**	
$\xi_{Öl}$	0,000	

$\dot{m}_{BA}$	0,000
$\dot{m}_{WB}$	0,000
$\dot{m}_{H2O}$	**0,215**
$\dot{m}_{Öl}$	0,000

total ER	
ξ_{BA}	0,001
ξ_{WB}	0,000
ξ_{H2O}	**0,251**
$\xi_{Öl}$	0,001

Reaction	
$\dot{m}_{BA,formed}$	2,476
$\dot{m}_{H2O,converted}$	1,758
$\dot{m}_{H2O,converted}$	0,718
$\dot{m}_{H2O,remaining}$	0,287

WE=WR		
ξ_{BA}	0,001	
ξ_{WB}	0,000	
ξ_{H2O}	**0,197**	
$\xi_{Öl}$	0,000	

$\dot{m}_{BA}$	0,004
$\dot{m}_{WB}$	0,000
$\dot{m}_{H2O}$	**0,790**
$\dot{m}_{Öl}$	0,002

$\dot{m}_{BA}$	0,004
$\dot{m}_{WB}$	0,000
$\dot{m}_{H2O}$	**1,005**
$\dot{m}_{Öl}$	0,002

RE		
ξ_{BA}	0,000	
ξ_{WB}	0,000	
ξ_{H2O}	**0,054**	
$\xi_{Öl}$	0,000	

$\dot{m}_{BA}$	0,0002
$\dot{m}_{WB}$	0,000
$\dot{m}_{H2O}$	**0,215**
$\dot{m}_{Öl}$	0,0004

VALVE V

RV=RE+RW		
ξ_{BA}	0,000	
ξ_{WB}	0,000	
ξ_{H2O}	**0,071**	
$\xi_{Öl}$	0,000	

RW		
ξ_{BA}	0,000	
ξ_{WB}	0,000	
ξ_{H2O}	**0,017**	
$\xi_{Öl}$	0,000	

$\dot{m}_{BA}$	0,0001
$\dot{m}_{WB}$	0,000
$\dot{m}_{H2O}$	**0,059**
$\dot{m}_{Öl}$	0,0001

SR=HR+IR+GR		
ξ_{BA}	0,007	
ξ_{WB}	0,001	
ξ_{H2O}	0,0002	
$\xi_{Öl}$	**0,634**	

$\dot{m}_{BA}$	0,028
$\dot{m}_{WB}$	0,004
$\dot{m}_{H2O}$	0,001
$\dot{m}_{Öl}$	**2,536**

$\dot{m}_{BA}$	0,0003
$\dot{m}_{WB}$	0,000
$\dot{m}_{H2O}$	**0,284**
$\dot{m}_{Öl}$	0,0006

HR		
ξ_{BA}	0,003	
ξ_{WB}	0,000	
ξ_{H2O}	0,0002	
$\xi_{Öl}$	**0,159**	

$\dot{m}_{BA}$	0,011
$\dot{m}_{WB}$	0,002
$\dot{m}_{H2O}$	0,00063
$\dot{m}_{Öl}$	**0,634**

IR		
ξ_{BA}	0,001	
ξ_{WB}	0,000	
ξ_{H2O}	0,0000	
$\xi_{Öl}$	**0,159**	

$\dot{m}_{BA}$	0,006
$\dot{m}_{WB}$	0,001
$\dot{m}_{H2O}$	0,00006
$\dot{m}_{Öl}$	**0,634**

GR		
ξ_{BA}	0,003	
ξ_{WB}	0,000	
ξ_{H2O}	0,0000	
$\xi_{Öl}$	**0,317**	

$\dot{m}_{BA}$	0,011
$\dot{m}_{WB}$	0,002
$\dot{m}_{H2O}$	0,00013
$\dot{m}_{Öl}$	**1,268**

CR		
ξ_{BA}	0,155	
ξ_{WB}	0,549	
ξ_{H2O}	0,000	
$\xi_{Öl}$	**0,226**	

$\dot{m}_{BA}$	0,621
$\dot{m}_{WB}$	2,198
$\dot{m}_{H2O}$	0,00000
$\dot{m}_{Öl}$	**0,905**

OR		
ξ_{BA}	0,000	
ξ_{WB}	0,002	
ξ_{H2O}	0,000	
$\xi_{Öl}$	**0,197**	

$\dot{m}_{BA}$	0,002
$\dot{m}_{WB}$	0,006
$\dot{m}_{H2O}$	0,0001
$\dot{m}_{Öl}$	**0,786**

total ZR	
ξ_{BA}	0,163
ξ_{WB}	**0,552**
ξ_{H2O}	0,000
$\xi_{Öl}$	1,057

$\dot{m}_{BA}$	0,650
$\dot{m}_{WB}$	**2,208**
$\dot{m}_{H2O}$	0,001
$\dot{m}_{Öl}$	**4,228**

RS=RH		
ξ_{BA}	0,774	
ξ_{WB}	0,110	
ξ_{H2O}	0,001	
$\xi_{Öl}$	**1,057**	

$\dot{m}_{BA}$	**3,097**
$\dot{m}_{WB}$	0,440
$\dot{m}_{H2O}$	0,00287
$\dot{m}_{Öl}$	**4,227**

HI		
ξ_{BA}	0,771	
ξ_{WB}	0,109	
ξ_{H2O}	0,001	
$\xi_{Öl}$	**0,898**	

$\dot{m}_{BA}$	**3,086**
$\dot{m}_{WB}$	0,438
$\dot{m}_{H2O}$	0,00224
$\dot{m}_{Öl}$	**3,593**

IG		
ξ_{BA}	0,770	
ξ_{WB}	0,109	
ξ_{H2O}	0,001	
$\xi_{Öl}$	**0,740**	

$\dot{m}_{BA}$	**3,080**
$\dot{m}_{WB}$	0,437
$\dot{m}_{H2O}$	0,002
$\dot{m}_{Öl}$	**2,959**

GC		
ξ_{BA}	0,767	
ξ_{WB}	0,109	
ξ_{H2O}	0,001	
$\xi_{Öl}$	**0,423**	

$\dot{m}_{BA}$	**3,069**
$\dot{m}_{WB}$	0,436
$\dot{m}_{H2O}$	0,002
$\dot{m}_{Öl}$	**1,691**

C_{orig} (n=4)

C_{orig} (n=5)

Table 16: Flow compositions, charge process, n=5

CHARGE, n=5

C_chg (n=5)

CR

		ξ	
$\dot{m}_{BA}$	3,076	ξ_{BA}	0,769
$\dot{m}_{MB}$	0,431	ξ_{MB}	0,108
$\dot{m}_{H2O}$	0,00000	ξ_{H2O}	0,000
$\dot{m}_{Oil}$	1,691	ξ_{Oil}	0,423

SR=HR+GR

		ξ	
$\dot{m}_{BA}$	0,006	ξ_{BA}	0,002
$\dot{m}_{MB}$	0,023	ξ_{MB}	0,006
$\dot{m}_{H2O}$	0,001	ξ_{H2O}	0,0002
$\dot{m}_{Oil}$	2,167	ξ_{Oil}	0,542

ZR

		ξ	
$\dot{m}_{BA}$	3,083	ξ_{BA}	0,771
$\dot{m}_{MB}$	0,453	ξ_{MB}	0,113
$\dot{m}_{H2O}$	0,001	ξ_{H2O}	0,000
$\dot{m}_{Oil}$	3,858	ξ_{Oil}	0,964

RL

		ξ	
$\dot{m}_{BA}$	0,004	ξ_{BA}	0,001
$\dot{m}_{MB}$	0,000	ξ_{MB}	0,000
$\dot{m}_{H2O}$	0,712	ξ_{H2O}	0,178
$\dot{m}_{Oil}$	0,002	ξ_{Oil}	0,000

R_chg

RS=RH

		ξ	
$\dot{m}_{BA}$	0,612	ξ_{BA}	0,153
$\dot{m}_{MB}$	2,178	ξ_{MB}	0,544
$\dot{m}_{H2O}$	0,00178	ξ_{H2O}	0,00045
$\dot{m}_{Oil}$	3,856	ξ_{Oil}	0,964

S (chg)

H

HI

		ξ	
$\dot{m}_{BA}$	0,608	ξ_{BA}	0,152
$\dot{m}_{MB}$	2,166	ξ_{MB}	0,541
$\dot{m}_{H2O}$	0,00101	ξ_{H2O}	0,000
$\dot{m}_{Oil}$	3,085	ξ_{Oil}	0,771

HR

		ξ	
$\dot{m}_{BA}$	0,003	ξ_{BA}	0,001
$\dot{m}_{MB}$	0,012	ξ_{MB}	0,003
$\dot{m}_{H2O}$	0,00077	ξ_{H2O}	0,0002
$\dot{m}_{Oil}$	0,771	ξ_{Oil}	0,193

I

IG

		ξ	
$\dot{m}_{BA}$	0,607	ξ_{BA}	0,152
$\dot{m}_{MB}$	2,160	ξ_{MB}	0,540
$\dot{m}_{H2O}$	0,00094	ξ_{H2O}	0,000
$\dot{m}_{Oil}$	2,313	ξ_{Oil}	0,578

IR

		ξ	
$\dot{m}_{BA}$	0,002	ξ_{BA}	0,000
$\dot{m}_{MB}$	0,006	ξ_{MB}	0,002
$\dot{m}_{H2O}$	0,00008	ξ_{H2O}	0,000
$\dot{m}_{Oil}$	0,771	ξ_{Oil}	0,193

G

GC

		ξ	
$\dot{m}_{BA}$	0,605	ξ_{BA}	0,151
$\dot{m}_{MB}$	2,155	ξ_{MB}	0,539
$\dot{m}_{H2O}$	0,00087	ξ_{H2O}	0,0002
$\dot{m}_{Oil}$	0,887	ξ_{Oil}	0,222

GO

		ξ	
$\dot{m}_{BA}$	0,002	ξ_{BA}	0,000
$\dot{m}_{MB}$	0,006	ξ_{MB}	0,002
$\dot{m}_{H2O}$	0,00008	ξ_{H2O}	0,000
$\dot{m}_{Oil}$	0,802	ξ_{Oil}	0,201

GR

		ξ	
$\dot{m}_{BA}$	0,001	ξ_{BA}	0,000
$\dot{m}_{MB}$	0,005	ξ_{MB}	0,001
$\dot{m}_{H2O}$	0,00006	ξ_{H2O}	0,000
$\dot{m}_{Oil}$	0,624	ξ_{Oil}	0,156

C_chg (n=5)

Table 17: Flow compositions, discharge process, n=5

Table 18: Flow compositions, charge process, n=6

CHARGE, n=6

CR

$\dot{m}_{BA}$ 3,014	ξ_{BA} 0,753	
$\dot{m}_{WB}$ 0,422	ξ_{WB} 0,105	
$\dot{m}_{H2O}$ 0,00000	ξ_{H2O} 0,000	
$\dot{m}_{Oil}$ 1,656	ξ_{Oil} 0,414	

SR=HR+GR

$\dot{m}_{BA}$ 0,006	ξ_{BA} 0,002	
$\dot{m}_{WB}$ 0,022	ξ_{WB} 0,006	
$\dot{m}_{H2O}$ 0,001	ξ_{H2O} 0,0002	
$\dot{m}_{Oil}$ 2,123	ξ_{Oil} 0,531	

ZR

$\dot{m}_{BA}$ 3,020	ξ_{BA} 0,755	
$\dot{m}_{WB}$ 0,444	ξ_{WB} 0,111	
$\dot{m}_{H2O}$ 0,001	ξ_{H2O} 0,000	
$\dot{m}_{Oil}$ 3,779	ξ_{Oil} 0,945	

RL

$\dot{m}_{BA}$ 0,003	ξ_{BA} 0,001	
$\dot{m}_{WB}$ 0,000	ξ_{WB} 0,000	
$\dot{m}_{H2O}$ 0,697	ξ_{H2O} 0,174	
$\dot{m}_{Oil}$ 0,002	ξ_{Oil} 0,000	

R_chg / RS=RH

$\dot{m}_{BA}$ 0,599	ξ_{BA} 0,150	
$\dot{m}_{WB}$ 2,134	ξ_{WB} 0,533	
$\dot{m}_{H2O}$ 0,00175	ξ_{H2O} 0,00044	
$\dot{m}_{Oil}$ 3,777	ξ_{Oil} 0,944	

S (chg)

H / HI

$\dot{m}_{BA}$ 0,596	ξ_{BA} 0,149	
$\dot{m}_{WB}$ 2,122	ξ_{WB} 0,530	
$\dot{m}_{H2O}$ 0,00099	ξ_{H2O} 0,000	
$\dot{m}_{Oil}$ 3,022	ξ_{Oil} 0,755	

HR

$\dot{m}_{BA}$ 0,003	ξ_{BA} 0,001	
$\dot{m}_{WB}$ 0,012	ξ_{WB} 0,003	
$\dot{m}_{H2O}$ 0,00076	ξ_{H2O} 0,0002	
$\dot{m}_{Oil}$ 0,755	ξ_{Oil} 0,189	

I / IG

$\dot{m}_{BA}$ 0,594	ξ_{BA} 0,149	
$\dot{m}_{WB}$ 2,116	ξ_{WB} 0,529	
$\dot{m}_{H2O}$ 0,00092	ξ_{H2O} 0,000	
$\dot{m}_{Oil}$ 2,266	ξ_{Oil} 0,567	

IR

$\dot{m}_{BA}$ 0,002	ξ_{BA} 0,000	
$\dot{m}_{WB}$ 0,006	ξ_{WB} 0,001	
$\dot{m}_{H2O}$ 0,00008	ξ_{H2O} 0,000	
$\dot{m}_{Oil}$ 0,755	ξ_{Oil} 0,189	

G / GC

$\dot{m}_{BA}$ 0,593	ξ_{BA} 0,148	
$\dot{m}_{WB}$ 2,111	ξ_{WB} 0,528	
$\dot{m}_{H2O}$ 0,00086	ξ_{H2O} 0,0002	
$\dot{m}_{Oil}$ 0,869	ξ_{Oil} 0,217	

GO

$\dot{m}_{BA}$ 0,002	ξ_{BA} 0,000	
$\dot{m}_{WB}$ 0,006	ξ_{WB} 0,002	
$\dot{m}_{H2O}$ 0,00008	ξ_{H2O} 0,000	
$\dot{m}_{Oil}$ 0,786	ξ_{Oil} 0,196	

GR

$\dot{m}_{BA}$ 0,001	ξ_{BA} 0,000	
$\dot{m}_{WB}$ 0,005	ξ_{WB} 0,001	
$\dot{m}_{H2O}$ 0,00006	ξ_{H2O} 0,000	
$\dot{m}_{Oil}$ 0,612	ξ_{Oil} 0,153	

C_chg (n=6)

W

Table 19: Flow compositions, discharge process, n=6

Table 20: Flow compositions, charge process, n=7

CHARGE, n=7

CR

ṁBA	2,952	ξBA	0,738
ṁMB	0,413	ξMB	0,103
ṁH2O	0,00000	ξH2O	0,000
ṁOil	1,623	ξOil	0,406

ZR

ṁBA	2,959	ξBA	0,740
ṁMB	0,435	ξMB	0,109
ṁH2O	0,001	ξH2O	0,000
ṁOil	3,702	ξOil	0,926

SR=HR+GR

ṁBA	0,006	ξBA	0,002
ṁMB	0,022	ξMB	0,006
ṁH2O	0,001	ξH2O	0,0002
ṁOil	2,079	ξOil	0,520

RL

ṁBA	0,003	ξBA	0,001
ṁMB	0,000	ξMB	0,000
ṁH2O	0,683	ξH2O	0,171
ṁOil	0,002	ξOil	0,000

RS=RH

ṁBA	0,587	ξBA	0,147
ṁMB	2,090	ξMB	0,523
ṁH2O	0,00171	ξH2O	0,00043
ṁOil	3,700	ξOil	0,925

H

ṁBA	0,584	ξBA	0,146
ṁMB	2,079	ξMB	0,520
ṁH2O	0,00097	ξH2O	0,000
ṁOil	2,960	ξOil	0,740

HI

ṁBA	0,003	ξBA	0,001
ṁMB	0,012	ξMB	0,003
ṁH2O	0,00074	ξH2O	0,0002
ṁOil	0,740	ξOil	0,185

I

ṁBA	0,582	ξBA	0,146
ṁMB	2,073	ξMB	0,518
ṁH2O	0,00090	ξH2O	0,000
ṁOil	2,220	ξOil	0,555

IR

ṁBA	0,002	ξBA	0,002
ṁMB	0,006	ξMB	0,006
ṁH2O	0,00007	ξH2O	0,000
ṁOil	0,740	ξOil	0,185

G

ṁBA	0,581	ξBA	0,145
ṁMB	2,068	ξMB	0,517
ṁH2O	0,00084	ξH2O	0,0002
ṁOil	0,851	ξOil	0,213

GO

ṁBA	0,002	ξBA	0,000
ṁMB	0,006	ξMB	0,002
ṁH2O	0,00008	ξH2O	0,000
ṁOil	0,770	ξOil	0,192

GR

ṁBA	0,001	ξBA	0,000
ṁMB	0,005	ξMB	0,001
ṁH2O	0,00006	ξH2O	0,000
ṁOil	0,599	ξOil	0,150

S (chg), SR, R, W, O, Ccng (n=7), Ccng (n=7)

Table 21: Flow compositions, discharge process, n=7

Table 22: Flow compositions, charge process, n=8

CHARGE, n=8

CR

	ṁ	ξ
BA	2,892	0,723
MB	0,405	0,101
H2O	0,00000	0,000
Oil	1,590	0,397

SR=HR+GR

	ṁ	ξ
BA	0,006	0,002
MB	0,022	0,005
H2O	0,001	0,0002
Oil	2,037	0,509

ZR

	ṁ	ξ
BA	2,898	0,725
MB	0,426	0,107
H2O	0,001	0,000
Oil	3,627	0,907

RL

	ṁ	ξ
BA	0,003	0,001
MB	0,000	0,000
H2O	0,669	0,167
Oil	0,002	0,000

RS=RH

	ṁ	ξ
BA	0,575	0,144
MB	2,048	0,512
H2O	0,00168	0,00042
Oil	3,625	0,906

H

HI

	ṁ	ξ
BA	0,572	0,143
MB	2,036	0,509
H2O	0,00095	0,000
Oil	2,900	0,725

HR

	ṁ	ξ
BA	0,003	0,001
MB	0,011	0,003
H2O	0,00073	0,0002
Oil	0,725	0,181

I

IG

	ṁ	ξ
BA	0,570	0,143
MB	2,031	0,508
H2O	0,00088	0,000
Oil	2,175	0,544

IR

	ṁ	ξ
BA	0,002	0,002
MB	0,006	0,006
H2O	0,00007	0,000
Oil	0,725	0,181

G

GC

	ṁ	ξ
BA	0,569	0,142
MB	2,026	0,507
H2O	0,00082	0,0002
Oil	0,834	0,208

GO

	ṁ	ξ
BA	0,002	0,000
MB	0,006	0,001
H2O	0,00008	0,000
Oil	0,754	0,189

GR

	ṁ	ξ
BA	0,001	0,001
MB	0,005	0,000
H2O	0,00006	0,000
Oil	0,587	0,147

C_chg (n=8) W S (chg)

R_chg C_dg (n=8) W

Table 23: Flow compositions, discharge process, n=8

5 Discussion of results and summary

The assumption concerning oil release is based on solid densities, and applies on relatively compact, spheric particles, which needs to be evaluated in experimental runs. In an extreme case, it could even be the other way around; under significant pore formation hence particle volume increase through dehydration of boric acid, caused by a "bloating" of the particles by the formation of steam; or with a formation of crystals and/or agglomerates. Such events would worsen the achievable packing density and limit the extraction of oil in the charge process when the created void volume is filled with process oil (and not with gas). In such a case, it could be that process oil is released in the discharge process and reused in the charge process. Given the uncertainty of this assumption, a set of experiments concerning changes in particle structure should be conducted before using an oil storage inlet only for the charge process.

For a more direct calculation and intuitive mass flow diagram, the recycled oil flow from the sedimentation column is shown as a direct route from the column to the reactor in the simplified block schemes, while in the actual design, it passes through the oil storage, from which it is fed into the conveyor screw. This requires comparable compositions of the extracted oil stream from the sedimentation column and the oil storage content; If that should not be the case, alternative piping (bypassing the oil storage) would solve eventual incoherencies.

5.1 Ideal processes

5.1.1 Summaries of calculations under ideal conditions

This chapter gives a quick overview on the calculation results for referencing and graphical interpretations, as well as comparisons between charge and discharge modes.

In the following table, major quantifications of the ideal charge and discharge process with steam are listed for comparisons.

Table 24: Summary of idealized calculations

	Ideal charge process (chg, id)	Ideal discharge process ($dcg_{(g)}, id$)
Target power[a]	$P_{th,dehyd} = 1\ kW$	$P_{th,rehyd} = -1\ kW$
Concentrate oil-to-solid ratio	$\gamma_C = 0.50\ \dfrac{kg_{oil}}{kg_{BA}}$	$\gamma_C = 0.42\ \dfrac{kg_{oil}}{kg_{MB}}$
Volume-specific energy content of input concentrate	$e_{v,C} = 0.74\ \dfrac{GJ}{m^3}$	$e_{v,C} = -1.36\ \dfrac{GJ}{m^3}$
Reactor inflow oil-to-solid ratio[a]	$\gamma_R = 1.11\ \dfrac{kg_{oil}}{kg_{BA}}$	$\gamma_R = 1.57\ \dfrac{kg_{oil}}{kg_{MB}}$
Reactor temperature[a]	$T_R = 150°C$	$T_R = 130°C$
Reactor residence time	$\tau_R = 54min$	$\tau_R = 15min$
Reactor volume	$V_R = 9.5l$	$V_R = 2.1l$
Oil separation ratios[b]	$\eta_H = 0.39$[a]	$\eta_H = 0.20$[a]
	$\eta_I = 0.08$[a]	$\eta_I = 0.12$[a]
	$\eta_G = 0.31$	$\eta_G = 0.24$
Input from concentrate	$\dot{m}_{CR}^{BA} = 3.82\ \dfrac{kg_{BA}}{h}$	$\dot{m}_{CR}^{BA} = 2.71\ \dfrac{kg_{MB}}{h}$
	$\dot{m}_{CR}^{oil} = 1.90\ \dfrac{kg_{oil}}{h}$	$\dot{m}_{CR}^{oil} = 1.14\ \dfrac{kg_{oil}}{h}$
Output to concentrate	$\dot{m}_{SC}^{BA} = 2.71\ \dfrac{kg_{MB}}{h}$	$\dot{m}_{SC}^{BA} = 3.82\ \dfrac{kg_{BA}}{h}$
	$\dot{m}_{SC}^{oil} = 1.14\ \dfrac{kg_{oil}}{h}$	$\dot{m}_{SC}^{oil} = 1.90\ \dfrac{kg_{oil}}{h}$
Steam flows (out/in)	$\dot{m}_{RL}^{H_2O(g)} = 1.11\ \dfrac{kg_{H_2O}}{h}$	$\dot{m}_{ER}^{H_2O(g)} = 1.11\ \dfrac{kg_{H_2O}}{h}$
Total recycled oil	$\dot{m}_{SR}^{oil} = 2.34\ \dfrac{kg_{oil}}{h}$	$\dot{m}_{SR}^{oil} = 2.34\ \dfrac{kg_{oil}}{h}$

Oil storage flows (out/in)	$\dot{m}_{SO}^{oil} = 0.75 \dfrac{kg_{oil}}{h}$	$\dot{m}_{OR}^{oil} = 0.75 \dfrac{kg_{oil}}{h}$
Preheating[b]	$\boldsymbol{T_{ZR} = 110°C}$[a]	$\boldsymbol{T_{ZR} = T_R = 130°C}$[a]
	$P_{th,Z} = 0.20kW$	$P_{th,Z} = 0.29kW$
	$P_{th,pre(R)} = 0.18kW$	-
Condenser/Evaporator heat	$P_{th,L} = -0.82kW$	$P_{th,E} = 0.81kW$
of which condensation/evaporation	$P_{th,L,cond} = -0.70kW$	$P_{th,E,evap} = 0.70kW$
Sedimentation heat	$P_{th,G} = -0.30kW$	$P_{th,G} = -0.35kW$

a) free parameters
b) partially free parameter set

On the following pages, some of these values were visualized in Sankey-Diagrams. In the energy balance, the boxes "Q" and "-Q" resemble the heating and cooling units, respectively, which were not further specified yet. The temperature levels at which the flows are induced or extracted are stated in the process units corresponding to each flow.
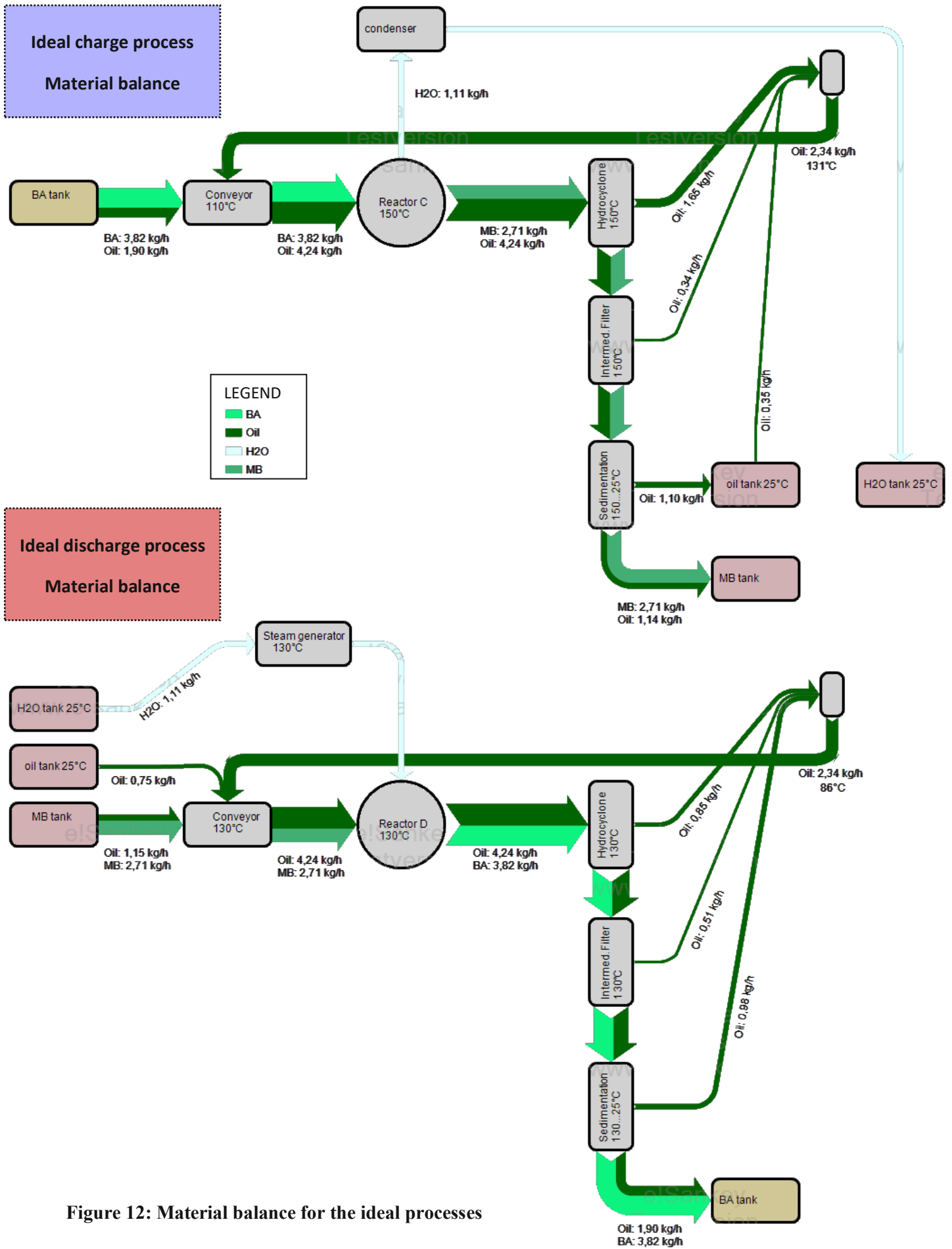
Figure 12: Material balance for the ideal processes

Ideal charge process

Energy balance

condenser
150...100...25°C

Sensible Heat: 0,12 kW
Condensation: 0,70 kW

Sensible Heat: 0,16 kW

Conveyor
110°C

Reactor C
150°C

Hydrocyclone
150°C

Sensible Heat: 0,13 kW

Oil
131°C

Sensible Heat: 0,36 kW

Reaction Enthalpy: 0,26 kW
Sensible Heat: 0,46 kW

Sensible Heat: 0,03 kW

Sensible Heat: 0,20 kW

Sensible Heat: 0,18 kW
Reaction Enthalpy: 1,00 kW

Intermed. Filter
150°C

Q
1,4kW

Sedimentation
150...25°C

Sensible Heat: 0,30 kW

-Q
1,1kW

Reaction Enthalpy: 0,26 kW

MB tank

LEGEND
Sensible Heat
Reaction Enthalpy
Condensation
Evaporation

Ideal discharge process

Energy balance

Steam generator
130°C

MB tank

Conveyor
130°C

Reactor D
130°C

Hydrocyclone
130°C

Sensible Heat: 0,08 kW

Sensible Heat: 0,05 kW

Oil 86°C

Reaction Enthalpy: 0,26 kW

Sensible Heat: 0,37 kW
Reaction Enthalpy: 0,26 kW

Sensible Heat: 0,43 kW

Sensible Heat: 0,03 kW

Sensible Heat: 0,29 kW

Sensible Heat: 0,11 kW
Evaporation: 0,70 kW

Reaction Enthalpy: 1,00 kW

Intermed. Filter
130°C

Q
1,1kW

Sedimentation
130...25°C

Sensible Heat: 0,35 kW

-Q
1,4kW

Figure 13: Energy balance for the ideal processes
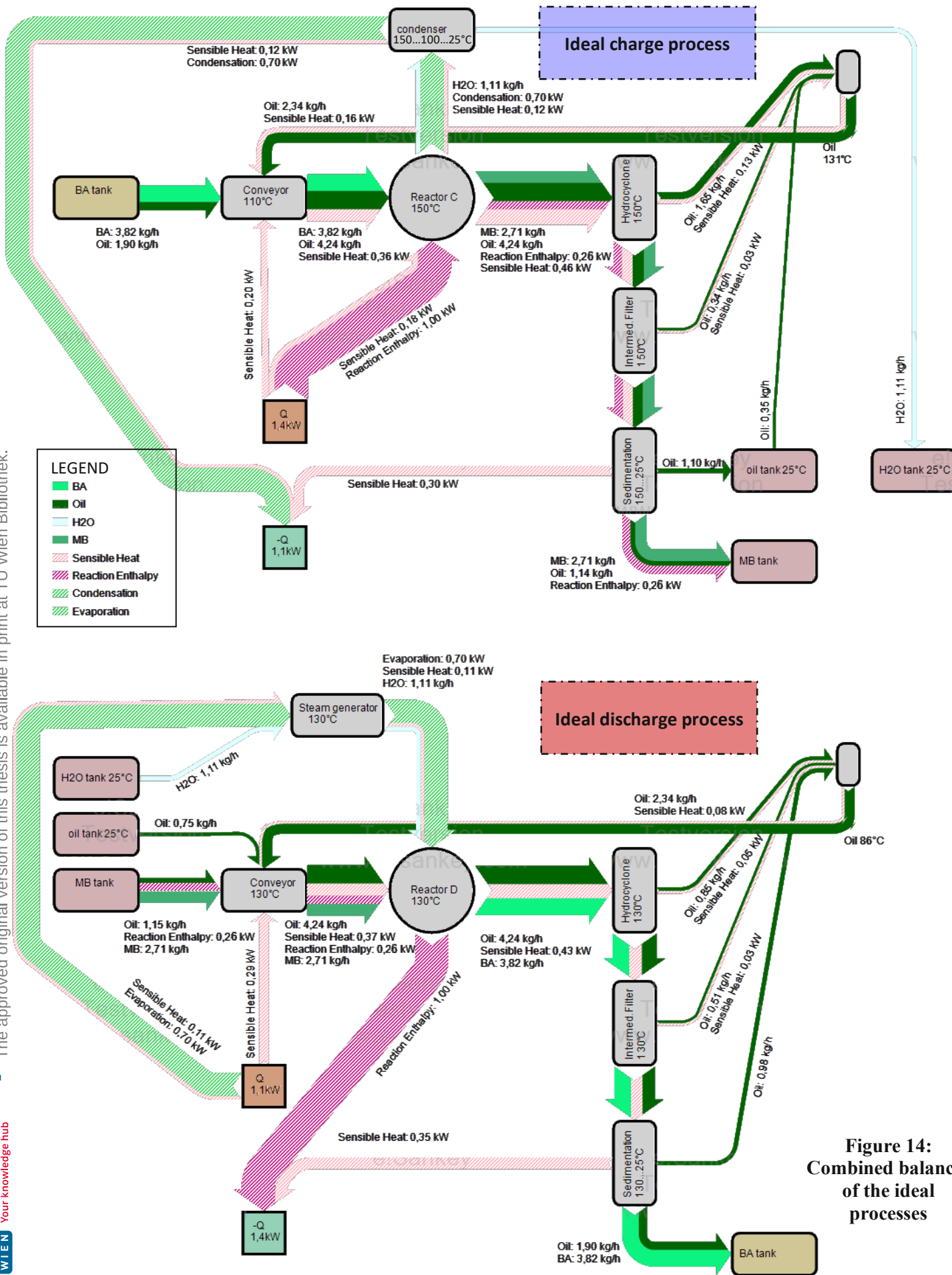
**Figure 14:
Combined balances
of the ideal
processes**

A remarkable result of these bilances are the "reaction enthalpy" flows of 0.26kW in Figure 13, the energy balance. This value was extracted from the energy balance over the charge reactor, as the remaining energy flow to close the balance, and with the uncertainties involved (for example using mean heat capacities), should be rounded to the next figure – Thus, the "effective stored energy" of the charge process relative to the principal design parameter, the reaction enthalpy power consumption, is emphasized here:

$$P_{sto,effective} \approx 0.3 * P_{th,dehyd}$$

This result aligns with the finding that the condensation heat of the charge process (and the evaporation heat of the steam discharge process) poses the largest fraction of the reaction enthalpy; Rephrasing that:

$$P_{th,cond} \approx 0.7 * P_{th,dehyd}$$

What comes to mind is that the actual design parameter to determine the mass flows should not be the reaction enthalpy alone, but also the recovery rate of condensation enthalpy, which accounts for most of the theoretically recoverable waste heat in charging (-1.1kW). This is where considerations on temperature level adaption should take place. Mechanical vapor recompression yields the potential to harvest this energy at reaction temperature – With a compression to 4.8 bar, condensation could be performed at the reaction temperature of 150°C [22]. Also, lowering the reaction temperature by operating the reactor under vacuum conditions, the necessary steam recompression could be lowered; For example, at 130°C, condensation could be performed at 2.7 bar [22].

The other heat waste flows, labelled as sensible heat in the diagrams are of lesser importance quantitatively and qualitatively, as most of the potential heat release is obtained at lower temperatures; Nevertheless, designing the preheating conveyor accordingly, it may be used there. See chapters 4.1.2.5 and 4.1.2.6 for the exact calculations.

It should be pointed out that there is a slight imbalance of the calculated heat flows between the charge and discharge processes – most likely due to using heat capacities for mean temperatures, based on the temperature difference, in the calculations on sensible heat. The differences are $1.38kW - 1.35kW$ between the charge input and discharge output power, and $1.10kW - 1.12kW$ between the discharge input and charge output power. With an exact calculation, these should vanish. Precise redeterminations, where necessary aligned with experimental findings, should be undertaken.

5.1.2 Variations of the ideal processes

5.1.2.1 Power

If the designed processes were meant to be upscaled, i.e., a higher power input/output was to be chosen, only the mass flow values and the reactor volume would change in the design presented in this thesis. With a higher input flow of boric acid (charge) or metaboric acid (discharge) come higher necessary oil flows and higher input/output flows of water and/or steam. All the other parameters for the materials and the process units remain constant. Thus, the chosen $P_{th,dehyd} = -P_{th,rehyd} = 1\,kW$ can be understood as a baseline for linear upscaling.

Table 25: Linear upscaling of the ideal processes

$P_{th,dehyd}$	$1kW$	$10kW$	$50kW$	$P_{th,rehyd}$	$-1kW$	$-10kW$	$-50kW$
$\dot{m}_{CR}^{BA_{chg,id}}$	$3.82\frac{kg}{h}$	$38.2\frac{kg}{h}$	$191.0\frac{kg}{h}$	$\dot{m}_{CR}^{MB_{dcg,id}}$	$2.71\frac{kg}{h}$	$27.1\frac{kg}{h}$	$135.5\frac{kg}{h}$
$V_R^{chg,id}$	$9.5l$	$95l$	$475l$	$V_R^{dcg,id}$	$2.1l$	$21l$	$105l$

This table is not to be understood as an exhaustive collection of values; The other values, for example oil flows and condensation/evaporation energies, are subject to the same factors.

5.1.2.2 Reactor residence times

As the estimated residence times are subject to further observation, the corresponding reactor volumes should not be considered as definitive suggestions. The impacts of a few different values on the reactor volume of the ideal 1kW scenario are listed below.

Table 26: Reactor residence time variations

$\tau_R^{chg,id}$	$30min$	$54min$	$150min$	$\tau_R^{dcg,id}$	$8min$	$15min$	$45min$
$V_{R(1kW)}^{chg,id}$	$5.3l$	$9.5l$	$26.4l$	$V_{R(-1kW)}^{dcg,id}$	$1.1l$	$2.1l$	$6.3l$

5.1.2.3 Discharge mode: steam vs. liquid water

Throughout this thesis, the rehydration in the discharge process was suggested to be operated under injection of steam, as opposed to a rehydration with liquid water, for its higher energy output in the reaction itself. Nevertheless, there are several advantages of a liquid rehydration, foremost lower apparative requirements. A more detailed comparison can be found in chapter 4.4.3. The following table gives a quick overview on some remarkable differences, which are direct consequences of the reaction enthalpy ratio of $\frac{941.3}{229.7} = 4.1$.

Table 27: Parameter comparison of steam/liquid rehydration

	$\frac{\Delta_r h_{BA}°}{kJ/kg_{BA}}$	$\frac{e_{v,C}}{GJ/m^3}$	$\frac{\dot{m}_{R_{in}(-1kW)}^{MB_{dcg,id}}}{kg/h}$	$\frac{\dot{m}_{R_{out}(-1kW)}^{BA_{dcg,id}}}{kg/h}$	$\frac{\dot{m}_{R_{out}(-1kW)}^{oil_{dcg,id}}}{kg/h}$
steam rehydration	941.3	-1.36	2.71	3.82	4.24
liquid rehydration	229.7	-0.33	11.11	15.66	17.38

Although the required mass flows for a rehydration with steam are much lower, it needs to be said that the evaporation heat for steam generation does not come out of thin air, especially considering that cheap sources of excess heat will be harder to find when the process aim itself consists in generating heat.

It may well be that the charge power is much higher then the discharge power in application; For example, if the former takes its energy from a local industrial plant providing 50kW of waste energy, and a few buildings with its own -10kW discharge plants receive tanks with metaboric acid concentrate and return the used boric acid concentrate. Nevertheless, due to weight and transport costs as well as the possibility to use the modified charge plant as the discharge plant in winter, when the waste energy can be directly distributed to consumers, it may be more efficient to operate both at the industrial site and deliver just the district heating energy and no materials; Which is why apparative requirements were not considered as key argument, and the steam rehydration accounted as the more promising base scenario.

5.2 Non-ideal processes

The calculated results were used to create exemplary Sankey diagrams for the material balances of two subsequent process cycles:
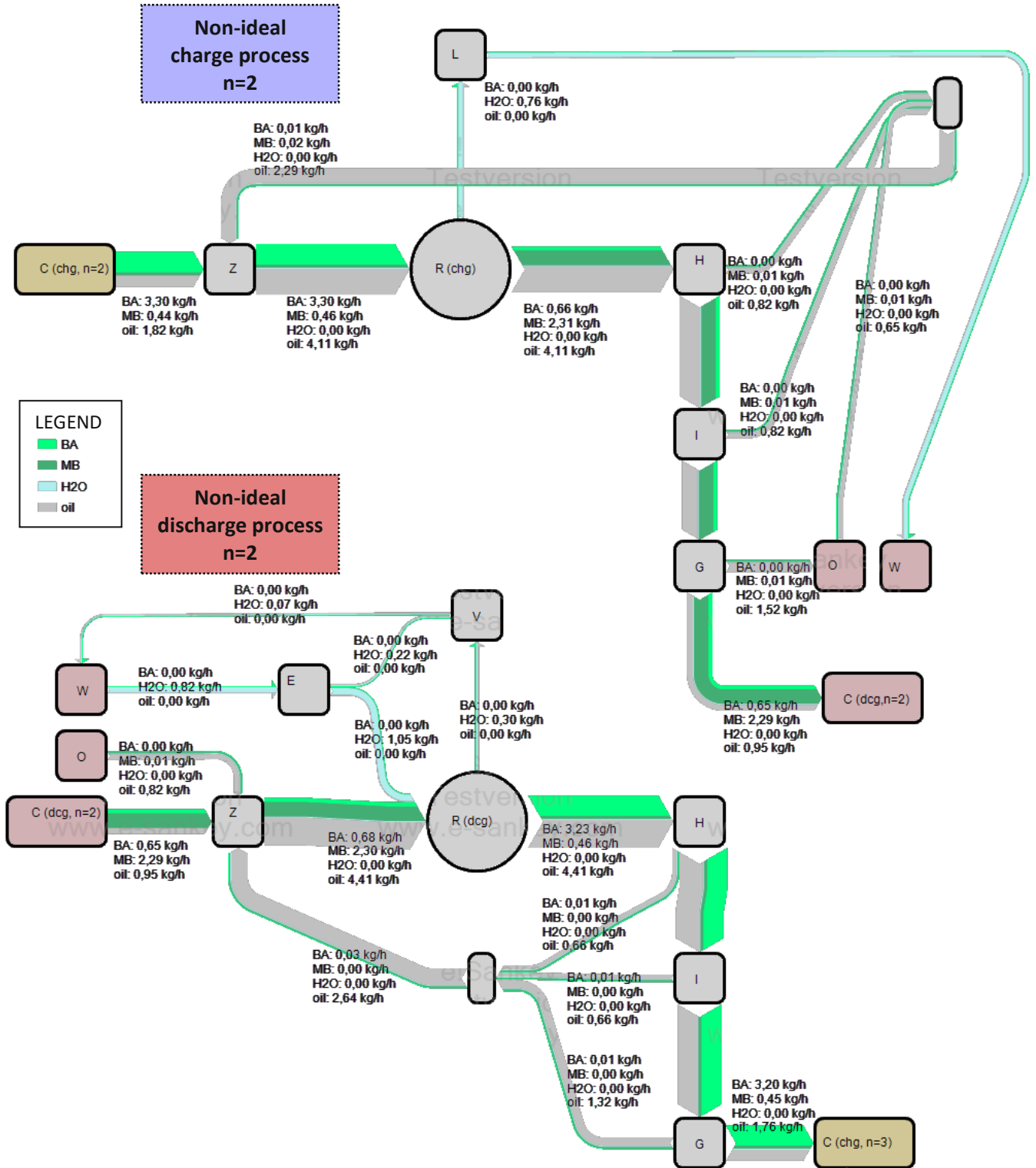
Figure 15: Material balance, non-ideal discharge process, n=2

Non-ideal charge process n=3

BA: 0,01 kg/h
MB: 0,02 kg/h
H2O: 0,00 kg/h
oil: 2,26 kg/h

BA: 0,00 kg/h
H2O: 0,74 kg/h
oil: 0,00 kg/h

C (chg, n=3)

Z

R (chg)

H

BA: 3,21 kg/h
MB: 0,45 kg/h
oil: 1,76 kg/h

BA: 3,21 kg/h
MB: 0,47 kg/h
H2O: 0,00 kg/h
oil: 4,02 kg/h

BA: 0,64 kg/h
MB: 2,27 kg/h
H2O: 0,00 kg/h
oil: 4,02 kg/h

BA: 0,00 kg/h
MB: 0,01 kg/h
H2O: 0,00 kg/h
oil: 0,80 kg/h

BA: 0,00 kg/h
MB: 0,01 kg/h
H2O: 0,00 kg/h
oil: 0,65 kg/h

LEGEND
BA
MB
H2O
oil

Non-ideal discharge process n=3

BA: 0,00 kg/h
MB: 0,01 kg/h
H2O: 0,00 kg/h
oil: 0,80 kg/h

I

G

O

W

BA: 0,00 kg/h
MB: 0,01 kg/h
H2O: 0,00 kg/h
oil: 1,49 kg/h

BA: 0,63 kg/h
MB: 2,25 kg/h
H2O: 0,00 kg/h
oil: 0,92 kg/h

C (dcg,n=3)

BA: 0,00 kg/h
H2O: 0,07 kg/h
oil: 0,00 kg/h

V

BA: 0,00 kg/h
H2O: 0,22 kg/h
oil: 0,00 kg/h

W

BA: 0,00 kg/h
H2O: 0,81 kg/h
oil: 0,00 kg/h

E

BA: 0,00 kg/h
H2O: 0,29 kg/h
oil: 0,00 kg/h

BA: 0,00 kg/h
H2O: 1,03 kg/h
oil: 0,00 kg/h

O

BA: 0,00 kg/h
MB: 0,01 kg/h
H2O: 0,00 kg/h
oil: 0,80 kg/h

C (dcg, n=3)

Z

R (dcg)

H

BA: 0,63 kg/h
MB: 2,24 kg/h
oil: 0,92 kg/h

BA: 0,66 kg/h
MB: 2,25 kg/h
H2O: 0,00 kg/h
oil: 4,32 kg/h

BA: 3,16 kg/h
MB: 0,45 kg/h
H2O: 0,00 kg/h
oil: 4,31 kg/h

BA: 0,01 kg/h
MB: 0,00 kg/h
H2O: 0,00 kg/h
oil: 0,65 kg/h

BA: 0,03 kg/h
MB: 0,00 kg/h
H2O: 0,00 kg/h
oil: 2,59 kg/h

BA: 0,01 kg/h
MB: 0,00 kg/h
H2O: 0,00 kg/h
oil: 0,65 kg/h

I

BA: 0,01 kg/h
MB: 0,00 kg/h
H2O: 0,00 kg/h
oil: 1,29 kg/h

BA: 3,13 kg/h
MB: 0,44 kg/h
H2O: 0,00 kg/h
oil: 1,73 kg/h

G

C (chg, n=4)

Figure 16: Material balance, non-ideal discharge process, n=3

These diagrams make the changes from one cycle to another more visible. Remember that the boldness of the lines does not correlate to the challenge of a pathway, which holds especially true for steam flows, given its volume.

In- and outflows of BA, MB, H_2O and oil were calculated for the whole series of processes as follows:

Table 28: Initial/final mass flow sums

Initial/final mass flow sum	Contributions
$\sum \dot{m}_{chg,n}^{i_{in}}$	$\dot{m}_{CR}^{i_{chg,n}}$
$\sum \dot{m}_{chg,n}^{i_{out}}$	$\dot{m}_{GC}^{i_{chg,n}} + \dot{m}_{GO}^{i_{chg,n}} + \dot{m}_{RL}^{i_{chg,n}}$
$\sum \dot{m}_{dcg,n}^{i_{in}}$	$\dot{m}_{CR}^{i_{dcg,n}} + \dot{m}_{OR}^{i_{dcg,n}} + \dot{m}_{WR}^{i_{dcg,n}}$
$\sum \dot{m}_{dcg,n}^{i_{out}}$	$\dot{m}_{GC}^{i_{dcg,n}} + \dot{m}_{RW}^{i_{dcg,n}}$

i… materials, n… cycle

These sums were used for Figure 17 below. As can be seen, the developed model does not handle the initial pure input well, creating an inconsistency in the first cycle $n = 1$. Also, some assumptions should be revised, considering that there is a slight decrease in the total reacting mass flows, i.e., the sum of BA, MB and H_2O mass flows at the beginning and the end of the processes. The increases from charge output to discharge input for $n \geq 2$ are due to the set value for water addition in WR. More important, the gradient for deterioration of the processes may be steeper in reality, and would be better modelled by using cycle-dependent parameters, not the fixed values from Table 7.
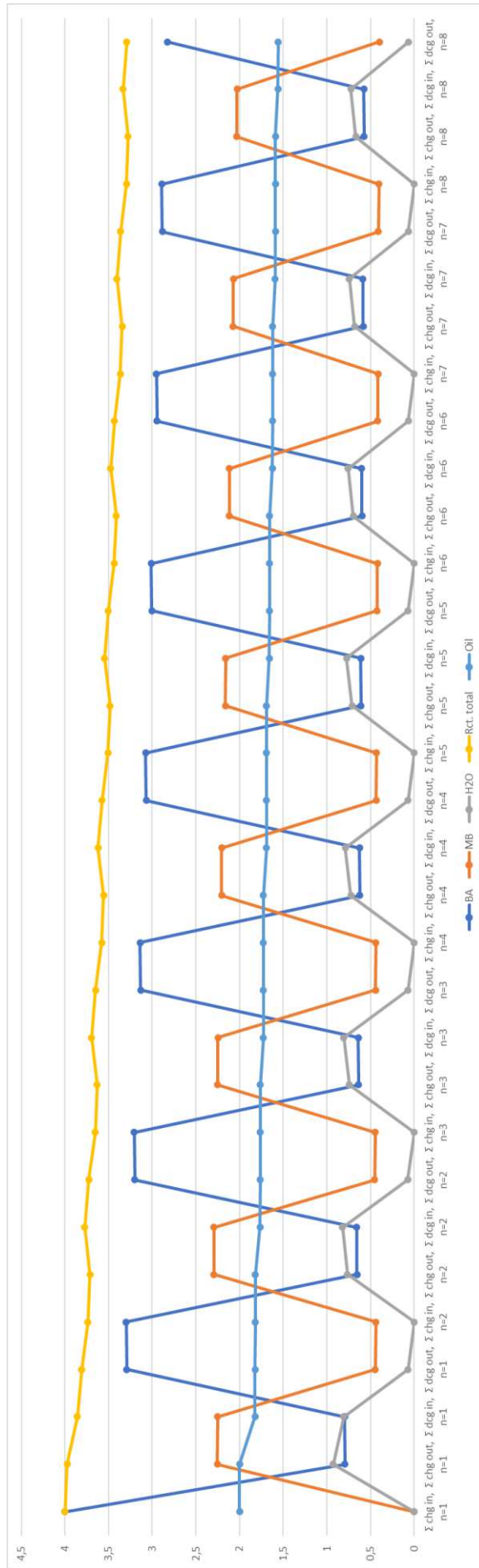
Figure 17: Mass flow sums for incomplete conversion and recovery

6 Conclusion

While the idealized processes serve as a starting point to understand the proposed experimental plant and underline the potential of the suspension reactor system, the obtained numbers are based on preliminary assumptions and guesswork. The range of results that could be covered by actual experimental runs on the developed plant concept is vast, and many parameters were set with the aim of scaffolding the calculations to obtain actual numbers. This thesis should therefore be understood as a first iteration and a framework of equations that can hopefully be of good service to future researchers, trying to analyze and optimize the process plant in use. On one hand, some of the units may cause more efforts than efficiency and may be completely abandoned; On the other hand, others cover a profound field of research, foremost the reactor, which was more than simplified in this work.

Based on the literature values for standard reaction enthalpies, one result that needs to be highlighted is that the actual gain through stored energy is comparatively small compared to its orbit of other energy flows. As the energy balances in this thesis do not include necessary energy inputs for handling the media through the plant (stirring, pumping etc.), not to mention the likely application of mechanical vapor recompression, the profitable application of the processes may be limited to large-scale heat capture, where the economic break-even point is more at hand than with low-power sources that still require the whole package of instrumental effort.

While it remains subject to precise redeterminations, the high share of condensation and evaporation energies of the processes that became clear early in this work suggests splitting the attention – Not only is it a question of the used TCES medium, but the dehydration and rehydration reaction kinetics as well as the efficient handling of water and steam give reason to award water as the key reaction component. In the comparison of rehydration processes with steam and liquid water, the reaction enthalpy difference by a factor of 4 highlights this necessity.

Clearly, there are legions of challenges to face – And from this point, it can be said that it is well worth the hassles. With a well-developed operation, TCES can turn out as a key player in tackling the global energy transition, given the availability of applicable materials and the potential of a low-maintenance capture from the plentiful waste heat sources – Ethically redistributing one of the very few human needs, warmth.

7 Outlook

While a few questions may have found an answer, more questions emerged that can be covered within the scope of this thesis. As it is often the case, with research revealing itself as a Pandora's box of evermore research.

The complexity of the proposed processes, not least due to their multi-phase nature, holds space for a handful of task forces. The behaviour of the materials should be thoroughly studied, under various process conditions. Quick examinations on dehydration behaviour led to a preliminary estimate on dehydration residence time, but no experimental results were gathered to estimate the necessary rehydration residence time, which is subject to examinations on the transport from injected steam bubbles to particles of metaboric acid, and in the case of liquid rehydration, also the characteristics of the formed steam in the suspension. Parameters for a mathematical model should at least cover steam bubble and particle sizes, the distribution of both in the suspension, particle porosity (and changes in such), reaction kinetics, turbulence (transport via convection) and suspension viscosity (transport via diffusion, outside and inside the particles).

In terms of energy efficiency, it is vital to utilize the heat that can be extracted from the condenser, and a mechanical vapor recompression should be considered, so that the condensation can be performed at reaction temperature to recycle the condensation heat directly to the reactor.

What was not examined in this work was the tendency of boric acid to sublimate and escape the reaction suspension. Also, the possibility to provoke spatial melting should be considered, especially when assessing the processes outside of laboratory conditions. An accumulation of a molten phase (or any other deterioration of the media) suggests developing yet another process – A recovery station to reestablish the original material properties after a number of cycles, to possible extents.

Good luck!

List of References

[1] T. C. Jones, "America, Oil, and War in the Middle East," *Journal of American History*, vol. 99, no. 1, pp. 208–218, 2012, doi: 10.1093/jahist/jas045.

[2] C. Clifford, "Russia's war with Ukraine offers critical lessons for global energy markets," *CNBC*, 03 Feb., 2022. https://www.cnbc.com/2022/03/02/russia-ukraine-war-lessons-for-global-energy-markets.html (accessed: May 5 2022).

[3] G. Brew, "How Oil Defeated The Nazis," 06 Jun., 2019. https://oilprice.com/Energy/Crude-Oil/How-Oil-Defeated-The-Nazis.html (accessed: May 5 2022).

[4] BP p.l.c., "bp Energy Outlook 2022," 2022. [Online]. Available: https://www.bp.com/content/dam/bp/business-sites/en/global/corporate/pdfs/energy-economics/energy-outlook/bp-energy-outlook-2022.pdf

[5] "Global Waste Heat to Power Market Size, Share and Analysis to Expand At 4.9% CAGR Through 2026," *MarketWatch*, 4/18/2022, 4/18/2022. https://www.marketwatch.com/press-release/global-waste-heat-to-power-market-size-share-and-analysis-to-expand-at-49-cagr-through-2026-2022-04-18 (accessed: May 5 2022).

[6] N. Pfleger, T. Bauer, C. Martin, M. Eck, and A. Wörner, "Thermal energy storage - overview and specific insight into nitrate salts for sensible and latent heat storage," *Beilstein journal of nanotechnology*, vol. 6, pp. 1487–1497, 2015, doi: 10.3762/bjnano.6.154.

[7] G. Krese, R. Koželj, V. Butala, and U. Stritih, "Thermochemical seasonal solar energy storage for heating and cooling of buildings," *Energy and Buildings*, vol. 164, pp. 239–253, 2018, doi: 10.1016/j.enbuild.2017.12.057.

[8] C. Huber *et al.,* "Boric Acid: A High Potential Candidate for Thermochemical Energy Storage," *Energies*, vol. 12, no. 6, p. 1086, 2019, doi: 10.3390/en12061086.

[9] J. Widhalm, "Die thermochemische Energiespeicherung bezogen auf realitätsnahe Anwendungsfälle," TU Wien, 2016.

[10] M. Deutsch *et al.,* "Systematic search algorithm for potential thermochemical energy storage systems," *Applied Energy*, vol. 183, pp. 113–120, 2016, doi: 10.1016/j.apenergy.2016.08.142.

[11] D. R. Lide, *CRC Handbook of Chemistry and Physics - 80th edition 1999-2000*. Boca Raton, FL: CRC Press, 1999.

[12] M. e. a. Wuerth, *Thermochemical Energy Storage Employing Fluidized Bed Technology: Experimental Investigations with CaO/Ca(OH)2 on a 21kWh Reactor.* [Online]. Available: https://www.aiche.org/conferences/fluidization/2019/proceeding/paper/thermochemical-energy-storage-employing-fluidized-bed-technology-experimental-investigations (accessed: May 8 2022).

[13] Bartels. M, *Agglomeration in fluidized beds: detection and counteraction*, 2008. [Online]. Available: https://www.researchgate.net/publication/27344182_Agglomeration_in_fluidized_beds_detection_and_counteraction

[14] H. Bürgmayr, "Master Thesis: Thermochemische Energiespeicher - innovative Materialsysteme im Suspensionsreaktor," ICEBE, TU Wien, Vienna, 2021.

[15] F. V. Vitiello, "Master Thesis: Transport phenomena in thermo-chemical solar energy systems: Application to the case-study of calcium oxalate monohydrate," TU Wien, Università Degli Studi Di Napoli Federico II, Vienna/Naples.

[16] G. Brauer, Ed., *Handbuch der präparativen anorganischen Chemie: Band I,* 3rd ed. Stuttgart: Enke, 1975.

[17] W. H. Zachariasen, "The crystal structure of monoclinic metaboric acid," *Acta Cryst*, vol. 16, no. 5, pp. 385–389, 1963, doi: 10.1107/S0365110X6300102X.

[18] Freyhardt, Wiebcke, and Felsche, "The monoclinic and cubic phases of metaboric acid (precise redeterminations)," *Acta crystallographica. Section C, Crystal structure communications*, 56 (Pt 3), pp. 276–278, 2000, doi: 10.1107/S0108270199016042.

[19] M. W. Chase Jr., "NIST-JANAF Thermochemical Tables, Fourth Edition," *J. Phys. Chem. Ref. Data, Monograph 9*, 1998. [Online]. Available: https://webbook.nist.gov/

[20] Fragoltherm, *Produktinformation Fragoltherm Q-32-N.* received upon request in May, 2021.

[21] *Saturated Steam - Properties for Pressure in Bar.* [Online]. Available: https://www.engineeringtoolbox.com/saturated-steam-properties-d_457.html (accessed: May 9 2022).

[22] *Water - Thermophysical Properties.* [Online]. Available: https://www.engineeringtoolbox.com/water-thermal-properties-d_162.html (accessed: May 14 2022).